MATHEMATICAL ANALYSIS ON CATALYTIC DEHYDROGENATION OF CYCLOHEXANE USING MICROPOROUS MEMBRANE

A DISSERTATION

Submitted in partial fulfilment of the
requirements for the award of the degree
of
MASTER OF TECHNOLOGY
in
CHEMICAL ENGINEERING
(With Specialization in Computer Aided Process Plant Design)

By

TANVI GABA

CENTRAL LIBRARY
Acc. No. G13816
Date 24/10/08
31/10/08
I.I.T. ROORKEE

DEPARTMENT OF CHEMICAL ENGINEERING
INDIAN INSTITUTE OF TECHNOLOGY ROORKEE
ROORKEE - 247 667 (INDIA)
JUNE, 2008

CANDIDATE'S DECLARATION

I hereby certify that the work which is being presented in this dissertation entitled **"Mathematical Analysis on catalytic dehydrogenation of cyclohexane using microporous membrane"** in partial fulfillment of the requirement for the award of the degree of **Master of Technology in Chemical Engineering** with specialization in **Computer Aided Process Plant Design (CAPPD)**, submitted in the Department of Chemical Engineering of Indian Institute of Technology Roorkee, India, is an authentic record of my work carried out during the period from June, 2007 to June, 2008 under the supervision of **Dr.(Mrs.) Shashi,** Assistant Professor, Department of Chemical Engineering Indian Institute of Technology Roorkee, Roorkee.

The matter embodied in this dissertation has not been submitted by me for the award of any other degree.

I.I.T.Roorkee
Date: 13th June 08

Tanvi
(TANVI GABA)

This is to certify that the above statement made by the candidate is correct to the best of our knowledge.

Shashi
13/6/08
(Dr.(Mrs.)Shashi)
Assistant Professor
Department Of Chemical Engineering
Indian Institute of Technology, Roorkee
Roorkee-247667

ABSTRACT

A steady state, isothermal one dimensional mathematical model has been developed for dehydrogenation of cyclohexane carried out in a microporous membrane reactor. The performance of three reactor configurations viz. conventional fixed bed, full length membrane reactor and hybrid reactor have been studied at two feed conditions: one is without hydrogen and the other is with hydrogen. Hydrogen has been added co-feed to increase the stability of catalyst and membrane and to reduce the possibility of coking. FAU type zeolite microporous membrane has been used. The expressions which relate permeance of components through FAU type membrane to temperature have been formulated on the basis of experimental data available in open literature. The model equations have been solved by using MATLAB. The simulated results at a given set of operating conditions and boundary conditions have been found to be in good agreement with the experimental results.

The variation in conversion along the length of the reactor and with temperature has been studied for all three reactor configurations and feed conditions. This study reveals that the conversion is maximum in full length membrane reactor and minimum in fixed bed reactor. The conversion in hybrid reactor has been found to be in between fixed bed and full length membrane reactor. On being endothermic reaction the conversion increases with temperature. Although the conversion is lower in hybrid reactor than full length membrane reactor the performance of hybrid reactor may be considered superior at the expense of high cost and high reactant loss in full length membrane reactor. In case of co-feeding of hydrogen with cyclohexane, the conversion in all cases is lower than without hydrogen due to high hydrogen concentration in the reactant. This reduction in conversion may be accepted on commercial level in order to maintain stability of membrane and catalyst.

ACKNOWLEDGEMENTS

Gratitude is the memory of heart and in carrying out this seminar work. persistent inspiration, unflinching support and encouragement of countless persons have served as the driving force.

I am completely indebted to my guide Dr. (Mrs.) Shashi, Assistant Professor, Department of Chemical Engineering, Indian Institute of Technology Roorkee, Roorkee without whom this concept of working in the area of the "Mathematical Analysis on catalytic dehydrogenation of cyclohexane using microporous membrane" would not have taken birth in my mind. I would like to sincerely acknowledge her valuable guidance, relentless support, discerning thoughts and load of inspiration that led forward to develop deeper into the issue.

I am highly thankful to Dr. Shrichand, Professor and Head, Department of Chemical Engineering, Indian Institute of Technology Roorkee. Roorkee for providing me all the necessary facilities in the department to complete this work.

I wish to express my profound sense of gratitude to Dr. Surendra Kumar, Professor, Department of Chemical Engineering, Indian Institute of Technology Roorkee. Roorkee for his constructive suggestions, moral support and constant encouragement during the course of this work.

I would also like to thank my family for their continuous support and blessings throughout my education.

I would like to especially thank Ms. Tripta Garg for her kind cooperation and pleasant manner. Special thanks are due to Sh. Ziaur Rehman and Sh. Mange Ram of Reaction Engineering Research (RER) Lab, Sh. Akhilesh Sharma, Sh Narendra Kumar and Sh. Raj Kumar of CAD center of the Department.

I am thankful to my friends Vishal, Saurabh, Mohit, Shweta, Shilpi. Vaani for their love, support and constant motivation.

Tanvi

Place: Roorkee
(TANVI GABA)
Date:
I.I.T. Roorkee

CONTENTS

ABSTRACT i

ACKNOWLEDGMENT ii

CONTENTS iii

LIST OF FIGURES vii

LIST OF TABLES xiii

NOMENCLATURE xv

1. **CHAPTER I** 1
   - 1.0. Introduction 1
   - 1.1. Membrane Technology 3
     - 1.1.1. Functions of Membrane 4
   - 1.2. Classification of Membranes 7
     - 1.2.1. Organic Membranes 7
       - 1.2.1.1. Polymeric Membranes 7
     - 1.2.2. Inorganic Membranes 7
   - 1.3. Gas Separation in Inorganic Membranes 9
   - 1.4. Zeolite Membranes 12
     - 1.4.1. Uses of Zeolite Membranes 14
     - 1.4.2. Faujasite type Zeolite Membrane 15
   - 1.5. Membrane Reactor Concepts 15
     - 1.5.1. Membrane Reactor Configuration 19
   - 1.6. Permeation Mechanism 23

2. **CHAPTER II – LITERATURE REVIEW** 25
   - 2.0. Introduction 25
   - 2.1. Experimental Reviews 25
   - 2.2. Modeling Reviews 30

3. **CHAPTER III – MODEL DEVELOPMENT** 51
   - 3.0. Introduction 51
   - 3.1. Kinetic Models 52

3.1.1. Reaction 52
3.1.2. Rate Expression 52
3.2. Catalyst 52
3.3. Membrane 52
3.4. Assumptions 53
3.5. Choice of Control Volume 53
3.6. Material Balance 54
3.7. Mathematical Model 56
3.7.1. Set of Mathematical Equations 56
3.7.2. Boundary Conditions 56
3.7.3. Constitutive Relationship 56
3.8. Solution 59

4. **CHAPTER IV – RESULTS AND DISCUSSIONS** **61**
4.0. Introduction 61
4.1. Feed without Hydrogen 61
4.1.1. Model Validation 61
4.1.2. Effect of Temperature on Conversion of Cyclohexane 61
4.1.2.1. Conventional Fixed Bed 61
4.1.2.2. Full length Membrane Reactor 62
4.1.2.3. Hybrid Reactor 62
4.1.3. Variation of Molar Flow Rate along the Length of Reactor 69
4.1.3.1. Full length Membrane Reactor 69
4.1.3.2. Hybrid Reactor 91
4.2. Feed with Hydrogen 92
4.2.1. Effect of Temperature on Conversion of Cyclohexane 105
4.2.2. Variation of Molar Flow Rate along the Length of Reactor 105
4.2.2.1. Full length Membrane Reactor 105
4.2.2.2. Hybrid Reactor 106

5. CHAPTER V – CONCLUSIONS AND RECOMMENDATIONS 143

5.1. Conclusions 143

5.2. Recommendations 144

REFERNCES 145

LIST OF FIGURES

Fig. No.	Title	Page No.
Fig 1.1	Schematic of possible functions of membrane in a reactor.	5
Fig. 1.2	Mechanism of gas transport through microporous membranes.	13
Fig. 1.3	The structure of Faujasite	16
Fig 1.4	Classification of membrane reactor concepts acc to membrane functions	17
Fig. 1.5	The permeation module	20
Fig. 1.6(a)	Full length membrane reactor with reactants fed in the tube side	21
Fig. 1.6(b)	Full length membrane reactor with reactants fed in the shell side	21
Fig.1.6(c)	Hybrid membrane reactor with reactants fed in the shell side	21
Fig.3.1	Schematic diagram of a membrane reactor	51
Fig.3.2	Selection of control volume for membrane reactor	54
Fig.4.1	Comparison of percent conversion of cyclohexane at various temperatures with experiment values	63
Fig.4.2	Variation of percent conversion of cyclohexane with temperature for fixed bed reactor with no H_2 in the feed side	65
Fig.4.3	Variation of percent conversion of cyclohexane with temperature for membrane reactor with no H_2 in the feed side	67

Fig. No.	Title	Page No.
Fig.4.4	Variation of percent conversion of cyclohexane along the length of hybrid reactor at 448 K with no H_2 in the feed	73
Fig.4.5	Variation of percent conversion of cyclohexane along the length of hybrid reactor at 473 K with no H_2 in the feed	75
Fig.4.6	Variation of percent conversion of cyclohexane along the length of hybrid reactor at 490 K with no H_2 in the feed	77
Fig.4.7	Variation in the molar flow rate along the length of the membrane reactor in the reaction side at 448 K with no H_2 in the feed	79
Fig.4.8	Variation in the molar flow rate along the length of the membrane reactor in the reaction side at 473 K with no H_2 in the feed	81
Fig.4.9	Variation in the molar flow rate along the length of the membrane reactor in the reaction side at 490 K with no H_2 in the feed	83
Fig.4.10	Variation in the molar flow rate along the length of the membrane reactor in the permeate side at 448 K with no H_2 in the feed	85
Fig.4.11	Variation in the molar flow rate along the length of the membrane reactor in the permeate side at 473 K with no H_2 in the feed	87
Fig.4.12	Variation in the molar flow rate along the length of the membrane reactor in the permeate side at 490 K with no H_2 in the feed	89

Fig. No.	Title	Page No.
Fig 4.13	Variation in the molar flow rate along the length of the hybrid reactor in the reaction side at 448 K with no H_2 in the feed	93
Fig.4.14	Variation in the molar flow rate along the length of the hybrid reactor in the reaction side at 473 K with no H_2 in the feed	95
Fig.4.15	Variation in the molar flow rate along the length of the hybrid reactor in the reaction side at 490 K with no H_2 in the feed	97
Fig.4.16	Variation in the molar flow rate along the length of the hybrid reactor in the permeate side at 448 K with no H_2 in the feed	99
Fig.4.17	Variation in the molar flow rate along the length of the hybrid reactor in the permeate side at 473 K with no H_2 in the feed	101
Fig.4.18	Variation in the molar flow rate along the length of the hybrid reactor in the permeate side at 490 K with no H_2 in the feed	103
Fig.4.19	Variation of percent conversion of cyclohexane with temperature for fixed bed reactor with $H_2 = 0.02$ mol % in the feed side	107
Fig.4.20	Variation of percent conversion of cyclohexane with temperature for membrane reactor with H_2=.02 mol % in the feed side	109
Fig.4.21	Variation of percent conversion of cyclohexane along the length of hybrid reactor at 448 K with $H_2 = 0.02$ mol % in the feed	111

Fig. No.	Title	Page No.
Fig.4.22	Variation of percent conversion of cyclohexane along the length of hybrid reactor at 473 K with H_2 = 0.02 mol % in the feed	113
Fig.4.23	Variation of percent conversion of cyclohexane along the length of hybrid reactor at 490 K with H_2 = 0.02 mol % in the feed	115
Fig.4.24	Variation in the molar flow rate along the length of the membrane reactor in the reaction side at 448 K with H_2 = 0.02 mol % in the feed	117
Fig.4.25	Variation in the molar flow rate along the length of the membrane reactor in the reaction side at 473 K with H_2 = 0.02 mol % in the feed	119
Fig.4.26	Variation in the molar flow rate along the length of the membrane reactor in the reaction side at 490 K with H_2 = 0.02 mol % in the feed	121
Fig.4.27	Variation in the molar flow rate along the length of the membrane reactor in the permeate side at 448 K with H_2 = 0.02 mol % in the feed	123
Fig.4.28	Variation in the molar flow rate along the length of the membrane reactor in the permeate side at 473 K with H_2 = 0.02 mol % in the feed	125
Fig.4.29	Variation in the molar flow rate along the length of the membrane reactor in the permeate side at 490 K with H_2 = 0.02 mol % in the feed	127
Fig.4.30	Variation in the molar flow rate along the length of the membrane reactor in the permeate side at 490 K with H_2 = 0.02 mol % in the feed	129

Fig. No.	Title	Page No.
Fig.4.31	Variation in the molar flow rate along the length of the hybrid reactor in the reaction side at 473 K with H_2 = 0.02 mol % in the feed	131
Fig.4.32	Variation in the molar flow rate along the length of the hybrid reactor in the reaction side at 490 K with H_2 = 0.02 mol % in the feed	133
Fig.4.33	Variation in the molar flow rate along the length of the hybrid reactor in the permeate side at 448 K with H_2 = 0.02 mol % in the feed	135
Fig.4.34	Variation in the molar flow rate along the length of the hybrid reactor in the permeate side at 473 K with H_2 = 0.02 mol % in the feed	137
Fig.4.35	Variation in the molar flow rate along the length of the hybrid reactor in the permeate side at 490 K with H_2 = 0.02 mol % in the feed	139

LIST OF TABLES

Table No.	Title	Page No.
Table 3.1.	Operating conditions	57
Table 4.1	Permeances of components through FAU type zeolite membrane at different temperatures	71
Table 4.2	Yield of hydrogen at different temperatures	71

NOMENCLATURE

$F_{i,F}$	Molar flow rate of i^{th} component in the feed side	(mol s^{-1})
$F_{i,F,0}$	Molar flow rate of i^{th} component in feed side at the inlet of the reactor	(mol s^{-1})
$F_{i,P}$	Molar flow rate of i^{th} component in the permeate side	(mol s^{-1})
$F_{i,P,0}$	Molar flow rate of i^{th} component in permeate side at the inlet of the reactor	(mol s^{-1})
J_i	Flux of i^{th} component	(mol m^{-2} s^{-1})
k	Reaction rate constant	(mol m^{-3} Pa^{-1} s^{-1})
K_B	Adsorption equilibrium constant of benzene	(Pa^{-1})
K_P	Equilibrium constant	(Pa^{3})
L	Length of reactor	(m)
p_i	Partial pressure of i^{th} component in feed side	(Pa)
p_C	Partial pressure of cyclohexane in feed side	(Pa)
p_H	Partial pressure of hydrogen in feed side	(Pa)
p_B	Partial pressure of benzene in feed side	(Pa)
P_F	Total feed pressure	(Pa)
P_P	Total permeate pressure	(Pa)
Q_i	Permeance of i^{th} component	(mol m^{-2} s^{-1} Pa^{-1})
r_C	Dehydrogenation rate of cyclohexane	(mol m^{-3} s^{-1})
r_3	Inner radius of shell	(m)
r_2	Outer radius of tube	(m)
T	Temperature	(K)
x_i	Mole fraction of i^{th} component in the feed side	(-)
X_C	Conversion of cyclohexane	(-)
y_i	Mole fraction of i^{th} component in the feed side	(-)
z	Distance from the inlet of reactor	(m)
	Greek letter	
ν_i	Stoichiometric coefficient of i^{th} component	(-)

Subscripts

Ar	Argon
B	Benzene
C	Cyclohexane
H	Hydrogen
i	ith Component

CHAPTER I

INTRODUCTION

From the viewpoint of preventing global warming due to the release of gases such as carbon dioxide, fossil-fuel is going to be outplaced by hydrogen which is expected as the third generation energy source. Further, to promote energy saving by using energy effectively and reducing the release of carbon dioxide, cogeneration of electric power facilities has been attracting public attention. Electricity is the most well-known energy carrier. We use electricity to move the energy in coal, uranium, and other energy sources from power plants to homes and businesses. We also use electricity to move the energy in flowing water from hydropower dams to consumers. It is much easier to use electricity than the energy sources themselves. Like electricity, hydrogen is an energy carrier and must be produced from another substance. Hydrogen is not widely used today but it has great potential as an energy carrier in the future. Hydrogen can be produced from a variety of resources (water, fossil fuels, biomass) and is a byproduct of other chemical processes. Unlike electricity, large quantities of hydrogen can be easily stored to be used in the future. Hydrogen can also be used in places where it's hard to use electricity. Hydrogen can store the energy until it's needed and can be moved to where it's needed.

Recently, fuel cell power generation systems which use hydrogen for power generation have been rapidly researched and developed to be used widely in various power generation fields such as power generation facilities for cars, homes, automatic vending machines, portable devices and so on. A fuel cell generates electricity and thermal energy simultaneously by reacting hydrogen and oxygen into water. These electric and thermal energies are used for hot-water supply and air-conditioning. So, a fuel cell is available as a distributed power supply for home use. Development of internal combustion engines such as micro-turbines and micro-engines besides fuel cells have also been under development.

Hydrogen is shown to be the future fuel from the point of view of human fuel evolution. The fuel evolution experienced the history from coal through petroleum to natural gas following the direction of increasing the content of hydrogen, therefore, it must finally reach the destination of pure hydrogen. Every step of the fuel evolution initiated a progress in human civilization, therefore, the large-scale utilization of hydrogen fuel will certainly elevate the human civilization to a higher horizon. Hydrogen is the cleanest fuel, and has a heating value three times higher than petroleum. However, it is not a natural source, but a man-made fuel; therefore, hydrogen bears a manufacture cost, which made it costing three times higher than the petroleum products. Therefore, any method of storage is not allowed to considerably increase the cost of hydrogen fuel. There are still problems in the realization of the renewed hydrogen from water, but the market supply and the cost of hydrogen do not constitute the bottleneck of hydrogen vehicles today although the hydrogen used presently may not be renewed. There is only one bottleneck for the hydrogen vehicle program, the storage of hydrogen. Just think about as large as 49 m^3 that 4 kg hydrogen occupies, which is required for a practical driving distance, one can imagine how difficult is the job of hydrogen storage. Storage basically implies to reduce the enormous volume of the hydrogen gas. The reversibility of the hydrogen uptake and release excludes all covalent hydrocarbon compounds as hydrogen carriers because the hydrogen is only released from the compounds if being heated to temperatures above 800 ^{0}C. The methods of interest include compression, liquefaction, physisorption, metallic hydrides, complex hydrides and organic hydrides[28].

Storage of hydrogen in a pressurized cylinder is not likely to be applied in the future due to the low density and high cost at high pressures. Liquid hydrogen could be applied if the unit cost becomes comparable with gasoline, yet the inevitable boiling-off of liquid might be of concern. Metallic hydrides of heavy metals cannot get rid of the constraint of gravimetric density, and the relatively high temperature of ab- and desorption and the large amount of energy required for releasing hydrogen remain the barriers for the light metal hydrides. Physisorption of hydrogen on nanotubes/nanofibers of any materials seems hopeless for enhancing the hydrogen density due to the small surface area. To solve such problems, an organic hydride system which uses hydrocarbons such as cyclohexane and decarin has attracted a great deal of public attention as-a hydrogen storage system which excels in safety, transportability, storage ability, and cost-reduction. These hydrocarbons are liquid at ordinary temperature and easy to be transported. For example, benzene and cyclohexane are cyclic hydrocarbons of the same number of carbons. However, benzene is an unsaturated hydrocarbon having double bonds of carbons but cyclohexane is a saturated hydrocarbon having no double bond. Cyclohexane is obtained by hydrogenation of benzene and benzene is obtained by dehydrogenation of cyclohexane. In other words, hydrogenation and dehydrogenation of hydrocarbon enable storage and supply of hydrogen. Since there is no requirement of heavy containers, such as in the case of high-pressure cylinders needed for carrying liquid hydrogen, the effective content of hydrogen on the weight basis for cycloalkane systems is considerably higher. Also due to the endothermic nature of the dehydrogenation of cyclic hydrocarbons, chemical equilibrium is favored at higher temperature; the reactions are performed at high temperature under steady-state operations in gas phase.

The dehydrogenation of cyclohexane is represented as:

$$C_6H_{12} \leftrightarrow C_6H_6 + 3H_2 \qquad (1.1)$$

Basically this reaction is endothermic reversible reaction and so attainable conversion under ordinary condition is limited by thermodynamics. The higher conversion can be achieved if one of the reaction products is selectively removed from the reactant through a separation unit such as membrane. The two most important, and often the most expensive, steps in a chemical process are usually the chemical reactor and the separation of the product stream. Both the process economics and the efficient use of natural resources could be improved by the combination of these two operations into a single unit operation, leading to potential savings in energy and reactant consumption and reduced by-product formation. One promising way to accomplish this combination is the use of membrane separation and catalytic reaction together in a multifunctional reactor. Until relatively recently, the use of membranes was restricted to low temperature processes with mild chemical environments, which could be tolerated by polymeric materials but with the invention of inorganic membranes they can be fabricated to high temperature processes.

1.1 Membrane technology

The energy consumption of the chemical industry accounts for about one third of the total consumption by all the manufacturing industries. It is estimated that more than a half of the energy for the chemical industry is used for separation or concentration of substances. Separation or concentration by membranes is known to require less energy about 70% according to estimation than distillation. Membranes may also have additional functions such as transportation, sensing or reaction. Membranes can, therefore, not only minimize the energy consumption of separation and concentration processes in chemical plants, but also have a great potential to provide a simple, cost effective platform for complicated multistage chemical reactions, leading to reduced energy consumption and substance-related risks including that of exposure to toxic substances or explosion.

1.1.1 Functions of membrane

A given membrane under appropriate circumstances can perform more than one generic function. The introduction of another membrane into the reactor can increase the number of generic membrane functions in the reactor or achieve the same generic membrane function. Figure 1.1 also indicates other activities concurrently taking place in the so-called nonreactor (or permeate) side of the membrane as well as in the reactor side of the membrane. A list of the generic membrane functions performed by a membrane or two in a reactor are as below:

- Separation of products from the reaction mixture
- Separation of a reactant from a mixed stream for introduction into the reactor
- Controlled addition of one reactant or two reactants
- Nondispersive phase contacting (with reaction at the phase interface or in the bulk phases)
- Segregation of a catalyst (and cofactor) in a reactor
- Immobilization of a catalyst in (or on) a membrane
- Membrane is the catalyst
- Membrane is the reactor
- Solid-electrolyte membrane supports the electrodes, conducts ions, and achieves the reactions on its surfaces
- Transfer of heat
- Immobilizing the liquid reaction medium

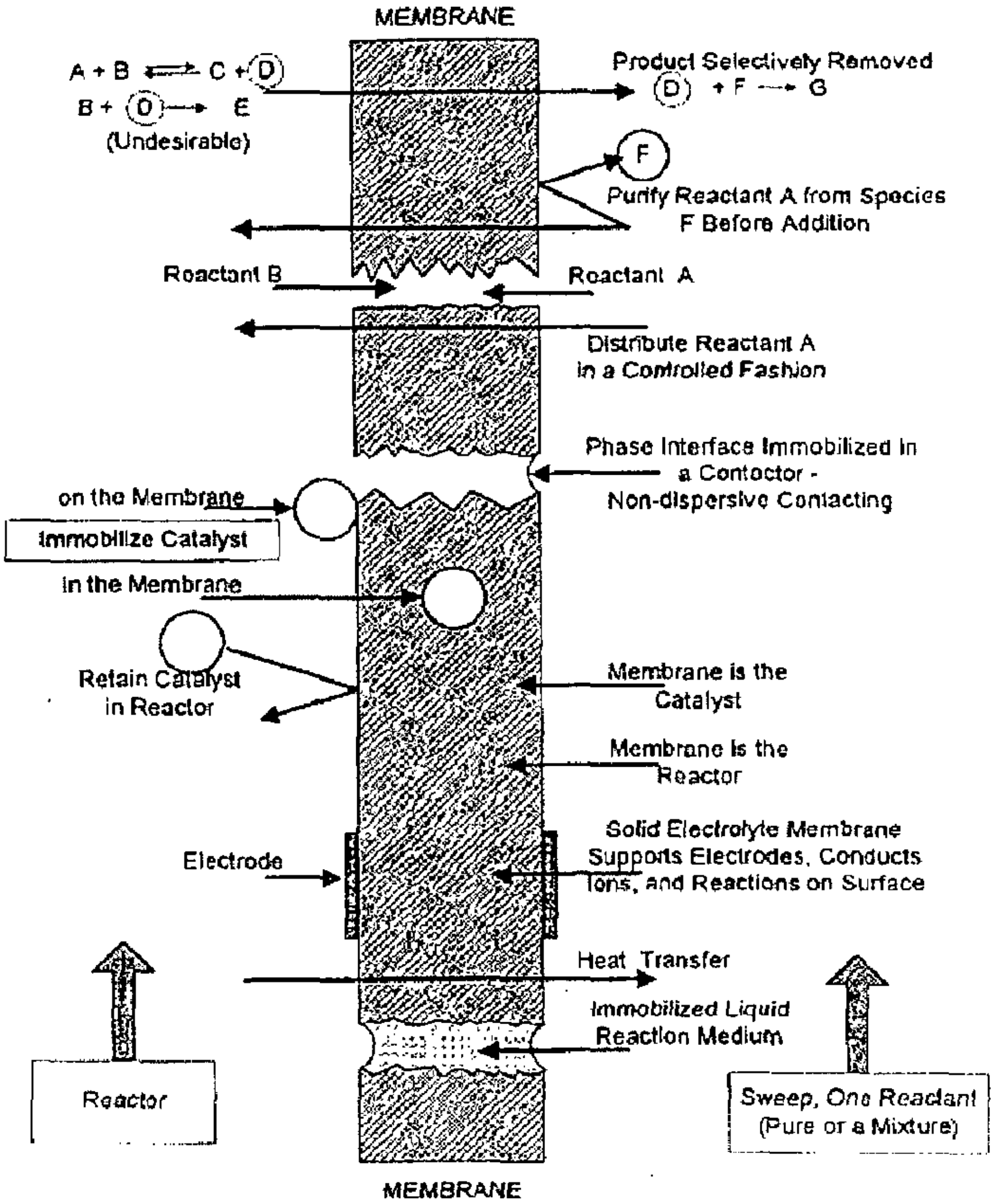
MEMBRANE
A + B ⇌ C + D
B + D → E
(Undesirable)
Product Selectively Removed
D + F → G
F
Purify Reactant A from Species F Before Addition
Reactant B
Reactant A
Distribute Reactant A in a Controlled Fashion
Phase Interface Immobilized in a Contactor - Non-dispersive Contacting
on the Membrane
Immobilize Catalyst
in the Membrane
Retain Catalyst in Reactor
Membrane is the Catalyst
Membrane is the Reactor
Electrode
Solid Electrolyte Membrane Supports Electrodes, Conducts Ions, and Reactions on Surface
Heat Transfer
Immobilized Liquid Reaction Medium
Reactor
Sweep, One Reactant (Pure or a Mixture)
MEMBRANE

Fig:1.1 Schematic of possible functions of membrane in a reactor[23].

1.2 Classification of membranes

Membranes can be classified as organic membranes and inorganic membranes.

1.2.1 Organic membranes

Organic membranes are mainly polymeric type membranes

1.2.1.1 Polymeric membranes

In polymeric membranes, membranes can take the form of polymeric interphases that also selectively transfer certain chemical species over others. There are several mechanisms that could be deployed in their functioning. Knudsen diffusion, solution-diffusion are prominent mechanisms. Polymeric membranes are of particular importance in gas separation applications.

ADVANTAGES

- High permselectivity
- Fast permeation
- Well-developed technology to produce thin polymeric membranes already exists.
- Cheaper than inorganic membranes

DISADVANTAGES

- Limited resistance to temperature
- Limited resistance to harsh environments
- Does not work in corrosive environment.

1.2.2 Inorganic membranes

Recent advances in inorganic materials have expanded the range of membrane use, to include high temperature and chemically harsh environments. Inorganic membranes are versatile. They can operate at elevated temperatures, with metal membranes stable at temperatures ranging from 500-800° C and with many ceramic membranes usable at over 1000° C. They are also much more resistant to chemical attack. Because of the wide variety of materials that may be used in the fabrication of our inorganic membranes, resistance to corrosive liquids and gases, even at elevated temperatures, can be realized. Inorganic membranes compete with organic membranes for commercial use. In many of the harsh operational environments listed above, organic membranes will not perform well, or will not survive at all. For these environments, only inorganic membranes offer needed solutions. Few advantages and disadvantages of inorganic membranes are listed below:

ADVANTAGES[4]

- Long term stability at high temperatures
- Resistance to harsh environments
- Resistance to high pressure drops
- Inertness to microbial degradation
- Easy cleanability after fouling
- Easy catalytic activation

DISADVANTAGES

- High capital costs
- Brittleness
- Low membrane surface per module volume
- Difficulty in achieving high selectivity in large scale microporous membranes
- Generally low permeability of highly selective membranes at medium temperatures
- Difficult membrane-to-module sealing at high temperatures

The materials of membrane construction can be classified as either dense or porous. Dense materials include palladium membranes that are semipermeable to hydrogen, and solid oxide electrolyte dense membranes such as modified zirconias and perovskites, which have reasonably high oxygen permeation rates at high temperatures. Porous inorganic membranes[8] can be divided into macroporous ($d_p > 50$ nm), mesoporous ($50 > d_p > 2$ nm) and microporous ($d_p < 2$ nm). Macroporous materials, such as "-alumina membranes, provide no separative function, but may be used to support layers of smaller pore size to form composite membranes, or in applications where a well-controlled reactive interface is required. Mesoporous materials for membranes have generally had pore sizes in the 4 - 5 nm range, so that permeation is governed by Knudsen diffusion. Typical materials are Vycor glass, and composite membranes of γ-alumina supported on successively larger-pore layers of α-alumina support. Microporous membranes offer the potential for molecular sieving effects, with very high separation factors, and materials such as carbon molecular sieves, porous silicas and zeolites have been studied. The most active areas of development for membrane materials are currently synthesis of supported thin films such as supported Pd films on porous aluminas or on porous stainless steel, and supported zeolite films.

1.3 Gas separation in inorganic membranes [27]

The performance of membranes as chemical reactors is generally dependent on their gas separation capability. The mechanisms involved in the separation of gases are widely different for dense and porous membranes.

Dense membranes

The effectiveness of gas separation by dense membranes of palladium and other metals is dependent on two opposing factors: permeability and selectivity. The dense membranes have high selectivities, but low permeabilities. The gases are dissolved in dense films depending on the solubility, transport occurs because of a concentration gradient and dissolution takes place on the other side of the membrane. The permeability is low because of the very low diffusion coefficients for gases in solids.

The gas separation in solid electrolytes is dependent on the ionic activity of the membrane material. The application of a thin film of a dense membrane, metal or solid oxide, on a porous ceramic support can drastically decrease the thickness of the membrane. The permeability is inversely proportional to the thickness and hence the reduction in the thickness improves the permeability of the dense membranes. This enhances the prospects for the application of these membranes in reactor/ separator systems.

Porous membranes

Five different mechanisms may be involved in the transport of gases across a porous membrane: Knudsen diffusion, surface diffusion, capillary condensation, laminar flow and molecular sieving. The contribution of the different mechanisms are dependent on the properties of the membranes and the gases as well as on the operating conditions of temperature and pressure.

Knudsen Diffusion

Knudsen diffusion occurs when the mean free path is relatively long compared to the pore size, so the molecules collide frequently with the pore wall. Knudsen diffusion is dominant for pores that range in diameter between 2 and 50 nm. Knudsen diffusion is described by the Einstein relation as follows:

$$D_s(c) = \lim_{t\to\infty} \frac{1}{6Nt}\left\langle \sum_{i=1}^{N} \left| \mathrm{r}_i(t) - \mathrm{r}_i(0)\right|^2 \right\rangle$$

where D_s is the self-diffusion coefficient, which depends on the concentration c, t is time, N is the total number of particles in the system, and r_i is the position vector of particle i.

Surface Diffusion

Surface diffusion is also used to explain a type of pore diffusion in which solutes adsorb on the surface of the pore and hop from one site to another through interactions between the surface and molecules.

Capillary condensation

Capillary condensation is known to occur when multilayer adsorption from adsorbate molecules proceeds to the point where pore spaces are filled with condensed liquid and separated from the gas phase by menisci.

Molecular (Fickian) Diffusion

Molecular, or transport, diffusion occurs when the mean free path is relatively short compared to the pore size, and is described by Fick's law as follows

$$j = -D_t(c)\nabla c$$

where j is the mass flux, D_t is the transport diffusion coefficient (or Fickian diffusion coefficient), and Δc is the concentration gradient. The transport diffusivity relates the macroscopic flux of molecules in a system to a driving force in the concentration. This diffusion mode is applicable to Brownian motion, where the movement of each particle is random and not dependent on its previous motion.

Viscous Flow

Viscous flow is the flow of a gas through a channel under conditions where the mean free path is small in comparison with the transverse section of the channel, so the flow characteristics are determined mainly by collisions between the gas molecules.

In a commercial ceramic membrane with pore sizes greater than 4 nm, Knudsen diffusion is likely to be the dominant mechanism of gas transport at low pressures and elevated temperatures. Capillary condensation and surface diffusion are unlikely to exist at elevated temperatures in membranes with pore sizes in the range of 2 nm. Molecular sieving does not take place, because the pore sizes are much larger than the gas molecules. The contribution of viscous flow, resulting from a pressure difference across the pores, will be quite small and even if it is present, it does not contribute to the separation process. This leaves Knudsen diffusion as the only transport mechanism contributing to the separation of various components in a gaseous mixture at elevated temperatures in a porous membrane. Gas permeation by Knudsen diffusion varies inversely with the square root of the molecular weight. The ideal separation factor for binary gas mixtures therefore equals the inverse of the square root of the ratio of the molecular masses. The actual separation factor, however, is found to be smaller, this being attributed to back diffusion, nonseparative diffusion, concentration polarization on the feed or permeate side and/or the occurrence of viscous flow (in large pores). The transport of gases through porous membranes by Knudsen diffusion alone imposes a severe constraint on the selectivity in a reaction/ separation system.

1.4 Zeolite membranes

Zeolite membranes form one of the newest branches of the inorganic membrane field. Unlike the most microporous metal oxides (e.g., SiO_2, Al_2O_3 and TiO_2) that have tortuous pore channels, zeolites are microporous aluminosilicate materials that have a well-defined, uniform pore system of molecular dimensions (enabling shape or size selective catalysis or separation) due to their porous crystalline structure. Zeolites are relatively stable at high temperatures, can be acidic or basic in nature and can exhibit hydrophilic or organophilic properties. These molecular sieves can be tailor made for a specific application through ion exchange, dealumination–realumination, isomorphous substitution and insertion of catalytically active guests such as transition-metal ions, complexes, basic alkali metal or metal oxide clusters. In addition to their thermal and chemical stability, make zeolites ideally suited for the combination of separation and reaction under process conditions.

Zeolitic membranes [8] can be classified as either symmetric membranes (self-supported) or asymmetric membranes (supported). In fact, the synthesis of two different kinds of zeolite membrane has been reported self-supported membrane and composite membrane. The first type of membrane is also constituted by a pure zeolitic phase; instead, a zeolitic thin layer formed on a support composes the second type.

Generally, the preparation of self-supported zeolitic films introduces some drawbacks related to the dimension, to the lack of homogeneous thickness and finally to the mechanical stability of the same membrane. Insofar, zeolitic films are synthesized in presence of momentary support (removed therefore after the preparation) or permanent (to form zeolite composite membranes). In order to prepare these membranes, zeolite crystals need to grow on porous substrates for forming a continuous thin film, having the zeolitic pores as the only available

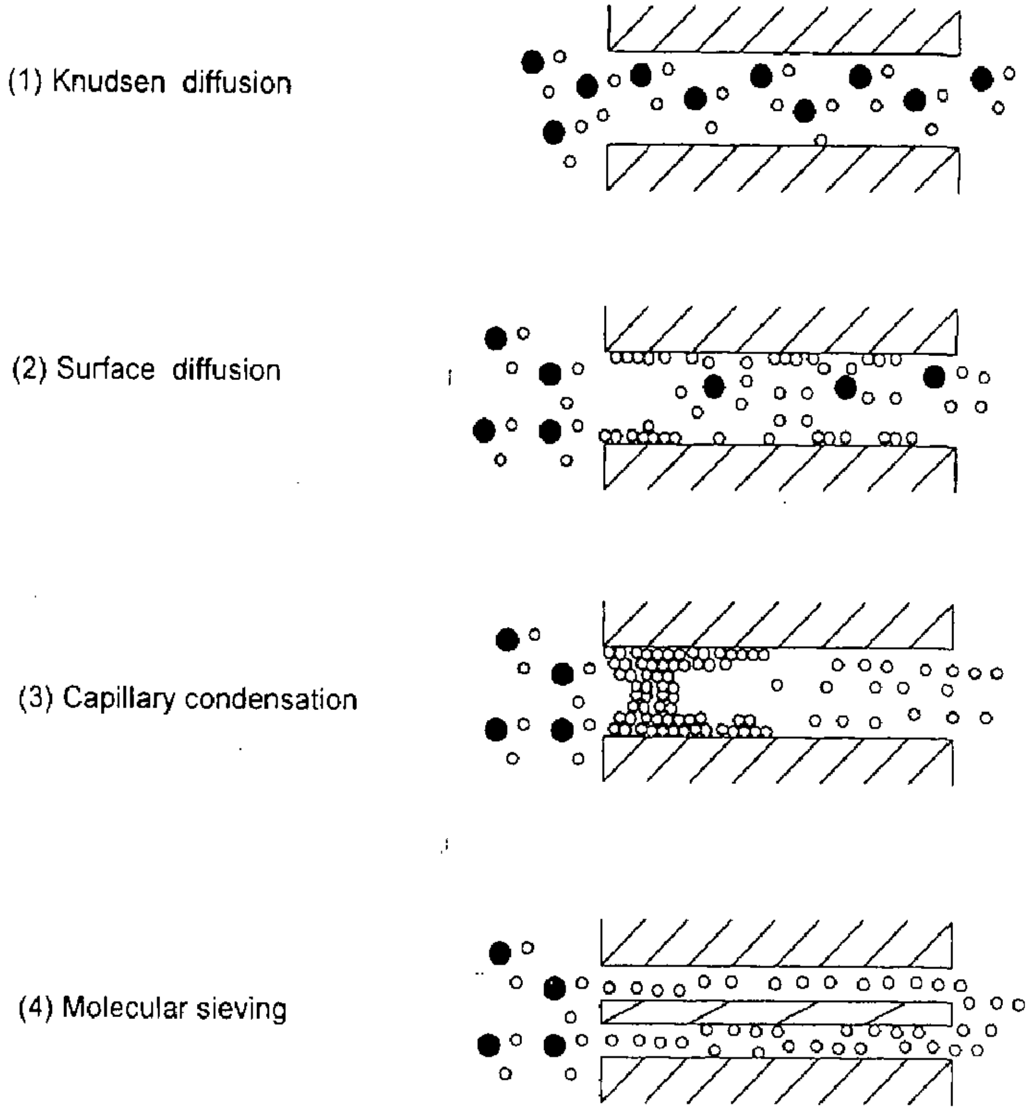

Fig:1.2 Mechanism of gas transport through microporous membranes[10].

pathways for gas or reactive molecules transport These defect-free composite membranes can be highly selective zeolite catalytic membranes. The term defects denote trans-membrane pathways larger than the intracrystalline zeolite pores. Following the IUPAC definitions and corresponding sizes, the defects in zeolite membranes can be classified into macro-defects, meso-defects, and micro-defects. Macro-defects are usually cracks and pinholes (with size >500 Å), while meso-defects (with <500Å and >20Å size) and micro-defects (with size <20Å) are primarily formed by non-perfect intergrowth between zeolite crystals in hydrothermal synthesis. The larger defects can be eliminated by repeated crystallization. Elimination of small defects may be possible by chemical vapor deposition of silica via reaction with a silicon alkoxide or other silylation agents. These treatments involve reduction of the pore openings on the external surface of the crystals. A prerequisite for the optimization of the applications as catalytic and filter membranes is the ability to prepare very thin (<1.5 mm) and oriented layers. These objectives can be reached only through an accurate knowledge of the specific conditions of preparation of the membranes.

1.4.1 Uses of Zeolite membranes

- Zeolite membranes have been used for the separation of vapor mixtures containing compounds with close boiling-points or with similar molecular weights; mixtures of alcohols of hydrocarbons and non-condensable gases; and mixtures of non-condensable gases (e.g., H_2/CH_4, CO_2/CH_4, CO_2/N_2, O_2/N_2 and CO/air).
- Zeolitic membranes find important application in catalytic membrane reactors to improve the yield and selectivity of reactions that are limited by equilibrium. The membrane can allow two reactions in the same reactor, in which case it separates the two reactions, so that only one component (one of the products of the first reaction) can permeate through the membrane to then function as a reagent for the second reaction.
- Zeolite interfaces are excellent candidates for micro-scale applications because of their high specificity in adsorption and catalysis, on account of which zeolites have been considered as the inorganic counterparts of enzymes
- The specificity of zeolites has been used on a variety of sensors, both reactive and non-reactive. Thus, zeolites have been employed to improve conventional chemical electrodes by modifying their surface
- The hydrophilic zeolite A membranes are especially recommended for the separation of water by pervaporation or steam permeation

Most of the applications proposed to date for zeolite membranes and films belong to the realm of large scale processing, often involving the production of commodities. None of these has yet materialized in industry, which is probably not only due to the high price of zeolite membranes but also due to a variety of reasons such as the lack of suitable methods for mass production for most types of zeolite membranes, and the perceived technological risks that are common to any novel industrial development. All of these hurdles would be considerably alleviated by developing zeolite membranes for small- and micro-scale applications, thereby facilitating industrial implementation of membrane technology in the near future.

1.4.2 Faujasite type zeolite membranes

Three different zeolite structures are: faujasite[FAU] group zeolites, zeolite A[LTA] and ZSM-5[MFI]. All of them have found important applications and therefore synthesized in an industrial scale. Zeolite X and Y are the synthetic analogues to the natural faujasite. The difference between the two is the Si/Al ratio which is 1-1.5 and 1.5-3 in zeolite X and Y, respectively. Figure 1.3 shows the structure of faujasite type of zeolite membrane.

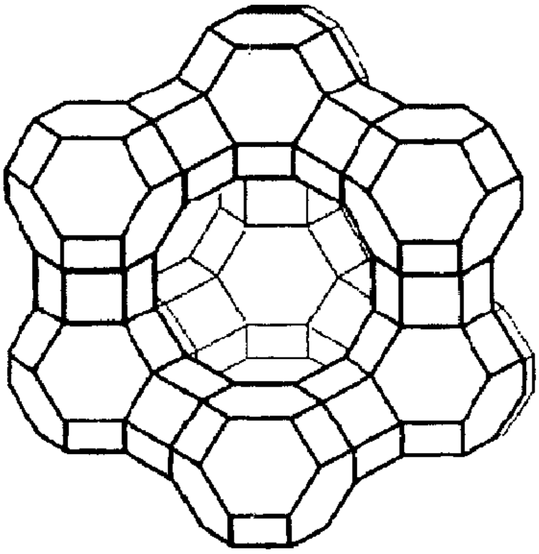

Fig:1.3: The structure of faujasite.

In membrane applications, a high flux of the permeating species increases the efficiency. A thin membrane offers less resistance and is therefore desirable. Recently, FAU-type zeolite (NaX, NaY) membranes have been applied to the separation of hydrocarbon mixtures. Jeong et al. [14-16] reported on the synthesis of an NaY-type zeolite membrane on a porous α-Al_2O_3 support tube using a hydrothermal synthesis. The separation properties of the resulting membrane for binary mixtures of benzene and cyclohexane were investigated, and a separation factor of 107 was found at 373 K. The high separation factor can be attributed to the selective adsorption of benzene and the blocking of cyclohexane by benzene, adsorbed in the pores. Therefore, benzene selective FAU-type zeolite membranes would be expected to be useful for the dehydrogenation of cyclohexane in a membrane reactor. To our knowledge, it may be the first contribution of a zeolite membrane for this purpose.

1.5 Membrane reactor concepts

According to the IUPAC definition a membrane reactor is a device that combines a membrane-based separation process with a chemical reaction step in one unit. Various possibilities exist for such a combination. The most widely used concept is the selective removal of products from the reaction zone (Fig. 1.4a), which is applied first of all to equilibrium limited reactions to increase the yield beyond the corresponding equilibrium value, or, generally speaking, to repress undesired secondary reactions of the products. In a different approach only particular reactants are supplied selectively via a membrane to the reaction zone (Fig. 1.4b), e.g. to establish an optimum concentration profile along the reactor. A third concept refers to a membrane that creates a well-defined reaction interface (or region) between two reactant streams (Fig. 1.4c).

The mass transport across a membrane can be permselective if only some components of a mixed stream permeate through the membrane (Fig. 1.4a and b) or non-permselective if all species permeate at comparable rates (Fig. 1.4c). Permselective transport is found first of all in dense membranes. It is governed by a solution-diffusion mechanism. Non-permselective transport normally occurs in macro- and mesoporous membranes. In the latter Knudsen diffusion is often the dominating transport mechanism. Microporous membranes represent a bit of both:
dominating transport mechanism. Microporous membranes represent a bit of both:
permselective and non-permselective transport is possible depending on the size of the permeating molecules in view of the pore size of the membrane as well as on the chemical nature of the permeating molecules and the membrane material. When the membrane reactor is used for carrying out a catalysed reaction the

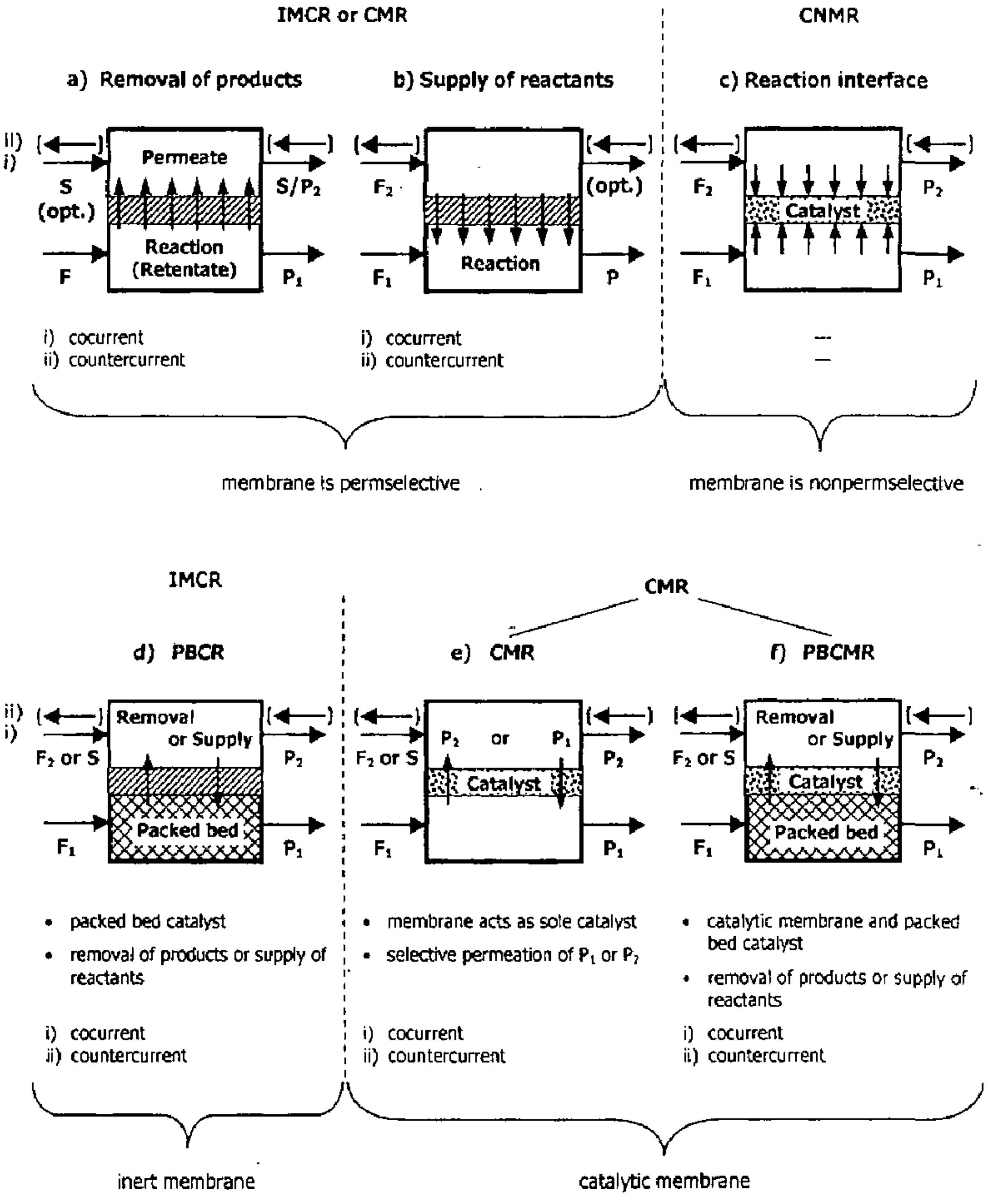
IMCR or CMR
CNMR
a) Removal of products
b) Supply of reactants
c) Reaction interface
ii)
i)
S
(opt.)
Permeate
Reaction
(Retentate)
F
S/P₂
P₁
F₂
Reaction
F₁
(opt.)
P
F₂
Catalyst
F₁
P₂
P₁
i) cocurrent
ii) countercurrent
i) cocurrent
ii) countercurrent
—
—
membrane is permselective
membrane is nonpermselective
IMCR
CMR
d) PBCR
e) CMR
f) PBCMR
ii)
i)
Removal
or Supply
F₂ or S
P₂
Packed bed
F₁
P₁
F₂ or S
P₂ or P₁
Catalyst
F₁
P₂
P₁
F₂ or S
Removal
or Supply
Catalyst
Packed bed
F₁
P₂
P₁
• packed bed catalyst
• removal of products or supply of reactants
i) cocurrent
ii) countercurrent
• membrane acts as sole catalyst
• selective permeation of P₁ or P₂
i) cocurrent
ii) countercurrent
• catalytic membrane and packed bed catalyst
• removal of products or supply of reactants
i) cocurrent
ii) countercurrent
inert membrane
catalytic membrane

F_1/F_2 = Reactant Feed; S = Sweep; P_1/P_2 = Product.

Fig 1.4: Classification of membrane reactor concepts acc to membrane functions [7].

questions arises whether the membrane itself has a catalytic function or not. If the membrane acts as a catalyst we refer to this as a catalytic membrane reactor (CMR, Fig. 1.4e and f), if not we have an inert membrane catalytic reactor (IMCR, Fig 1.4d). The CMR-case may be further subdivided into two categories, i.e. when the membrane acts as the sole catalyst (Fig. 1.4e), and when a conventional catalyst is present in addition to the membrane (Fig. 1.4f). Other authors have introduced similar acronyms for an easy reference to the different membrane reactor types. Some authors refer to a catalytic non-permselective membrane reactor (CNMR) as to a reactor with a catalytic membrane which is not permselective but provides for a well-defined interface for two (or more) reactants flowing on opposite sides of the membrane (Fig. 1.4c). In contrast their definition of a catalytic membrane reactor (CMR) requires a permselective membrane (Fig. 1.4e). In both cases the membrane acts as the sole catalyst. The same authors assigned the acronyms PBMR and FBMR to the packed-bed and fluidised-bed membrane reactor where the membrane is permselective but not catalytic (Fig. 1.4d). The opposite cases, i.e. with catalytic and permselective membrane, are referred to as PBCMR and FBCMR, respectively (Fig. 1.4f). Coronas and Santamaria [6] used the notations CMR and IMR to distinguish between the catalytic and the inert membrane reactor. According to their definition the CMR has no other type of catalyst except the membrane. Consequently a third category "combined" is introduced to refer to membrane reactor configurations where the catalyst is placed both inside and outside the membrane. No further distinction is made in view of the permselectivity, i.e. whether the membrane performs a separation task, whether it provides a reaction interface for different reactant streams, or whether it acts only as a special type of catalyst support, e.g. to minimise the mass transport resistance when the whole feed stream is passed through it in cross-flow.

1.5.1 Membrane Reactor Configuration

The membrane reactors are usually operated in parallel or cross flow mode, with the reactants on one side and the permeate on the other. The permeate is driven by the sweep gas as shown in Fig 1.5. The basic idea of a membrane reactor is to separate the reaction chanber into several compartments which interact by heat and mass transfer. This idea allows for many variations.

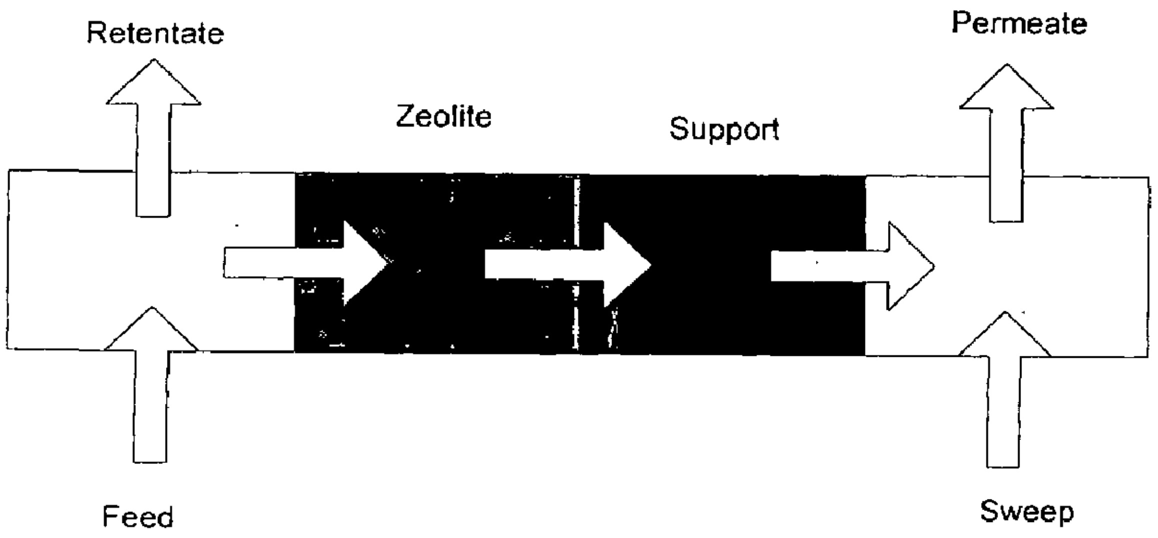

Fig 1.5: The permeation module

Two common type of membrane reactor types are shown in Fig.1.6(a) and Fig 1.6(b). Another type of membrane reactor 'hybrid membrane reactor', which is a combination of impermeable region and membrane as shown in Fig 1.6(c). A packed bed membrane reactor is a type of catalytic membrane reactor which is a combination of a heterogeneous catalyst and perm selective membrane. A membrane is a barrier in the form of a thin film or layer that can be selectively permeated by some components of the mixture. In the case a packed-bed membrane reactor, the membrane is in the form of a tube and is packed with catalyst. This allows both the reaction in the catalyst bed and the separation of the mixture components through the membrane to take place simultaneously. In the full length membrane reactor feed is introduced in the tube side where the membrane is incorporated. One of the reactant products is selectively removed from the membrane by permeating the one component through that, is basic principle in enhancing the conversion by shifting the equilibrium in the forward side. In case of hybrid reactors, initial portion of the tubular region is fixed with the impermeable region and next part is arranged with the membrane of suitable type. In this case the reaction is carried out in the initial stages of the reactor, and then it permeates through the membrane. It has the advantage over the full length membrane reactor as it does not permeate the reactant components initially which is possible in the later case.

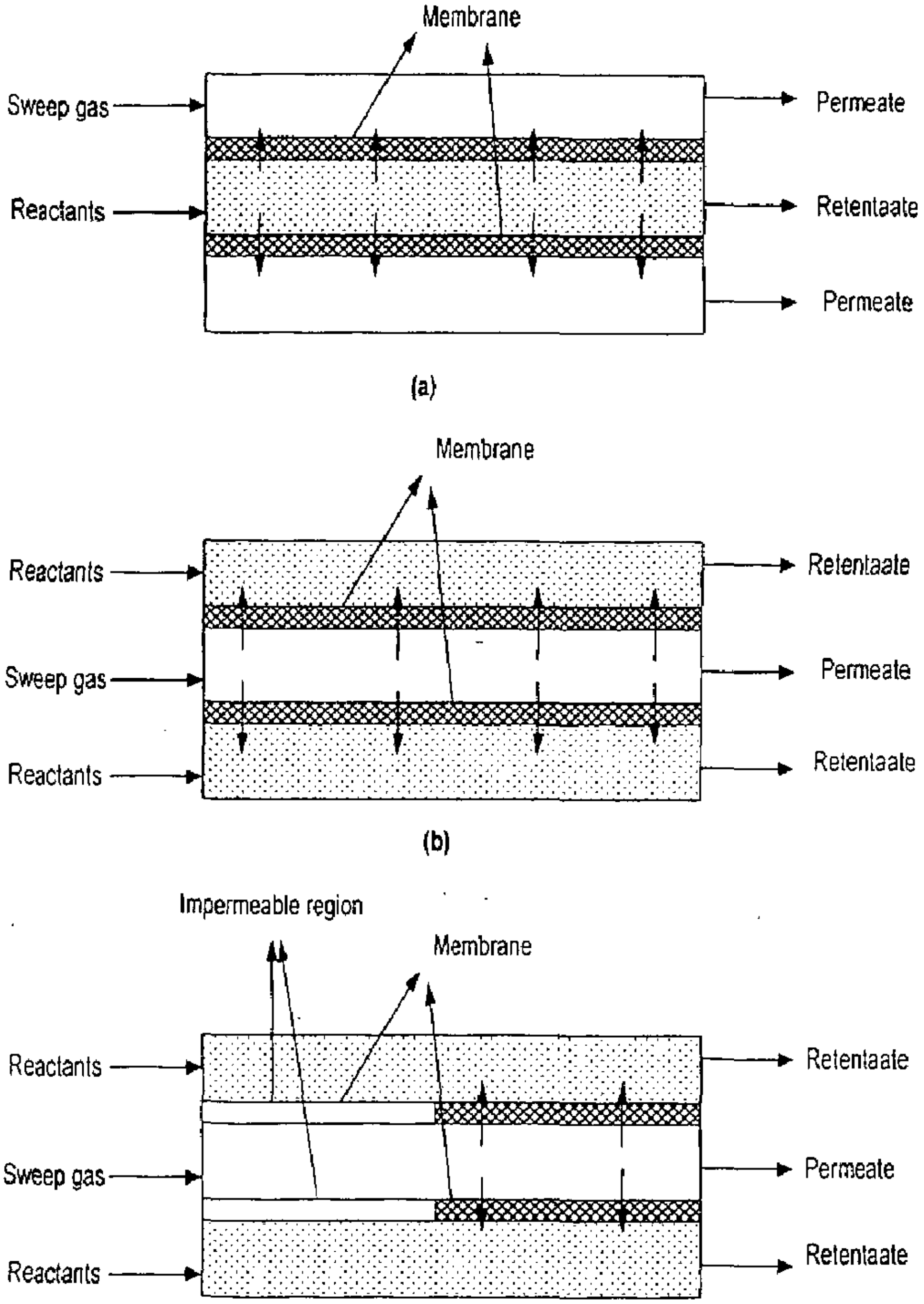
Membrane
Sweep gas
Permeate
Reactants
Retentaate
Permeate
Membrane
Reactants
Retentaate
Sweep gas
Permeate
Reactants
Retentaate
Impermeable region
Membrane
Reactants
Retentaate
Sweep gas
Permeate
Reactants
Retentaate

(a)

(b)

(c)

Fig 1.6: (a) Full length membrane reactor with reactants fed in the tube side (b) Full length membrane reactor with reactants fed in the shell side (c) Hybrid membrane reactor with reactants fed in the shell side.

1.6 Permeation Mechanism

Earlier researchers described transport through porous membranes as adsorption on the external surface, transport into the pores, inter-crystalline diffusion, transport out of the pores, and desorption. The operating conditions and the molecule determine which step is rate determining.

Previous studies indicate that interfacial effects can be neglected for our conditions. Thus only intercrystalline transport will be taken into account and equilibrium adsorption will be assumed at interfaces. Different mechanisms contribute to the selectivity of the zeolite membranes. In zeolite pores, adsorption and diffusion plays major roles for some molecules, whereas for other molecules sieve effects dominate. Diffusion also takes place through the intercrystalline regions, where the pores can be larger than zeolite pores, and these are referred to as non zeolite pores. Depending on the sizes of non zeolite pores and diffusing molecules, other transport mechanisms such as molecular, Knudsen, surface diffusion or viscous flow may occur. Pore blocking by adsorption and capillary condensation can be beneficial for restricting the permeation of few molecules specially reactants. The permeation of hydrocarbons through FAU-type zeolite membranes proceeds via the following steps:

- Adsorption on the external surface
- Transport from the external surface into the pores
- Diffusion between vacant sites
- Transport out of the pores to the external surface
- Desorption from the external surface.

CHAPTER II

LITERATURE REVIEW

2.0 INTRODUCTION

The literature review is the heart of every research area. It provides the contribution of various research workers in the concerned research area. The review of open literature helps in framing out the work plan of further research in that area. In the present work, we are planning to study the performance of membrane reactor to carry out the dehydrogenation of cyclohexane. Enormous literature is available on this dehydrogenation reaction. Here in this chapter it is not possible to include all the studies. Therefore the studies on only those aspects have been included which are relevant to the present research work. This chapter comprises mainly two type of research reviews:

- Review of experimental studies
- Review of modeling studies.

2.1 Experimental Reviews

Kusakabe et al. [19] have synthesized NaY-type zeolite membranes on a porous support tube by a hydrothermal process. The membranes were ion-exchanged with Li^+ and K^+ ions, and permeances through the membranes were determined for an equimolar mixture of CO_2 and N_2, as well as for single-components therefore, at a temperature range of 0 - 400^0C. The permeance to CO_2 showed a maximum at 100^0C, but CO_2 / N_2 selectivity decreased with increasing temperature. The zeolite membranes that were exchanged with K^+ and Li^+ ions gave higher and lower CO_2/N_2 selectivities, respectively, than were found for the NaY-type membrane. The permeation properties of the ion-exchanged zeolite membranes were analyzed using a sorption- diffusion model. The high CO_2/N_2 selectivity of the K-exchanged membranes can be explained by the decrease in N_2 sorptivity for the mixed feed.

Hasan et al. [10] have measured the permeances of gases with kinetic diameters ranging from 2.6 to 3.9Å were measured through silica hollow fiber membranes over a temperature range of 298 to 473 K at a feed gas pressure of 20 atm. Permeances at 298 K ranged from 10 to 2.3 X 10^5 Barrer/cm for CH_4 and He, respectively, and were inversely proportional to the kinetic diameter of the penetrant. From measurements of CO_2 adsorption at low relative pressures, the silica hollow fibers are microporous with a mean pore size estimated to be between 5.9 and 8.5 Å. X-ray scattering measurements show that the orientation of the pores is completely random. Mass transfer through the silica hollow fiber membranes is an activated process. Activation energies for diffusion through the membranes were calculated from the slopes of Arrhenius plots of the permeation data. The energies of activation ranged from 4.61 to 14.0 kcal/mol and correlate well with the kinetic diameter of the penetrants. The experimental activation energies fall between literature values for zeolites 3A and 4A. Large separation factors were obtained for O_2/N_2 and CO_2/CH_4 mixtures. The O_2/N_2 mixed gas separation factors decreased from 11.3 at 298 K to 4.8 at 423 K and were up to 20% larger than the values calculated from pure gases at temperatures below 373 K. Similar differences in the separation factors were observed for CO_2/CH_4 mixtures after the membrane had been heated to at least 398 K and then cooled in an inert gas flow. The differences between the mixture and ideal separation factors is attributed to a competitive adsorption effect in which the more strongly interacting gases saturate the surface and block the transport of the weakly interacting gases. Based on Fourier transform infrared (FFIR) spectroscopy results, this unusual behavior is attributed to the removal of physically adsorbed water from the membrane surface.

Lechuga et al. [20] have studied experimentally dehydrogenation of cyclohexane to benzene in a pure membrane reactor, a conventional packed bed reactor, and hybrid membrane reactors consisting of a packed bed reactor segment followed by a membrane reactor segment. The conversions achieved in pure membrane reactors were higher than those achieved with hybrid membrane reactors. In terms of global conversions based on the amounts of product present in both retentate and sweep streams, the conversion achieved in a pure membrane reactor was 60 to 128% higher than that achieved in a conventional packed bed reactor. However, the increase in the conversion level achieved was not attributed primarily to the selective removal of hydrogen via the membrane but to reduction of the partial pressures of the reactants in the retentate stream caused by the transport of the organic constituents through the membrane into the retentate stream, thereby decreasing their partial pressures and shifting the equilibrium extent of reaction. For the pure membrane reactor experiments, between 34 and 36% of the organic constituents fed left the reactor in the retentate stream. The experimental results indicated that the rate of permeation through the membrane was fast compared to the reaction rate and/or the axial flow rates.

Ali et al. [2] reported the dehydrogenation of cyclohexane over different catalysts containing 0.35 wt% of each of the following metals: Pt, Rh, Re, U, PtIr, PtRh, PtRe and PtU on γ-Al_2O_3 in a pulsed micro-reactor system at the temperature range 200-500^0 C. Also the effect of chlorine and fluorine contents (1, 3 and 6 wt%) on the activities of these catalysts were investigated and the following conclusions were drawn:

- Most of the catalysts under study enhance cyclohexane dehydrogenation up to 350^{0}C beyond which the activity may not improve via further increase of temperature or even decline. This may be attributed to the stronger adsorption of the produced benzene molecules, thus retarding further cyclohexane adsorption and reactor.
- Combination of Ir, Rh or Re with Pt enhances the catalytic activity, whereas U inhibits this activity.
- Halogenation of the monometallic or bimetallic catalysts with chlorine or fluorine enhances the catalytic activity except for the catalysts containing Ir(F), PtIr(Cl), PtRh(Cl) and PtRh(F).
- The optimum concentration of halogen for enhancing cyclohexane dehydrogenation is 3% by weight, which may be attributed to the increasing hydrogen spillover and improving the metal dispersion in the support.

Dittmeyer et al. [7] have discussed two different membrane reactor concepts which both rely on supported palladium, on the one hand as a permselective membrane material, and on the other hand as base component of a membrane-type hydrogenation catalyst. Dense palladium composite membranes can be used for hydrogen separation from packed-bed catalysts in gas-phase hydrocarbon dehydrogenation reactions. Mesoporous membranes containing dispersed bimetallic Pd/X-clusters can be employed as so-called catalytic diffusers for liquid-phase hydrogenation, e.g. of nitrate and nitrite in water. The principles of both concepts are introduced, recently obtained experimental data are evaluated in connection with literature results, and the perspectives for further development are highlighted.

Kariya et al. [18] reported highly efficient evolution of hydrogen achieved in the dehydrogenation of cycloalkanes such as cyclohexane, methylcyclohexane, and decalin over Pt catalyst supported on active carbon (AC) under "wet–dry multiphase conditions". Formation rate of hydrogen is largely dependent on reaction conditions such as reactant/catalyst ratio, temperature, and support. The highest initial rate of formation of hydrogen, $k = 8.0\times10^{-3}$ mol min^{-1}, was obtained in the dehydrogenation of cyclohexane over Pt/AC at 623K and the reactant/catalyst ratio = 3.3ml g^{-1}. The addition of second metals such as Mo, W, Re, Rh, Ir, and Pd on the carbon-supported Pt catalysts enhances the dehydrogenation rate due to the promotion of C–H bond cleavage and/or desorption of aromatic products. A physical mixture of Pt/AC and Pd/AC catalysts exhibits higher activities than the monometallic Pt/AC catalyst owing to the synergistic effects of spillover, migration, and recombination of hydrogen over Pt and Pd catalysts.

Itoh et al. [11] have examined the recovery of hydrogen from cyclohexane as one of the promising chemical hydrogen carriers using a palladium membrane reactor. First, the rate expression for the cyclohexane dehydrogenation under higher pressures, necessary for the reactor design and analysis was established. The operation conditions of the palladium membrane reactor to obtain a higher hydrogen recovery were then predicted by computer simulation. As a result, it was shown that the hydrogen recovery rate became higher as the pressure on the hydrogen permeation side was lowered below atmospheric pressure or as the reaction pressure increased. Also, it was found that the reaction temperature significantly affected the conversion of cyclohexane to benzene, and preferably, the temperature should be around 573K for accomplishing a higher recovery rate of hydrogen. Based upon the simulated results, the reaction was carried out at

573K and 1–4 bar while the perm-side pressure was kept in the range 0.1–1 bar. It was clearly shown that as the perm-side pressure was lowered, the conversion as well as the hydrogen recovery rate increased. Near 0.1 bar of perm-side pressure, about 80% of the hydrogen contained in cyclohexane was successfully recovered.

Jeong et al. [14] reported about an FAU-type zeolite membrane on a porous α-Al_2O_3 support tube, for use in the selective separation of benzene and hydrogen from cyclohexane. The membrane was used for the catalytic dehydrogenation of cyclohexane in a membrane reactor packed with a Pt/Al_2O_3 catalyst. The reaction was carried out in the temperature range of 423–523K over a 1.0 wt.% Pt/Al_2O_3 catalyst prepared by means of an impregnation method. Prior to the reaction in the membrane reactor, the activity of the catalyst was evaluated as a function of time, and the catalyst was found to exhibit a stable performance during a 3-day period of operation. In the membrane reactor system, an increase of the sweep flow rate resulted in a higher cyclohexane conversion, due to the rapid removal of products from the feed side of the membrane, thus leading to a high turnover rate. The conversion of cyclohexane was significantly affected by the cyclohexane feed rate. In a membrane reactor with a benzene selective FAU-type zeolite membrane, cyclohexane conversion was found to be 72.1% at 473 K, whereas the calculated equilibrium value is 32.2%, when the sweep flow rate was maintained at 100 cm^3 (STP) min^{-1} and the cyclohexane feed rate was maintained at 1.1 mol h^{-1}.

Biniwale et al. [3] carried out dehydrogenation of cyclohexane over Pt/alumite and Pt/activated carbon catalysts for hydrogen storage and supply to fuel cell applications. An unsteady state has been created using spray pulsed injection of cyclohexane over the catalyst surface to facilitate the endothermic reaction to occur efficiently. Higher temperature of the catalyst surface is more favorable for the reaction, thus the heat transfer phenomena and temperature profile under alternate wet and dry conditions created using spray pulsed injection becomes important. IR thermography has been used for monitoring of temperature profile of the catalyst surface simultaneously with product analysis. The heat flux from the plate-type heater to the catalyst has been estimated using a rapid temperature recording and thermocouple arrangement. The estimated heat flux under transient conditions was in the range of 10-15 kW/m^2, which equates the requirement for endothermic reactions to the injection frequency of 0.5 Hz, as used in this study. The analysis of temperature profiles, reaction products over two different supports namely activated carbon cloth and alumite, reveals that the more conductive support such as alumite is more suitable for dehydrogenation of cyclohexane.

2.2 Modeling Reviews

In order to study the performance of a membrane reactor, a number of modeling studies have been conducted. Most of the models are concerned with equilibrium limited reactions since these systems have been mostly studied experimentally. The dehydrogenation of cyclohexane has been extensively studied as a model reaction in various membrane reactors. The reaction is as follows:

$$C_6H_{12} \xrightleftharpoons{423-500K} C_6H_6 + 3H_2, \quad \Delta H = 206 \text{ kJ/mol} \tag{2.1}$$

This section present the models developed by the different researchers for the performance of the membrane reactors and for different reaction mechanisms with possible modeling and experimental conclusion to assist further research in the novel technology. This chapter briefly gives the brief discussion on the literature on only the aspects of membrane reactors used for different reaction systems and for their modeling work.

Mohan and Govind [21] has studied dehydrogenation of cyclohexane on Pd-Al_2O_3 or Pt-Al_2O_3 in a permeable wall membrane reactor. It is assumed that catalyst is only present inside the tube with no reaction occurring on the shell side. Their model assumes the following assumptions:

1. Isothermal operation.
2. Negligible pressure drop on the tube and shell side.
3. Plug flow on both tube and shell sides
4. No axial or radial flow.

For the tube side, $Z>0$

$$\frac{dF_A^{'}}{dZ} = -\alpha f_A - hu_A(x_A - y_A P_r) \tag{2.2}$$

$$\frac{dF_B^*}{dZ} = bf_A - hu_B(x_B - y_BP_r) \tag{2.3}$$

$$\frac{dF_C^*}{dZ} = -cf_A - h(x_C - y_CP_r) \tag{2.4}$$

$$\frac{dF_I^*}{dZ} = -hu_I(x_I - y_IP_r) \tag{2.5}$$

For the shell side, Z>0

$$\frac{dQ_A^*}{dZ} = hu_A(x_A - y_AP_r) \tag{2.6}$$

$$\frac{dQ_B^*}{dZ} = hu_B(x_B - y_BP_r) \tag{2.7}$$

$$\frac{dQ_C^*}{dZ} = h(x_C - y_CP_r) \tag{2.8}$$

$$\frac{dQ_I^*}{dZ} = hu_I(x_I - y_IP_r) \tag{2.9}$$

where,

f_A = dimensionless rate expression for the reaction ($x_A^a - x_B^b x_C^c P_t^{(b+c-a)} / K_p$)

F_i = molar flow rate of ith component in the tube side, mol/s

F_i^* = dimensionless flow of gas on the tube side, F_i/F_{A0}

h = ratio of permeation rate to the reaction rate, ($P^c A_m P_t / kv_t P_t^a t_m$)

L = Length of the reactor

P_t = tube-side pressure, Pa

P_s = shell side pressure, Pa

P_r = Ps/Pt

Q_i = molar gas flow rate on the shell side, mol/s

Q_i^* = dimensionless flow of gas on the shell side, Q_i/Q_{A0}

T = reaction temperature, K

u_i = permselectivity of gas i with respect to the fastest gas

v_t = tube side volume per unit length of perm-reactor m^3/m

x_i = mole fraction of gas in the tube side

X = conversion

X_R = conversion ratio, perm reactor conversion/equilibrium conversion.

y_i= mole fraction of gas on the shell side

Z = dimensionless perm reactor length, kP_tLV_t / F_{A0}, Damkohler number.

They have drawn the following conclusions

- For a fixed length of perm-reactor there exists an optimum ratio of permeation rate to the reaction rate h corresponding to the maximum conversion
- There exists a maximum(optimum) conversion in a cocurrent perm-reactor that is achieved when the forward reaction rate becomes zero.
- When there is no back permeation of the reactant from the product (shell) side to the reactant (tube) side the optimum conversion in a perm-reactor is a function of amount of permeation of cyclohexane. Thus the smaller the pressure ratio (Pr) and h, the higher the conversion.
- When there is back permeation of the reactant from the shell side to the tube side, the optimum conversion in the perm-reactor is independent of h. For a perm-rector operating in this regime there is limiting length z beyond which there is no appreciable change in conversion.
- A membrane that exhibits a high permselectivity for the products over the reactants should be used in order to achieve large values of conversion.
- There exists a critical value of inert flow rate on the shell side for a given inert flow rate on the tube side, which corresponds to the optimum conversion ratio of 1.0.

Itoh [12] has developed a model of component gases in a reactor using a palladium hollow tube. The quantitative representation for this was developed by taking a material balance of each component in dimensionless differential section of the reactor dL. Hence,

$$\frac{du_c}{dL} = r_c V_r \tag{2.10}$$

$$\frac{du_h}{dL} = -3r_c V_r - \alpha_H \left(\sqrt{P_{T_r} \frac{u_H}{\sum u_i}} - \sqrt{P_{T_s} \frac{v_H}{\sum v_i}} \right) \tag{2.11}$$

$$\sum u_i = u_C + u_B + u_H + u_A$$

$$\sum v_i = v_A + v_H \tag{2.12}$$

$$u_B = u_C^0 - u_C$$

$$v_H = u_H - 3(u_C^0 - u_C) \tag{2.13}$$

$$u_A = u_A^0, v_A = v_A^0, v_C = v_B = 0 \tag{2.14}$$

where, u_i and v_i (i=C,H,B, and A) are the flow rates of component i in the reaction and separation sides, respectively. V_r is the gross volume of the reaction section P_{Tr} and P_{Ts} are the total pressures in the reaction and separation side respectively. The disappearance rate of cyclohexane, r_C can be expressed by

$$r_C = \frac{-k(K_p p_C / p_H^3 - p_B)}{1 + K_B K_p p_c / p_H^3} \tag{2.15}$$

where, p_i is the partial pressure of component i in the reaction side. Equations (2.10) to (2.15) were numerically integrated by the Runge Kutta method with initial conditions,

$$\begin{gathered} L = 0, u = u_C^0, u_B = 0, u_H = 0 \\ u_A = u_A^0, v_H = 0, v_A = v_A^0 \end{gathered} \tag{2.16}$$

Sun and Khang [24] have analyzed the performance of a catalytic membrane reactor (CMR) in comparison with three different reactor types: the inert membrane reactor with catalyst pellets placed on the feed side of the membrane (IMRCF), the plug flow reactor packed with catalyst pellets (PFR), and the mixed flow reactor in which catalysts are well-mixed with reactants (MFR). Three general categories of reactions are considered: (1) the volume is increased after reaction (gas-phase reaction with Δn > 0), (2) the volume remains constant after reaction (liquid-phase reaction, or gas-phase reaction with Δn = 0), and (3) the volume is decreased after reaction (gas-phase reaction with Δn < 0). The purpose of this paper is to further analyze the performance of the catalytic membrane reactor in comparison with the inert membrane reactor and also two other traditional ideal flow reactors-the plug flow reactor (PFR) and the mixed flow reactor (MFR). The comparison is made based on the same amount of catalyst and is made by using a well-established single-cell model (Itoh, 1987). The relationships among key dimensionless groups in the governing equations are discussed in detail:

CATALYTIC MEMBRANE REACTOR:

The feed-side (upstream) pressure, P_f, is higher than the permeate-side (downstream) pressure, P_p. The total molar flow rate and the composition of each input stream, as well as P_p and P_f, are maintained constant during the operation. A single or multiple reaction may take place in the catalytic membrane, and the reaction rate expression of each reaction is denoted by $r_i = k_i f_i(P)$, where i, k, and P are, respectively, the reaction number, the reaction rate constant, and the vector expression for the partial pressures of all the components. It is assumed that the system is isothermal and the interfacial mass-transfer resistance between the gas phase and the surface of the catalytic membrane is negligible compared to the internal mass-transfer resistance in the membrane. The membrane is assumed to have a microporous structure, and thus the gas diffusion through the membrane is assumed to follow the Knudsen diffusion behavior. It is also assumed that the contents in the feed-side chamber and the permeate-side chamber are well mixed. The model is called a single-cell model because no longitudinal variation is considered. The steady-state equations for the system are given are follows.

In the catalytic membrane

$$\frac{D_j}{RT}\frac{1}{r}\frac{d}{dr}\left[r\frac{dP_j}{dr}\right]+\sum_{i=1}^{m}\upsilon_{ij}k_i f_i(P)=0;(j=1,2,.....n) \tag{2.17}$$

$P_j = x_j P_f$ at r = r_f

$P_j = y_j P_p$ at r = r_p

In the feed side chamber (shell side)

$$Q_f^0 x_j^0 - Q_f x_j - 2\pi L\frac{D_j}{RT}\left(r\frac{dP_j}{dr}\right)\Bigg|_{r_f} = 0;(j=1,2,......n) \tag{2.18}$$

In the permeate side chamber (tube side)

$$Q_p^0 y_j^0 - Q_p y_j + 2\pi L\frac{D_j}{RT}\left(r\frac{dP_j}{dr}\right)\Bigg|_{r_p} = 0\ ;(j=1,2,......n) \tag{2.19}$$

The dimensionless forms of equations (2.17) to (2.19) are written as follows

$$\frac{1}{\exp(2\xi\delta)}\frac{d^2\psi_j}{d\xi^2}+\frac{\phi^2}{\alpha_j}\sum_{i=1}^{m}\upsilon_{ij}k_i f_i(\psi)=0,(j=1,2,.....n) \tag{2.20}$$

$\Psi j = xj$ at $\zeta = 1$

$\Psi j = yjPr$ at $\zeta = 0$

$$x_j^0 - \theta_f x_j - \alpha_j\phi\frac{d\psi_j}{d\xi}\Bigg|_{\xi=1} = 0,(j=1,2.......n) \tag{2.21}$$

$$\theta_P^0 y_j^0 - \theta_p y_j + \alpha_j \phi \left.\frac{d\psi_j}{d\xi}\right|_{\xi=0} = 0, (j = 1, 2, ...n) \tag{2.22}$$

where ψ_j, α_j, ξ, and θ are, respectively, the dimensionless partial pressure of component j, the ratio of diffusivities between component j and component i or the ideal separation factor between the two components, the dimensionless radius, and the dimensionless molar flow rate. The dimensionless diffusional space time, ϕ, and the Thiele modulus, φ, are defined as

$$\phi = \frac{2\pi L D_1 P_f}{\delta R T Q_f^0} \tag{2.23}$$

$$\varphi = r_p \delta \left(\frac{R T k_1 P_f^{\beta_1 - 1}}{D_1} \right)^{1/2} \tag{2.24}$$

For category 1, the performances of PFR and MFR operated at the feed-side pressure *(P)* are better than those of CMR or IMRCF. Between two membrane reactors, the performance of CMR is slightly better than that of IMRCF at a longer diffusional space time (low pressure drop across the membrane). For category 2, both types of membrane reactors (CMR and IMRCF) perform better than the traditional PFR and MFR because of the equilibrium shift induced by a selective product separation. For category 3, the performance of IMRCF at a longer diffusional space time is better than any other reactors in the studied case. The catalytic membrane reactor is not suitable for this category due to the undesirable equilibrium effect induced by the pressure variation.

Shelekhin et al. [22] had studied the gas permeability properties of He, H, CO_2, O_2, N_2, and CH_4 in microporous silica membranes as a function of temperature and pressure. A mathematical model of compressible flow in a hollow fiber tube with permeable walls was developed and solved to describe gas transfer in the membranes. The permeation rate of He in the microporous membrane was comparable to that in industrially produced polymeric membranes. Selectivity factors in the membrane were found to be a function of differences in the gas kinetic diameters. The ideal selectivity factor for He/CH, was more than 10,000 at 30^{0}C. Selectivity factors decreased with increasing temperature. The developed model was as follows:

Equation of continuity (mass balance)

Let w be the mass flow rate (kg/sec) along the tube. Then

$$\frac{dw}{dz} = -2\pi r_i f_i \tag{2.25}$$

where f_i is the mass flux through the tube wall at the inside radius (kg/m^2-sec), or simply the permeation flux.

Equation of motion (momentum balance):

Let p be pressure, A, be cross-sectional area (πr_i^2), B be wetted perimeter ($2\pi r_i$) and τ_w, be wall shear stress (kg/m-sec^2). Then

$$\frac{d}{dz}(\rho v_z^2) = -\frac{\tau_w B}{A_z} - \frac{dp}{dz} \tag{2.26}$$

As written, eqn. (2.26) involves p, v_z,, p, and τ_w, all of which vary with distance down the tube. The mass balance involves w, and measurements are made of p, so the equation will be reformulated in terms of these two variables.

- for ideal gas

$$\rho = \frac{pM}{RT}$$

- by definition

$$w = \rho v_z \pi r_i^2 = \frac{p v_z \pi r_i^2 M}{RT}$$

- by definition of λ

$$\tau_w = \frac{\rho v_z^2 \lambda}{2}$$

Assuming that the friction factor for laminar flow in a microporous tube is the same as in a nonporous one

$$\lambda = \frac{16}{\mathrm{Re}} = \frac{16\pi r_i \mu}{w}$$

Then using the above, together with the definitions of B and A_z, eqn (2.26) becomes:

$$\frac{dp}{dz} = \frac{-4 f_i \pi r_i - 8\pi\mu}{\dfrac{M\pi^2 r_i^4 p}{RTw} - \dfrac{w}{p}} \tag{2.27}$$

So eqns. (2.25) and (2.27) give two equations in the two unknowns p and w.

In order to get a constitutive relation for f_i it was needed to introduce an additional postulate: the permeability coefficient P does not depend on pressure in the microporous membranes. The mass flux or permeation rate per unit area is expressed in terms of a permeability P (barrer). Then by definition

$$f_i = \frac{\gamma PM(p-p_3)}{r_i \ln(r_0/r_i)}$$

where p_3 is the pressure on the shell side of the membrane.

Substituting f_i into eqn (2.25)

$$\frac{dw}{dz} = -2\pi\gamma\frac{PM(p-p_3)}{\ln(r_0/r_i)} \tag{2.28}$$

where

A_z= membrane inside cross sectional area

B= wetted perimeter

d= gas kinetic diameter

E= activation energy of permeation

f_i= mass flux through the tube wall at the inside radius

L= membrane length

M= gas molecular weight

N= no of pores per unit area

p=pressure

p_0=inlet pressure

p_1=pressure at the membrane outlet at z=L

p_3= pressure on the permeate side of the membrane

P= permeability coefficient

r= pore radius

r_i=inside diameter of the fiber

r_0= outside diameter of the fiber

w=mass flow rate

α= selectivity factor

τ_w= all shear stress

ρ = gas density

λ= friction factor

μ= viscosity

As shown in the publication, the microporous membranes exhibit excellent selectivity factors and simultaneously high transmembrane fluxes. There are still many challenges on the way to practical implementation, and the most important one is the mechanical stability of the membrane. Certainly, membrane module construction on the basis of these particular fibers would be an enormous problem, as the membranes are very brittle. Nevertheless, it would be a premature judgement to reject the possibility of further development of inorganic membranes based only on the mechanical properties of this particular membrane. The main achievement in the creation of this membrane is that it clearly shows the real possibility of microporous, high temperature and chemically resistant membrane preparation with transport properties competitive with polymeric membranes or even exceeding them.

Gokhale et al. [9] had simulated a dehydrogenation reaction of the form $A \leftrightarrow B + 3H_2$ in a cocurrent, isothermal, membrane-enclosed catalytic reactor to study the effects of reactant permeation rate, hydrogen-permeation selectivity, feed composition, and reactant space times on reaction conversion. Two dimensionless numbers, the Damkohler number and the permeation number, were used to quantify the effects of reactant space time and reactant loss on conversion respectively. The Damkohler number is the ratio of maximum reaction rate to inlet reactant flow rate, and the permeation number is the ratio of maximum reactant permeation rate to inlet reactant flow rate. For reactant space times at STP between 0.3 and 30 s, and hydrogen-permeation selectivities between 3 and 1000, conversion decreased as the maximum reactant permeation rate exceeded the inlet reactant flow rate because reactant loss controlled conversion. For hydrogen-permeation selectivities between 3 and 40, a membrane reactor gave maximum conversions when the maximum reactant permeation rate equaled the inlet reactant flow rate, and the reactant space times at STP had to be greater than 1.5 s to obtain conversions higher than the enhanced equilibrium conversion due to dilution by the inert sweep gas. The following model equations were formulated for concurrent membrane reactor:

Tube side(reaction side)

$$\frac{dF_i^t}{dz} = \nu_i R_A \pi r_1^2 - 2\pi r_1 \psi_i (x_i P_t - y_i P_s) \qquad (2.29)$$

Shell side (permeation side):

$$\frac{dF_i^s}{dz} = 2\pi r_1 \psi_i (x_i P_t - y_i P_s) \qquad (2.30)$$

The rate of dehydrogenation, R_A is given by:

$$R_A = k_f \left(p_A - \frac{p_B p_{H_2}}{K_{eq}}\right) \qquad (2.31)$$

Eqs. (2.29) and (2.30) can be written in dimensionless form as follows:

Tube side (reaction side):

$$\frac{df_i^t}{d\xi} = \nu_i Da R^* - \alpha_i \Pi (x_i - y_i P_r) \qquad (2.32)$$

Shell side (permeation side)

$$\frac{df_i^s}{d\xi} = \alpha_i \Pi (x_i - y_i P_r) \qquad (2.33)$$

where,

F_i^t=tube side molar flow rate of species i (mol/s)

F_i^s= shell side molar flow rate of species i (mol/s)

F_0= inlet flow rate of reactant(mol/s)

I= inert inlet flow rate (mol/s)

k_f= rate constant for forward reaction

K_{eq}=equilibrium constant(atm)

ψ_i =permeance of species i

L=reactor length

p_i= concentration of species i(atm)

P_0= standard pressure of 1 atm

P_t= tube side pressure

P_s=shell side pressure (atm)

P_r=pressure ratio=P_s/P_t

r_1=inner radius of the membrane tube

R_A= net reaction rate

R^*= dimensionless reaction rate, R_A/R_m

R_m= maximum reaction rate

x_i= tube side mol fraction of spècies i

y_i= shell side mole fraction of component i.

Da= Damkohler number

f_i^t =dimensionless flow rate of species i on the tube side

f_i^s =dimensionless flow rate of species i on the shell side

Itoh et al. [13] has proposed a membrane reactor, which is a double-tubular reactor equipped with a selective membrane tube as the inner tube was proposed. Such a reactor makes it possible to obtain a product yield of a reversible reaction beyond its equilibrium value by continuous removal of products during reaction. The following assumptions were made so as to develop basic equations for analysis.

- Attainment of isothermal conditions.
- Plug flow and negligible pressure drop in the axial direction exist on both the inner and the outer sides.
- Absence of axial or radial profiles.
- Permeability of each gas is independent of its concentration.

Taking mass balance of each gas component across a longitudinal length dl of the inner and outer sides of the membrane reactor, two simultaneous ordinary differential equations are obtained; they are represented in dimensionless form as

$$\frac{dU_i}{dL}=\frac{2\pi \bar{P}_i P_s l_0}{(u_i^0+v_i^0)\ln(r_{out}/r_{in})}\left(\frac{P_{out}}{P_s}\frac{1-U_i}{1+\beta-U_i-\beta U_j}-\frac{P_{in}}{P_s}\frac{U_i}{U_i+\beta U_j}\right) \tag{2.34}$$

$$\frac{dU_j}{dL}=\frac{2\pi \bar{P}_j P_s l_0}{(u_i^0)\ln(r_{out}/r_{in})}\left(\frac{P_{out}}{P_s}\frac{1-U_j}{1+1/\beta-U_j-U_i/\beta}-\frac{P_{in}}{P_s}\frac{U_j}{U_j+U_i/\beta}\right) \tag{2.35}$$

where

$$U_i=\frac{u_i}{u_i^0+v_i^0},U_j=\frac{u_j}{u_j^0},L=\frac{l}{l_0}$$

$$\beta=\frac{u_j^0}{u_i^0+v_i^0}$$

Also the following relations in terms of mass balance are valid.

$$V_i=1-U_i \tag{2.36}$$

$$V_j=1-U_j \tag{2.37}$$

where $\bar{P}_i$ and $\bar{P}_j$ are the permeabilities of component i and j respectively. P_s[Pa] is the reference pressure for obtaining dimensionless form and was 1.013 X 10^5Pa. P_{in} and P_{out} are the total pressures of the inner and the outer side respectively. Equations (2.34)-(2.37) were solved numerically under the initial condition that

$$L = 0; U_i = \frac{u_i^0}{u_i^0 + v_i^0}, U_j = 1 \tag{2.38}$$

The disappearance rate of cyclohexane r_C [mol.m^{-3}.s^{-1}], can be expressed by:

$$r_C = -\frac{k_C(K_p p_C / p_H^3 - p_B)}{1 + K_B K_p p_C / p_H^3} \tag{2.39}$$

k_C= 0.221 exp(-4270/T) [mol. m^{-3}. Pa^{-1}. s^{-1}]
K_B=2.03 x 10^{-10}exp(6270/T) [Pa^{-1}]
K_P=4.89 x 10^{35} exp(-26490/T) [Pa^3]

where p_i is the partial pressure of component i.

The permeabilities ($\bar{P}_H$ and $\bar{P}_C$) were obtained by using them as unknown parameters in the calculations and through greater agreement between the calculated results and experimental data. Dehydrogentaion experiments were carried out under atmospheric pressure in the range of 453-493 K. The conversions obtained were increased beyond those attainable at the equilibrium condition with an increase in flow rate of the sweep gas, that is, in the separation speed of the products, especially hydrogen.

Weyten et al. [26] has studied the comparison between the performance of the CVI-silica membrane and a Pd/Ag membrane when used as the H_2 selective membrane. The H_2 transport mechanism through a dense Pd/Ag membrane is quite different from the transport mechanism through a microporous silica membrane. The H_2 flux through noble metals (like the Pd/Ag membrane) is a special case of a solution/diffusion mechanism. The H_2 molecules are adsorbed and catalytically dissociated on the metal surface and can subsequently diffuse through the metal matrix. On the other side of the membrane, the recombination and desorption takes place. The rate of diffusion can be described in terms of Fick's first law

$$\Phi_{H_2} = \frac{F}{l}(p_h^n - p_l^n) = F_0(p_h^n - p_l^n) \tag{2.40}$$

Where Φ is the gas flux, p_h the pressure at the feed side and p_l the pressure at shell side. The permeation (F_0) is defined as gas flux through the membrane divided by the pressure difference (Δp), which act as the driving force.

Traditionally, the diffusion through the microporous silica membrane is described by the Knudsen/ Poiseulle law:

$$F_0 = \frac{\Phi}{\Delta p} = F_{0,k} + F_{0,p} = K_0 + B_0\,\bar{p} \tag{2.41}$$

where mean pressure $\bar{p} = 1/2(p_h+p_l)$[Pa].

The performance of the Pd/Ag membrane is far superior to the performance of the SiO_2 membrane. H_2 fluxes of more than 0.1 mol/m^{2}s were measured and the H_2/Ar permselectivity exceeds 4500. When it is run under comparable conditions, the performance of the Pd/Ag membrane reactor is much better. The increase in propane conversion persists at values of the propane feed stream that are about six times higher (105 mmol/s). Since the H_2 is selectively removed from the reaction mixture, it is not available for any competitive side reactions. The production of methane, which limits the propene selectivity of the reaction in a conventional plug-flow reactor, is much less in a catalytic membrane reactor. This means that the selectivity in the membrane reactor is higher than in the plug-flow reactor when they are run under similar conditions.

Jeong et al. [16] proposed a model for the permeation of hydrocarbons through the FAU-type zeolite membrane which proceeds in five steps

1. adsorption on the external surface;
2. transport from the external surface into the pores;
3. diffusion between vacant sites;
4. transport out of the pores to the external surface;
5. desorption from the external surface.

The activation energy for step 3 is higher than the energies for the other processes, suggesting that pore diffusion is rate-determining. The diffusion flux of component i for a binary mixture in the membrane, $N(i)$, can be described as:

$$N(i) = -\rho\Theta_{sat}(i)D_{eff}(i)\frac{d\theta(i)}{dz} \tag{2.42}$$

where ρ represents the density of zeolite, $\Theta_{sat}(i)$ the adsorbed amount of component i at saturation, $D_{eff}(i)$ the effective diffusivity, θ(i) the fractional surface occupancy, and z the distance from the feed-side surface of the membrane. The adsorbed amount on the feed-side surface of the membrane is assumed to be in equilibrium with the partial pressure in the outside gas. Since the diffusivity of the less adsorbed component is usually larger than that of the more adsorbed component, the separation factor for permeation of the binary mixture is smaller than the selectivity for adsorption. This model is consistent with the permeation data in the present study through the FAU-type zeolite membrane at 373K for the binary systems of C_6 hydrocarbons other than benzene.

They have also investigated the permeation and separation properties of an FAU-type zeolite membrane for mixtures of benzene and saturated hydrocarbons at 373 K. The membrane has been found to be stable after repeated temperature cycling and long-term use over 1 year. The membrane was benzene selective, and high separation factors for benzene/cyclohexane systems were obtained all over the mole fraction of benzene on the feed side. The benzene flux increased slightly with an increase of mole fraction of benzene on the feed side while the cyclohexane flux sharply decreased. The effect of the mole fraction of benzene on permeation properties was more prominent than that of cyclohexane. For an equimolar mixture of benzene and cyclohexane, the adsorption selectivity for benzene/cyclohexane reached a value of approximately 19, whereas the separation factor for permeation of the binary mixture was over 100. Hence, the adsorption selectivity is not the single major factor for the high separation factor. The preferentially permeating benzene molecules may block the windows, and as a result, the diffusivity of cyclohexane through the windows may be greatly decreased. Thus, the high adsorption selectivity in favor of benzene and the blockage against cyclohexane can be major determinants of the high B/C separation factor. For an equimolar mixture of n-C_6 and MP, in contrast, the adsorption selectivity for n-C_6/MP was lower than 3. Thus, the separation factors for mixtures of these hydrocarbons can be explained based on the single-file diffusion mechanism.

Jeong et al. [15] have reported on the development of a simple mathematical model assuming isothermal operation and a plug flow pattern, in an evaluating of the performance of an FAU-type zeolite membrane reactor for use in the catalytic dehydrogenation of cyclohexane and the simulation results are compared with experimental data. The effect of co-feeding hydrogen with cyclohexane to the feed side on conversion is evaluated, and the relationship between the permeance and the separation factor is discussed. The following assumptions are taken:

- isothermal conditions;
- plug flow in both the feed and permeate sides;
- no axial or radial diffusion;
- permeation through the membrane is proportional to the difference in partial pressures between the feed and permeate sides;
- dehydrogenation reactions take place only on the catalysts packed in the feed side.

The mass balance equations for component i in the feed side and the permeate side in the membrane reactor are given as follows:

Feed side (catalyst bed):

$$\frac{dN_{i,F}}{dl} = \upsilon_i r_C S_R - 2\pi r Q_i (P_F x_i - P_P y_i) \tag{2.43}$$

Permeate side:

$$\frac{dN_{i,P}}{dl} = 2\pi r Q_i (P_F x_i - P_P y_i) \tag{2.44}$$

where N_i is the molar flow rate of component i. l is the distance from the inlet of the reactor. υ_i is the stoichiometric coefficient of component i. r_C is the dehydrogenation rate of cyclohexane. S_R is the cross-sectional area of catalyst bed. r is the outer radius of the porous support tube. Q_i is the permeance of component i. P_F and P_P are the total feed and permeate pressures. x_i and y_i are the mole fractions of component i in the feed and permeate sides, respectively.

The following reaction rate equation of cyclohexane, r_C, was used

$$r_C = \frac{-k(K_p p_C / p_H^3 - p_B)}{1 + K_B K_p p_C / p_H^3} \tag{2.45}$$

where k, K_B, and K_p are, respectively, the reaction rate constant, the adsorption equilibrium constant for benzene, and the reaction equilibrium constant. p_i is the partial pressure of component i.

The model equations were numerically solved by the simplest Euler method using the above parameters. The conversion of cyclohexane, X_C, was calculated from the ratio of the molar fractions of cyclohexane at the outlets of the feed and the permeate sides to those for cyclohexane at the inlets of both sides as follows:

$$X_C = 1 - \frac{u_{x,1}x_{C,1} + u_{y,1}y_{C,1}}{u_{x,0}x_{C,0} + u_{y,0}y_{C,0}} \tag{2.46}$$

where $u_{x,0}$ and $u_{x,1}$ are the gas flow rates at the inlet and the outlet of the feed side, respectively. $u_{y,0}$ and $u_{y,1}$ are the gas flow rates at the inlet and the outlet of the permeate side, respectively.

The length of the impermeable region in the membrane reactor was found to be sufficient to permit an equilibrium conversion, and the selective permeation of benzene and hydrogen was effective in shifting the equilibrium. The conversion in the zeolite membrane reactor was much higher than the equilibrium conversion, and good agreement was found between the calculated values and the experimental ones. Based on the simulation results, the zeolite membrane reactor showed a better performance than the Knudsen membrane reactor. The co-feeding of hydrogen with cyclohexane into the reaction side, to prevent coking of the catalyst was effective. This can be attributed to the high hydrogen concentration on the reaction side. The increase in conversion in the zeolite membrane reactor was more dependent on the permeance than the separation factor.

Jia and Murad [17] have examined gas separations with faujasite zeolite membranes using the method of molecular dynamics. Two binary mixtures are investigated, oxygen/nitrogen and nitrogen/carbon dioxide. These mixtures have been found experimentally to exhibit contrasting behavior. In O_2 /N_2 mixtures the ideal selectivity (pure systems) is higher than the mixture selectivity, while in N_2 /CO_2 the mixture selectivity is higher than the ideal selectivity. One of the key goals of this work was to seek a fundamental molecular level understanding of such divergent behavior. Their simulation results (using previously developed intermolecular models for both the gases and zeolites investigated) were found to replicate this experimental behavior. By examining the loading of the membranes and the diffusion rates inside the zeolites, they have been able to explain such contrasting behavior of O_2 /N_2 and N_2/CO_2 mixtures. In the case of O_2/N_2 mixtures, the adsorption and loading of both O_2 and N_2 in the membrane are quite competitive, and thus the drop in the selectivity in the mixture is primarily the result of oxygen slowing the diffusion of nitrogen and nitrogen somewhat increasing the diffusion of oxygen when they pass through the zeolite pores. In N_2 /CO_2 systems, CO_2 is rather selectively adsorbed and loaded in the zeolite, leaving very little room for N_2 adsorption. Thus although N_2 continues to have a higher diffusion rate than CO_2 even in the mixture, there are so few N_2 molecules in the zeolite in mixtures that the selectivity of the mixture increases significantly compared to the ideal (pure system) values. They have also compared simulation results with hydrodynamic theories by using the model equation:

$$J = A\ln(\frac{1+KP_f}{1+KP_p}) + B(P_f^2 - P_p^2) + C(P_f - P_p), \tag{2.47}$$

where J is the flux, P_f and P_p the pressures on the feed and the permeate side and A,B,C, and K parameters of the equation. The first term of the equation refers to surface diffusion, while second to viscous flow and last to Knudsen diffusion contribution. Their simulations results fit the surface diffusion model quite well. On the other hand, the fit to the viscous flow and diffusion model is rather poor. Thus, in the hydrodynamic sense, their simulation confirms that surface diffusion is the dominant mechanism for membrane permeation in the N_2/O_2 system, except in the case of N_2 /CO_2 binary mixtures where Knudsen diffusion also makes a contribution to N_2 transport.

Abashar and Rabiah [1] has developed a rigorous two-dimensional model for the dehydrogenation of ethane and hydrogenation of benzene in a co-current packed bed membrane reactor. The following simplifying assumptions are used in the derivation of the conservation equations of the model:

- The reactor operates at steady state conditions and isothermally with negligible pressure drop.
- The membrane has exclusive selectivity for hydrogen.

- The reactions are considered to take place only in the tube side.
- Negligible diffusion resistances within the catalyst particles.
- Axial diffusion is negligible.
- The ideal gas law is obeyed.

Tube side

The differential mass balance equations on component i is given by:

$$\frac{\partial C_i^t}{\partial L} = \frac{D_{e_i}^t \varepsilon_1 L_0}{u_l} \frac{1}{r_1} \frac{\partial}{\partial r_1}\left[r_1 \frac{\partial C_i^t}{\partial r_1} \right] + \frac{(1-\varepsilon_1)L_0}{u_1} \times \sum_{j=1}^{n=2} \theta_j \gamma_{ij} R_j^{\cdot} \rho_j \quad 0 < r_1 < R_1,\ i=1\text{-}5 \qquad (2.48)$$

where i=1, 2, 3, 4 and 5 for C_2H_6, C_2H_4, H_2, C_6H_6 and C_6H_{12}, respectively, γ_{ij} the stiochiometric coefficient of component i in the j^{th} reaction (negative for reactants) and θ_j is the volume fraction of catalyst j.

The boundary conditions are:

$$L = 0, C_i^t = C_{if}^t; r_1 = 0, \frac{\partial C_i^t}{\partial r_1} = 0;$$
$$r_1 = R_1, C_i^t = C_i^c; i = 1-5 \qquad (2.49)$$

The effective diffusivity coefficient is calculated as:

$$D_{e_i} = \frac{1 - y_i}{\sum_{\substack{j=1 \\ j \neq i}}^{n} (y_i / D_{ij})} \qquad (2.50)$$

Ceramic Support

The differential mass balance equations on component i is given by:

$$\frac{D_{e_i}^c \varepsilon_2}{r_2} \frac{\partial}{\partial r_2}\left[r_2 \frac{\partial C_i^c}{\partial r_2} \right] = 0 \qquad R_1 < r_2 < R_2,\ i=1\text{-}5 \qquad (2.51)$$

The boundary conditions are

$$r_2 = R_1, C_i^t = C_i^c, D_{e_i}^t \varepsilon_1 \left.\frac{\partial C_i^t}{\partial r_1}\right|_{r_1 = R_1} = D_{e_i}^c \varepsilon_2 \left.\frac{\partial C_i^c}{\partial r_2}\right|_{r_2 = R_1} \qquad i = 1\text{-}5$$

$$r_2 = R_2, \left.\frac{\partial C_i^c}{\partial r_2}\right|_{r_2 = R_2} = 0, i = 1, 2, 4, 5 \qquad (2.52)$$

For H_2

$$\left.\frac{\partial C_3^c}{\partial r_2}\right| = \left(\frac{Q_0}{\delta D_{e_3}^c \varepsilon_2} \right)\left[\sqrt{P_{H_2}^t} - \sqrt{P_{H_2}^s} \right] \qquad (2.53)$$

Shell side

The differential mass balance on hydrogen gives:

$$\frac{dF_{H_2}^{s}}{dL} = Q_{H_2} \tag{2.54}$$

where,

A membrane area (m^2)

C_i^c concentration of component i in ceramic support (kg mol/m^3)

C_i^t concentration of component i in tube side (kg mol/m^3)

D_{ei} effective diffusion coefficient of component i (m2/s)

D_{ij} molecular diffusivity for component i in a binary mixture of i and j (m^2/s)

$F_{H_2}^{S}$ hydrogen molar flow rate in shell side (kg mol/s)

ΔH^0 standard heat of reaction (kJ/kg mol)

k_1 reaction rate constant of dehydrogenation reaction (kg mol/kg s Pa)

k_2 reaction rate constant of hydrogenation reaction (kg mol/kg s)

K_B adsorption constant for benzene (Pa−1)

K_1 equilibrium constant of dehydrogenation reaction (Pa)

L dimensionless reactor length

L_0 reactor length (m)

P_i partial pressure of component i (Pa)

P_t pressure in tube side (Pa)

P_s pressure of sweep gas (Pa)

Q_{H2} hydrogen permeation rate (kg mol/s)

Q_0 permeability constant (kg mol m/m^2 s Pa $^{0.5}$)

r_1 radial dimension in catalyst bed (m)

r_2 radial dimension in ceramic support (m)

R universal gas constant (kJ/kg mol K)

R_1 inner tube radius (m)

R_2 outer radius of composite tube (m)

R_1^{*} rate of dehydrogenation reaction (kg mol/kg s)

R_2^{*} rate of hydrogenation reaction (kg mol/kg s)

T temperature (K)

u_1 axial velocity (m^2/s)

y_i mole fraction of component i

γ_{ij} stiochiometric coefficient of component i in the jth reaction

δ membrane thickness (m)

ε_1 porosity of catalyst bed

ε_2 porosity of ceramic support

θ_j volume fraction of catalyst j

ρ_j density of catalyst j (kg/m^3)

The global orthogonal collocation technique is implemented to change the set of the partial differential equations Eqs. (2.48) and (2.51) into a set of ordinary equations. The radial derivatives are discretized using six orthogonal collocation points. Then, the new set of ordinary differential equations and the shell side equation (2.53) are integrated by an IMSL subroutine (DGEAR) based on a Runge–Kutta–Verner fifth and sixth-order method with automatic step size and double precision to ensure accuracy.

The results presented in this paper show that the integrated catalytic membrane reactor with catalyst pattern strategy is an attractive application for production of ethylene and cyclohexane. The introduction of the concept of dual functionality of the well-mixed catalyst bed has appreciable improvement of the reactor performance in terms of high conversions, low temperatures and reduced total reactor lengths. The combined effect of the membrane and reaction coupling is believed to enhance the ethane conversion to completion at relatively low temperatures (720–800 K). These are important results, since it is known that excessive temperatures have destructive effects on the catalysts, the mechanical and chemical stability of the membranes and the reactors. Effective operating regions with optimal conditions are observed and an effective reactor length criterion is used to evaluate the performance of the reactor. In light of the results presented the optimal effective reactor length is favored by high temperature and tube side pressure. It seems that the potential application of coupling ethane and benzene reactions in fixed bed membrane reactors is promising. Future research should focus on different catalyst layer configurations and rigorous optimization studies. Further improvements are still to be expected both in scientific knowledge and industrial practice in ethylene industry.

ENTRAL LIBRARY
Acc. No. 613816
Date 24/10/08

CHAPTER III

MODEL DEVELOPMENT

3.0 Introduction

In this chapter, mathematical model equations have been developed for the dehydrogenation of cyclohexane carried out in tubular membrane reactor. The catalyst is packed on the shell side. The feed is a mixture of cyclohexane, hydrogen and argon and is passed through the shell side. Argon, as a sweep gas is passed through the tube side. The products benzene and hydrogen as well as some of the reactant i.e. cyclohexane is permeated by the membrane to the tube side. The kinetic model, constitutive relationships along with boundary conditions and operating conditions are mentioned as well.

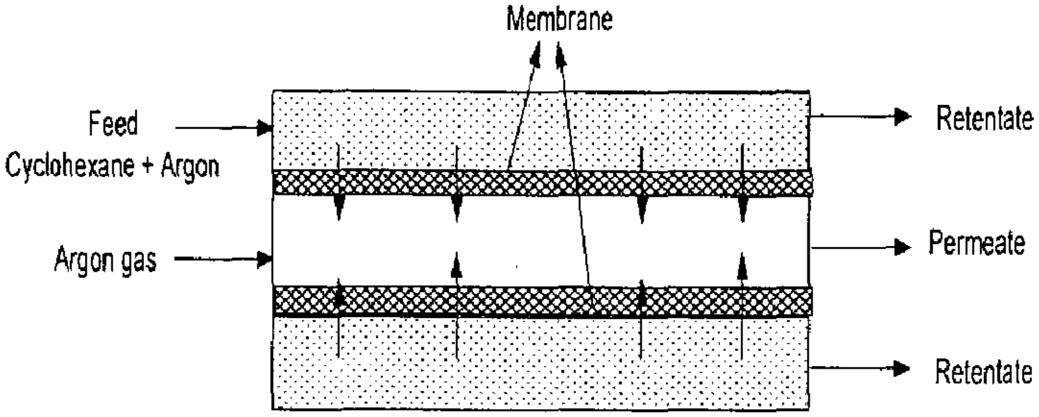

Fig 3.1: Schematic diagram of a membrane reactor

3.1 Kinetic Model

3.1.1 Reaction

Jeong.et.al. [15] studied the catalytic dehydrogenation of cyclohexane in an hybrid membrane reactor and observed that no by product, except benzene and hydrogen were present in the product stream.

The dehydrogenation reaction of cyclohexane is

$$C_6H_{12} \xrightleftharpoons{Pt/Al_2O_3} C_6H_6 + 3H_2 \qquad \Delta H=206.2\ \text{KJ/mol} \qquad (3.1)$$

3.1.2 Rate Expression

The dehydrogenation rate of reaction of cyclohexane r_C[12] is as follows:

$$r_C = \frac{k[K_p p_C - p_B p_H^3]}{p_H^3 + K_B K_p p_C} \qquad (3.2)$$

where k, K_B and K_P are the reaction rate constant, adsorption equilibrium constant for benzene, and the reaction equilibrium constant respectively. The expressions for the constants are

$k=0.44\ \exp(-4270/T)$ mol m^{-3} Pa^{-1} s^{-1} (3.3)

$K_B=2.03 \times 10^{-10} \exp(6270/T)$ Pa^{-1} (3.4)

$K_P=4.89 \times 10^{35} \exp(-26490/T)$ Pa^3 (3.5)

3.2 Catalyst

The dehydrogenation of cyclohexane is performed in the membrane reactor with 1 wt % Pt/Al_2O_3 as a catalyst. The reaction temperature is in the range of 423-500 K.

3.3 Membrane

The simulated membrane reactor was composed of a quartz glass tube containing an FAU-type zeolite membrane, which was fixed coaxially in the tubular reactor as shown in Fig 3.1. The flux of component i through membrane can be written as

$J_i=Q_i\Delta p_i$ (3.6)

where Q_i is the permeance of component i which depends upon membrane characteristics and temperature. In order to evaluate the permeance of cyclohexane, benzene and hydrogen at different temperatures for FAU type zeolite membrane experiment data have been taken from studies of Jeong.et.al. [14] and are fitted to a polynomial for each component.

The developed equations are as follows:

$$Q_C = 1.025 \times 10^{-14}\, T^3 - 2.365 \times 10^{-11}\, T^2 + 1.643 \times 10^{-8}\, T - 3.408 \times 10^{-6} \qquad (3.7)$$

$$Q_B = 1.14 \times 10^{-12}\, T^3 - 1.691 \times 10^{-9}\, T^2 + 8.317 \times 10^{-7}\, T - 1.341 \times 10^{-4} \qquad (3.8)$$

$$Q_H = 6.503 \times 10^{-13}\, T^3 - 9.703 \times 10^{-10}\, T^2 + 4.823 \times 10^{-7}\, T - 7.911 \times 10^{-5} \qquad (3.9)$$

3.4 Assumptions

A mathematical model is developed to study the performance of an FAU type zeolite membrane reactor under the following assumptions:

- Isothermal conditions
- No variation of pressure along the length
- Plug flow on both feed and permeate side
- Axial or radial diffusion excluded
- Non-reactive sweep gas
- Permeation through the membrane is proportional to the difference in partial pressures between feed and permeate side.

3.5 Choice of Control Volume

For developing the model we divide the length of reactor L into small elemental length dz (as shown in Fig 3.2) and carry out the mass balance around dz both on shell side and tube side. The concentration of all components present and other physical properties are assumed to be constant with in the control volume.

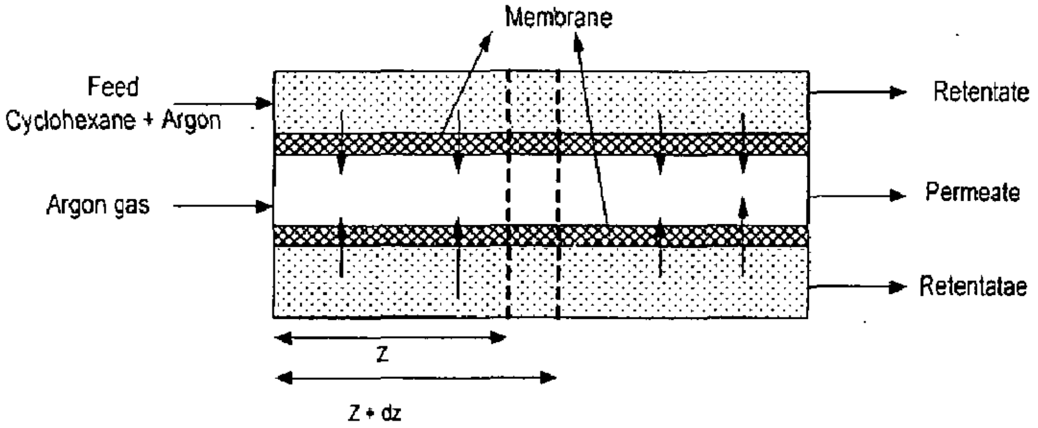

Fig.3.2: Selection of control volume for membrane reactor

3.6 Material Balance

The component mass balance equations in terms of molar flow rates are derived around the control volume as mentioned above and the final model is given by the following equations.

Shell side

rate$_{in}$ – rate$_{out}$ + rate of formation – permeation through the membrane = Rate of accumulation

$$F_{i,F}\big|_z - F_{i,F}\big|_{z+\Delta z} + \upsilon_i r_c \pi (r_3^2 - r_2^2)\Delta z - 2\pi r_2 J_i \Delta z = 0 \tag{3.10}$$

On dividing the equation (3.10) by dz and taking limit Δz→0

$$\frac{F_{i,F}\big|_z - F_{i,F}\big|_{z+\Delta z}}{\Delta z} + \upsilon_i r_c \pi (r_3^2 - r_2^2) - 2\pi r_2 J_i = 0$$

$$\frac{dF_{i,F}}{dz} = \upsilon_i r_c \pi (r_3^2 - r_2^2) - 2\pi r_2 J_i \tag{3.11}$$

Tube side

rate$_{in}$ – rate$_{out}$ + rate of formation + permeation through the membrane = Rate of accumulation

$$F_{i,P}\big|_z - F_{i,P}\big|_{z+\Delta z} + 2\pi r_2 J_i \Delta z = 0 \tag{3.12}$$

On dividing equation (3.12) by dz and taking limit Δz→0

$$\frac{F_{i,P}\big|_z - F_{i,P}\big|_{z+\Delta z}}{\Delta z} + 2\pi r_2 J_i = 0$$

$$\frac{dF_{i,P}}{dz} = 2\pi r_2 J_i \tag{3.13}$$

From equation (3.6) $J_i = Q_i \Delta p_i$, Thus shell side equation becomes:

$$\frac{dF_{i,F}}{dz} = \upsilon_i r_c \pi (r_3^2 - r_2^2) - 2\pi r_2 Q_i (P_F x_i - P_P y_i) \tag{3.14}$$

and equation (3.13) becomes:

$$\frac{dF_{i,P}}{dz} = 2\pi r_2 Q_i (P_F x_i - P_P y_i) \tag{3.15}$$

where i=C_6H_{12}, C_6H_6, H_2, Ar

The total material balance equations for all the species is given by:

Shell side (Reaction side)

C_6H_{12}: $$\frac{dF_{C,F}}{dz} = -r_C \pi (r_3^2 - r_2^2) - 2\pi r_2 Q_C (P_F x_C - P_P y_C) \tag{3.16}$$

C_6H_6: $$\frac{dF_{B,F}}{dz} = r_C \pi (r_3^2 - r_2^2) - 2\pi r_2 Q_B (P_F x_B - P_P y_B) \tag{3.17}$$

H_2: $$\frac{dF_{H,F}}{dz} = 3 r_C \pi (r_3^2 - r_2^2) - 2\pi r_2 Q_H (P_F x_H - P_P y_H) \tag{3.18}$$

Ar: $$\frac{dF_{Ar,F}}{dz} = -2\pi r_2 Q_{Ar} (P_F x_{Ar} - P_P y_{Ar}) \tag{3.19}$$

Tube side (Permeate side)

C_6H_{12}: $$\frac{dF_{C,P}}{dz} = 2\pi r_2 Q_C (P_F x_C - P_P y_C) \tag{3.20}$$

C_6H_6: $$\frac{dF_{B,P}}{dz} = 2\pi r_2 Q_B (P_F x_B - P_P y_B) \tag{3.21}$$

H_2: $$\frac{dF_{H,P}}{dz} = 2\pi r_2 Q_H (P_F x_H - P_P y_H) \tag{3.22}$$

Ar: $$\frac{dF_{Ar,P}}{dz} = 2\pi r_2 Q_{Ar} (P_F x_{Ar} - P_P y_{Ar}) \tag{3.23}$$

The relationship between total and partial pressures of each component can be expressed by the following equation:

$$p_i = \left(\frac{F_i}{\sum F_i} \right) P_F \tag{3.24}$$

where i=C_6H_{12}, C_6H_6, H_2 in the feed side

3.7 Mathematical Model

The mathematical model comprises of set of a mathematical equation, boundary conditions and constitutive relationships. They are presented sequentially in this section.

3.7.1 Set of Mathematical Equations

Model includes 8 differential equations presented by equations (3.16 – 3.19) for reaction side and equations (3.20 – 3.23) for permeate side. In these equations z is independent variable and 8 state variables $F_{C,F}$, $F_{B,F}$, $F_{H,F}$, $F_{Ar,F}$ for reaction side and $F_{C,P}$, $F_{B,P}$, $F_{H,P}$, $F_{Ar,P}$ for the permeate side.

3.7.2 Boundary Conditions

The initial conditions of the parameters at the inlet of the reactor are listed below:

At z = 0,

Reaction side:

$$F_{C,F} = F_{C,F,0} = 9.0434 \times 10^{-7} \text{ mol/s} \quad (3.25)$$

$$F_{B,F} = F_{B,F,0} = 0 \quad (3.26)$$

$$F_{H,F} = F_{H,F,0} = 0 \quad (3.27)$$

$$F_{Ar,F} = F_{Ar,F,0} = 8.1390 \times 10^{-6} \text{ mol/s} \quad (3.28)$$

Permeate side:

$$F_{C,P} = F_{C,P,0} = 0 \quad (3.29)$$

$$F_{B,P} = F_{B,P,0} = 0 \quad (3.30)$$

$$F_{H,P} = F_{H,P,0} = 0 \quad (3.31)$$

$$F_{Ar,P} = F_{Ar,P,0} = 4.5217 \times 10^{-5} \text{ mol/s} \quad (3.32)$$

3.7.3 Constitutive Relationship

Equations (3.2) to (3.5) represent the kinetic properties for the dehydrogenation of cyclohexane and equations (3.6) to (3.9) represent permeation properties of components through zeolite membranes.

Table 3.1: Operating conditions[15]

Name	Parameter Specification/Value
Reactor	
Length(m)	6×10^{-2}
Inner radius(m)	5×10^{-3}
Membrane Packing	
Membrane Type	FAU- type Zeolite membrane
Length(m)	6×10^{-2}
Inner Radius(m)	0.85×10^{-3}
Outer Radius(m)	1.05×10^{-3}
Catalyst	1.0 wt % Pt/Al_2O_3
Cross Sectional Area of the bed, feed side(m^2)	7.5×10^{-5}
Molar Flow Rate	
Feed Flow Rate, Feed side(mol/s)	9.0434×10^{-6}
Sweep Flow Rate, Permeate side(mol/s)	4.5217×10^{-5}
Composition	
Mole Fraction of Cyclohexane, Feed side	0.1
Mole Fraction of Diluent(Argon), Feed side	0.9
Mole fraction of Diluent(Argon), Tube side	1(pure)
Total Pressure	
Feed side(P_F)(Pa)	1.013×10^5
Permeate side(P_P)(Pa)	1.013×10^5
Permeance (Jeong.et.al.[3]	
Q_A (Argon)(mol m^{-2} s^{-1} Pa^{-1})	1.0×10^{-10}

3.8 Solution

In order to predict the performance of the model, solution of the model equation is very essential. The developed mathematical model consists of a set of nonlinear ordinary coupled differential equations. These equations constitutes initial value problem. So we can use ODE solvers of MATLAB to solve these equations. The model have been solved using operating conditions mentioned in Table 3.1 using solver "ode45" of MATLAB. The performance of the reactor is studied on the basis of conversion of cyclohexane. The model equations have been solved for fixed bed by putting permeance through membrane equal to zero at operating conditions of experimental studies carried out by Jeong.et.al. [15]. The percentage conversion of cyclohexane can be evaluated by the following expression:

$$\% X_C = \left(\frac{F_{C,0} - F_{C,1}}{F_{C,0}} \right) 100 \tag{3.33}$$

$F_{C,1}$ includes the flow rate of cyclohexane at the outlet of the permeate and at the outlet of the retentate side.

Percent selectivity and percent yield can be expressed by the following formulae

$$\% \text{ yield of } H_2 = \frac{H_2(Produced)}{Cyclohexane(feed)} X100 \tag{3.34}$$

$$\% \text{ selectivity of } H_2 = \frac{H_2(Produced)}{\sum_P P(Produced)} \tag{3.35}$$

where P (Produced) = P (retented) + P (permeated)

P = Hydrogen and Benzene

RESULTS AND DISCUSSION

4.0 INTRODUCTION

The present research study has been carried out for two feed conditions. In the first feed conditions cyclohexane and argon are mixed in 1:9 molar ratio and in the second feed condition hydrogen is also mixed with cyclohexane and argon in 1:8.8:0.2 molar ratio. For both the feed conditions, three reactor configurations have been considered viz conventional fixed bed, full length membrane reactor and hybrid reactor. These feeds have been introduced in all three reactor configuration and performance of the reactors have been studied. In the permeate side, argon is taken as the sweep gas in all cases. In the literature [15], it is mentioned that the permeation of argon through FAU type membrane is very low (1×10^{-10} mol m^{-2} s^{-1} Pa^{-1}) therefore in the present study permeation of argon is neglected as compared to the permeation of other components.

4.1 Feed without hydrogen

4.1.1 Model Validation

The mathematical model equations have been solved for conventional fixed bed reactor under operating and boundary conditions mentioned in chapter 3. The feed is considered to be a mixture of cyclohexane and argon only. The conversion of cyclohexane has been estimated at different feed temperatures. These model based conversions have been compared with the experimental study based conversion in Fig 4.1. The experimental values have been taken from Jeong et al. [15]. From Fig 4.1 it is clear that all model results are within ± 4% of the experimental results. Therefore it can be concluded that our model is correct and is able to predict the result within acceptable limit of errors.

4.1.2 Effect of temperature on conversion of cyclohexane

4.1.2.1 Conventional fixed bed

Fig 4.2 depicts the percent conversion of cyclohexane at various temperatures. The conversion increases with increase in temperature. The valid reason is that the dehydrogenation reaction is endothermic in nature. Therefore on increasing the temperature, the forward reaction rate increase which leads to increase in conversion of cyclohexane. The figure also depicts that the increase in conversion at higher temperature is much larger as compared to increase at lower temperature which is attributed to the same reason of endothermicity.

4.1.2.2 Full length membrane reactor

The membrane in the reactor acts as a separator for at least one of the products. In reversible reactions, the continuous removal of one of the products shifts the reaction equilibrium towards right. This shift enhances the conversion of the reactant. Here FAU type of membrane has been used which is permeable to all the components but selectivity is different for different components. The permeation of the component through membrane depends upon the permeance of that component and the driving force which is the partial pressure difference across the membrane in case of gaseous mixture. Therefore products as well as the reactants may permeate through the membrane. So as the reaction proceeds, the products get permeated through the membrane along with the small amounts of reactants. This separation increases the conversion from the conversion achieved in conventional fixed bed reactor where there is no separation of one of the products through membrane. This fact is clearly shown in Fig 4.3 where conversion at one temperature is higher than the conversion obtained in fixed bed reactor (Fig 4.2) at that temperature.

4.1.2.3 Hybrid Reactor

FAU is porous type of membrane. These membranes are permeable for all the components. The permeation of the component depends upon the pore size and molecular size of the component. In porous membranes, therefore, there always occurs the permeation of reactant specially at the inlet section of the reactant where partial pressure of the reactant is higher than the product. As a result there is loss of reactant. To avoid the loss of reactant, hybrid type of reactor is commonly employed to utilize membrane and to achieve higher conversion. The hybrid reactor is the combination of conventional fixed bed followed by membrane reactor. The reaction is carried out in fixed bed reactor. After achieving

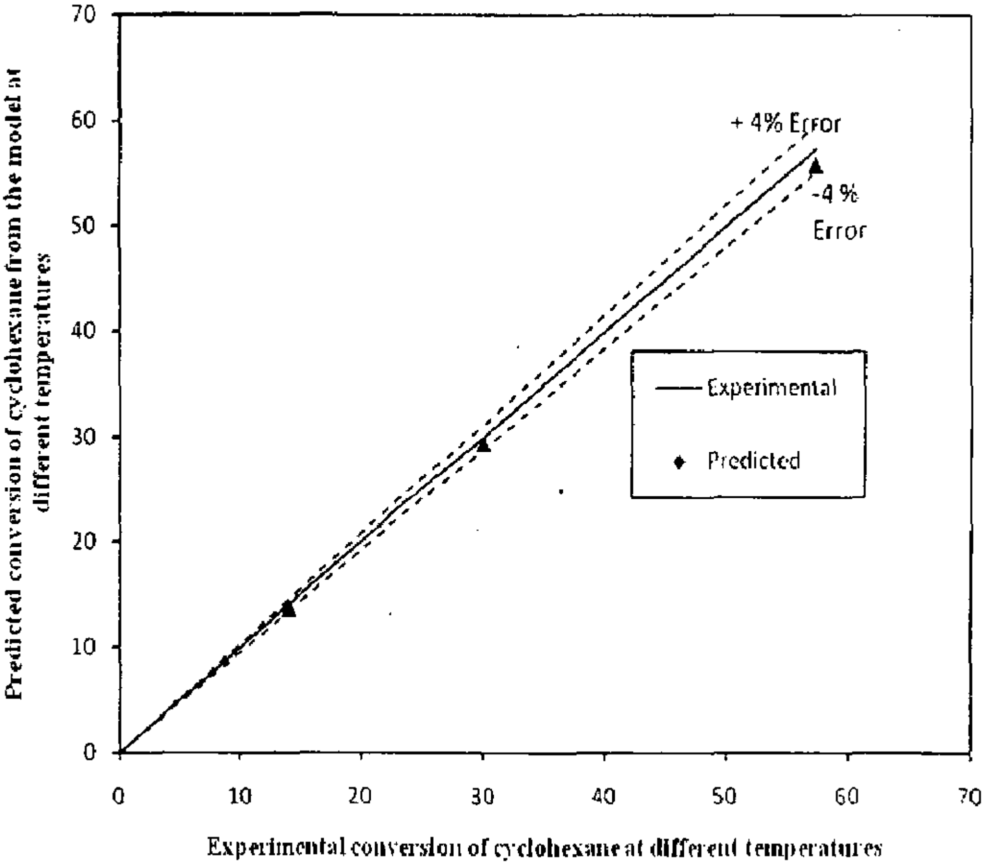

Fig 4.1: Comparison of percent conversion of cyclohexane at various temperatures with experiment values.

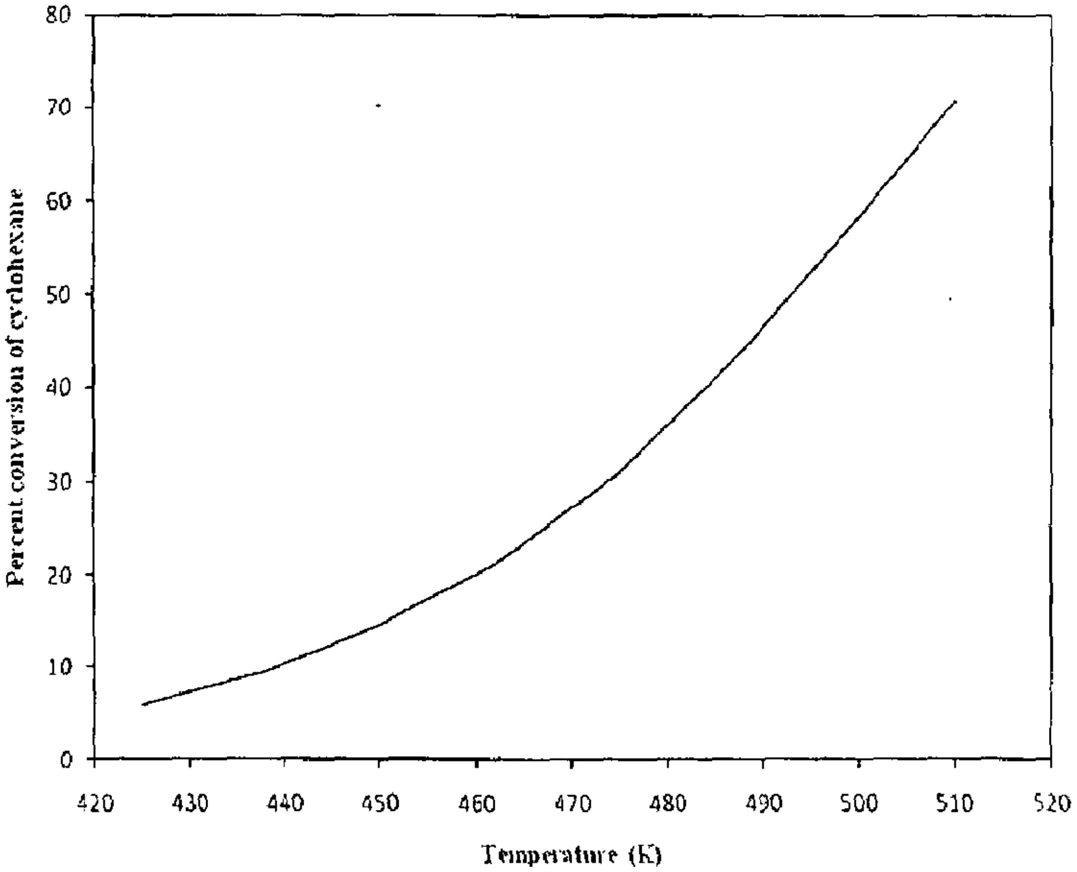

Fig.4.2: Variation of percent conversion of cyclohexane with temperature for fixed bed reactor with no H_2 in the feed side.

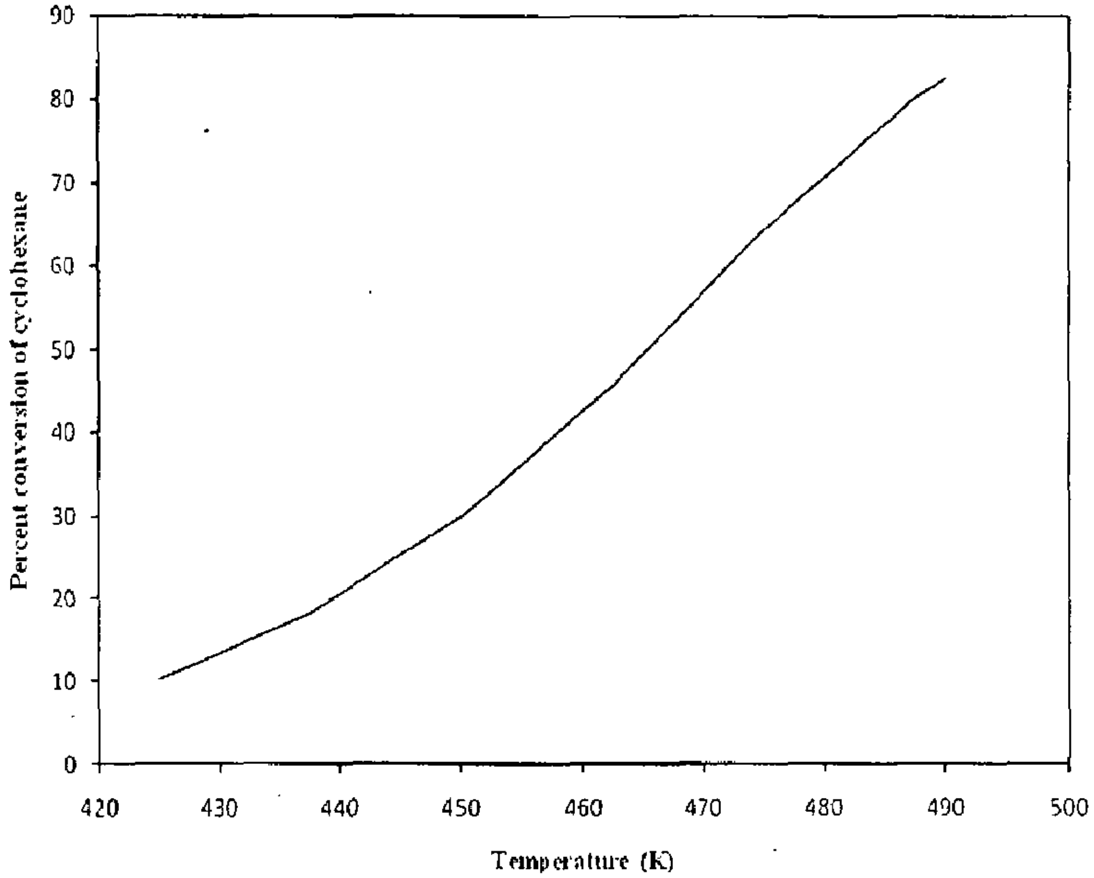

Fig.4.3: Variation of percent conversion of cyclohexane with temperature for membrane reactor with no H_2 in the feed side.

the equilibrium in fixed bed reactor, the reaction mixture is passed through the membrane reactor. The mixture which enters the membrane reactor is lean in reactant and rich in product. This shows low driving force for the permeation of the reactant and high driving force for the permeation of products through the membranes and shifts the equilibrium towards right to further increase the conversion of reactant and to enhance the yield of products.

In the present study, the equilibrium with fixed bed reactor has been achieved at length 0.04m. This bed is connected with membrane reactor of length 0.02m which gives the total length of hybrid reactor as 0.06m. Fig 4.4, 4.5 and 4.6 show the variation in conversion along the length of hybrid reactor. These figures indicate that the conversion is less than the conversion achieved from the pure membrane reactor (Fig 4.3) but higher than conversion in conventional fixed bed reactor (Fig 4.2). For instance at temperature 448 K the conversion in fixed bed is 13.65, for pure membrane reactor it is 27.82 where as for hybrid reactor it is 19.12. However at the expense of cost of membrane and loss of reactant, hybrid reactor is more economical than full length membrane reactor.

4.1.3 Variation of molar flow rate along the length of reactor

4.1.3.1 Full length membrane reactor

Fig 4.7, 4.8 and 4.9 shows the variation in molar flow rate of cyclohexane, benzene and hydrogen in the reaction side of full length membrane reactor at temperature of 448 K, 473 K and 490 K respectively. In Fig 4.7 we observe typical trends for the flow rate of reactants and products in a reactor. This figure is at temperature of 448 K. As the reaction proceeds the flow rate of cyclohexane decreases along the length of the reactor while the flow rate of benzene and hydrogen increases. Since benzene and hydrogen are produced in molar ratio of 1:3, molar flow rate of benzene is quite low as compared to hydrogen. The trends for hydrogen and benzene are observed to be different at higher temperature of 473 K and 490 K (Fig 4.8 and 4.9). The flow rate of hydrogen and benzene reaches at maximum value and then decreases. At 473 the flow rate of hydrogen decreases slowly while at 490 it decreases rapidly. The decrease in flow rate of benzene is very slow at both temperatures of 473 K and 490 K. These trends are due to very high permeation rate of hydrogen as compared to permeation rate of benzene at that temperature. The high temperature enhances not only the permeance (Table 4.1) but also the formation rates of hydrogen and benzene which in turn increase the driving force for permeation through membrane.

Table 4.2 shows the yield of hydrogen in membrane reactor. The yield of hydrogen increases with increase in temperature. As far as selectivity is concerned, the selectivity of hydrogen is 75% and of benzene is 25% at all temperatures and for all types of reactor configurations as only dehydrogenation reaction of cyclohexane is being considered in the present study and side reactions are assumed to be neglected. On this ground, the yield of benzene is one third of yield of hydrogen.

In Fig 4.10, 4.11 and 4.12 the molar flow rates of cyclohexane, benzene and hydrogen in the permeate side of the reactor are plotted against the length of full length membrane reactor at temperature 448, 473 and 490 K respectively. Fig 4.10 indicates that the flow rate of hydrogen is maximum while the flow rate of benzene is minimum at 448 K. In the beginning section, the flow rate of cyclohexane is higher than benzene and hydrogen but afterwards as the reaction proceeds it lies between benzene and hydrogen. This is because the permeance of benzene through FAU type of zeolite membrane is maximum and that of cyclohexane is minimum (Table 4.1). In the reaction side at 448 K, the endothermic dehydrogenation rate of cyclohexane and so the conversion is low. As a result the partial pressure of cyclohexane is high and partial pressure of benzene and hydrogen is low. Since molar formation rate of hydrogen is three times higher than molar formation rate of benzene, the partial pressure of hydrogen is three times the partial pressure of benzene. Thus in order to permeate through membrane, the driving force, which is the partial pressure difference across the membrane, is three times higher for hydrogen than for benzene. Therefore, inspite of having high permeance, the flow rate of permeated benzene is less than the flow rate of permeated hydrogen. Owing to the low conversion of cyclohexane, the partial pressure for cyclohexane is higher at the beginning section of the reactor which gives higher permeation for cyclohexane and so higher flow rate of cyclohexane in the permeate side. As the reaction proceeds the partial pressure of cyclohexane decreases but remains higher than partial pressure of benzene because of low conversion at low temperature and also formation of one mole of benzene from the consumption of one mole of cyclohexane. Therefore, in Fig 4.10, the flow rate of cyclohexane lies between hydrogen and

Table 4.1: Permeances of components through FAU type zeolite membrane at different temperatures

Component	Permeance at 448 K (mol m^{-2} s^{-1} Pa^{-1})	Permeance at 448 K (mol m^{-2} s^{-1} Pa^{-1})	Permeance at 448 K (mol m^{-2} s^{-1} Pa^{-1})
Cyclohexane	1.2762 x 10^{-7}	1.5689 x 10^{-7}	1.70237 x 10^{-7}
Benzene	1.6147 x 10^{-6}	1.6075 x 10^{-6}	1.5437 x 10^{-6}
Hydrogen	6.8928 x 10^{-7}	7.5087 x 10^{-7}	7.5511 x 10^{-7}

Table 4.2 Yield of hydrogen at different temperatures

Reactor configuration	Yield at 448 K	Yield at 473 K	Yield at 490 K
Conventional fixed bed	40.94	88.38	138.88
Full length membrane	83.4	184.2	247.6
Hybrid	57.34	130.94	202.26

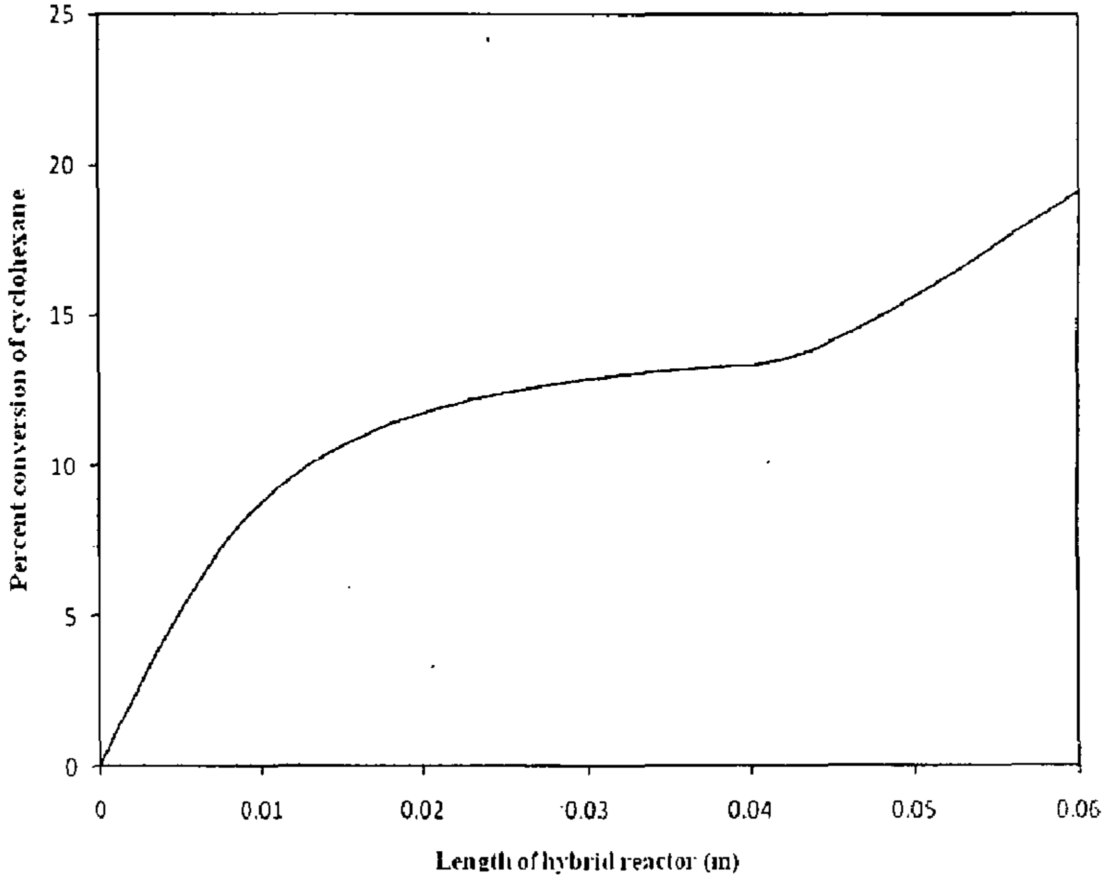

Fig.4.4: Variation of percent conversion of cyclohexane along the length of hybrid reactor at 448 K with no H_2 in the feed

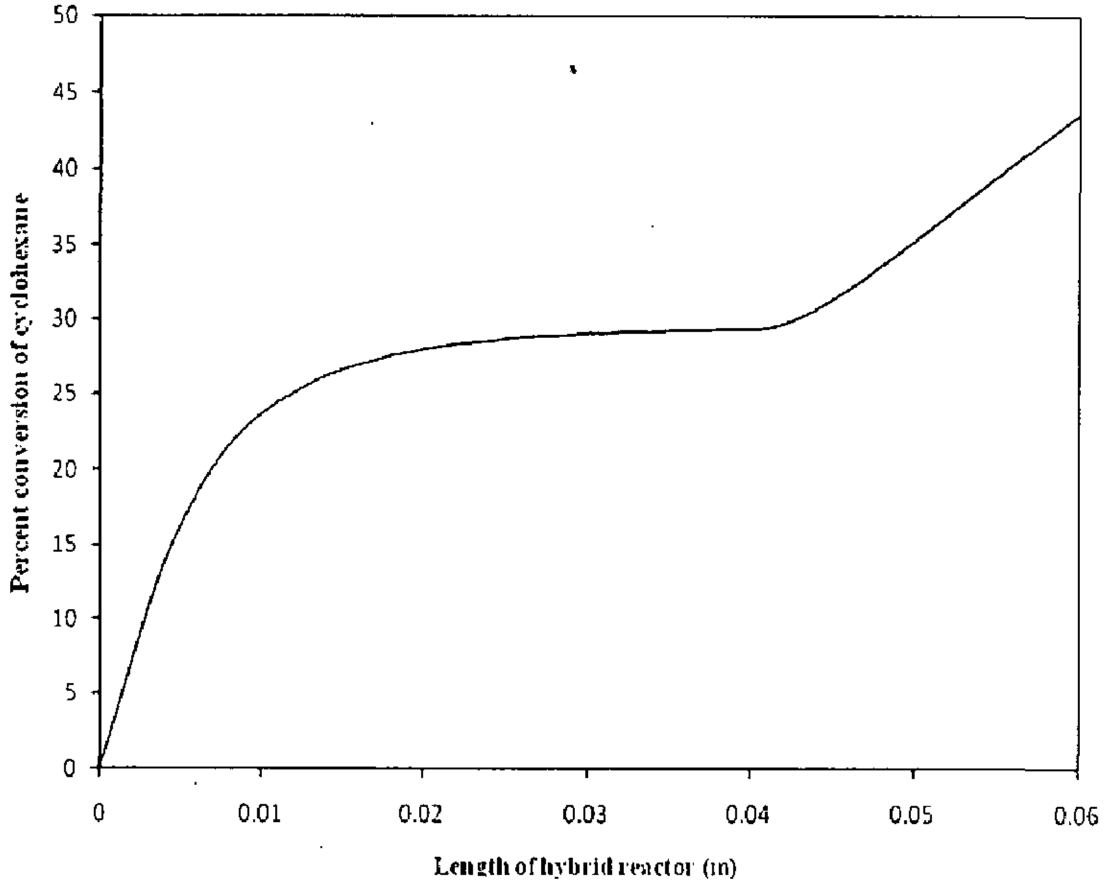

Fig.4.5: Variation of percent conversion of cyclohexane along the length of hybrid reactor at 473 K with no H_2 in the feed

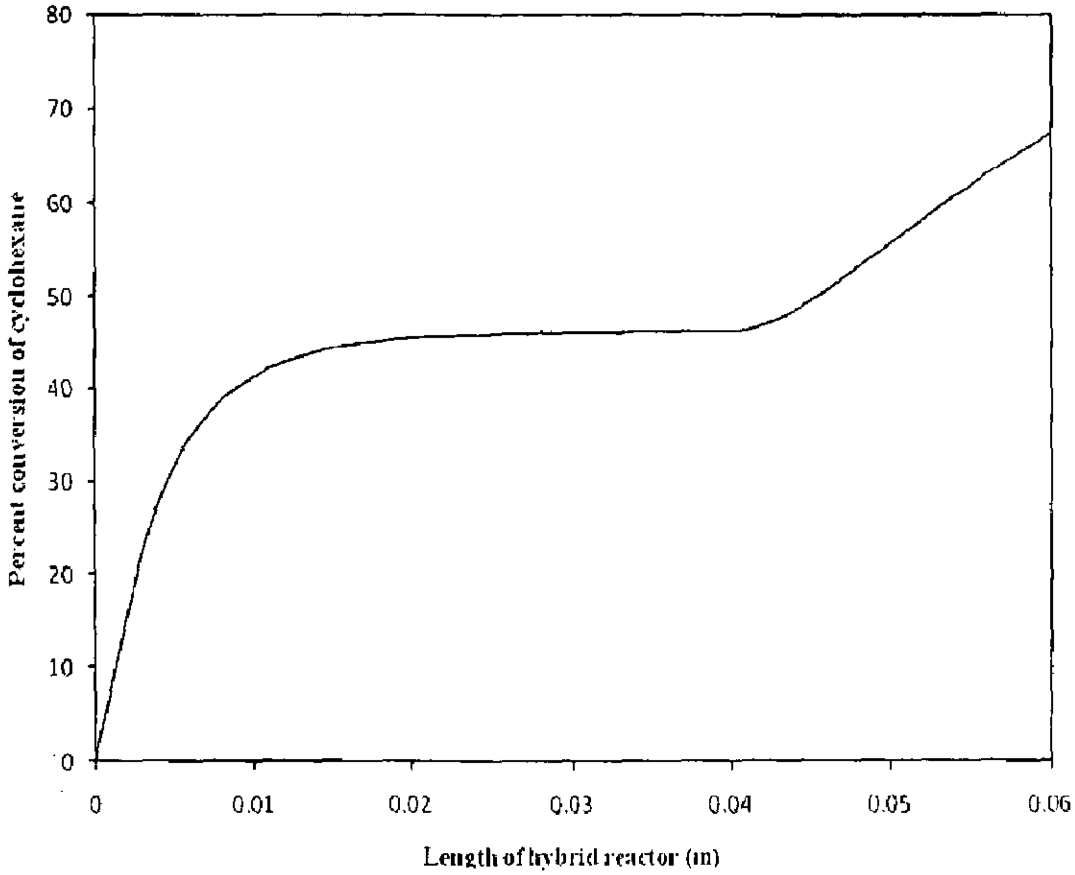

Fig.4.6: Variation of percent conversion of cyclohexane along the length of hybrid reactor at 490 K with no H_2 in the feed

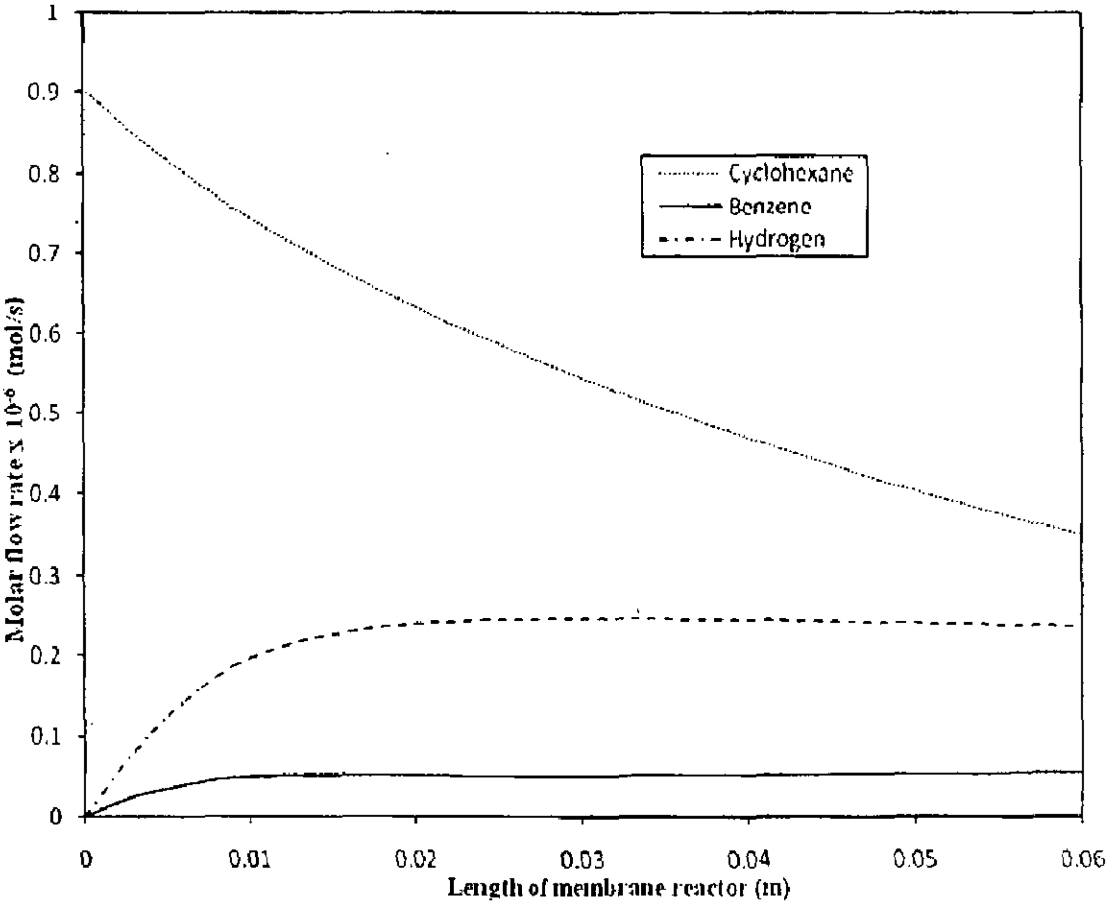

Fig.4.7: Variation in the molar flow rate along the length of the membrane reactor in the reaction side at 448 K with no H_2 in the feed.

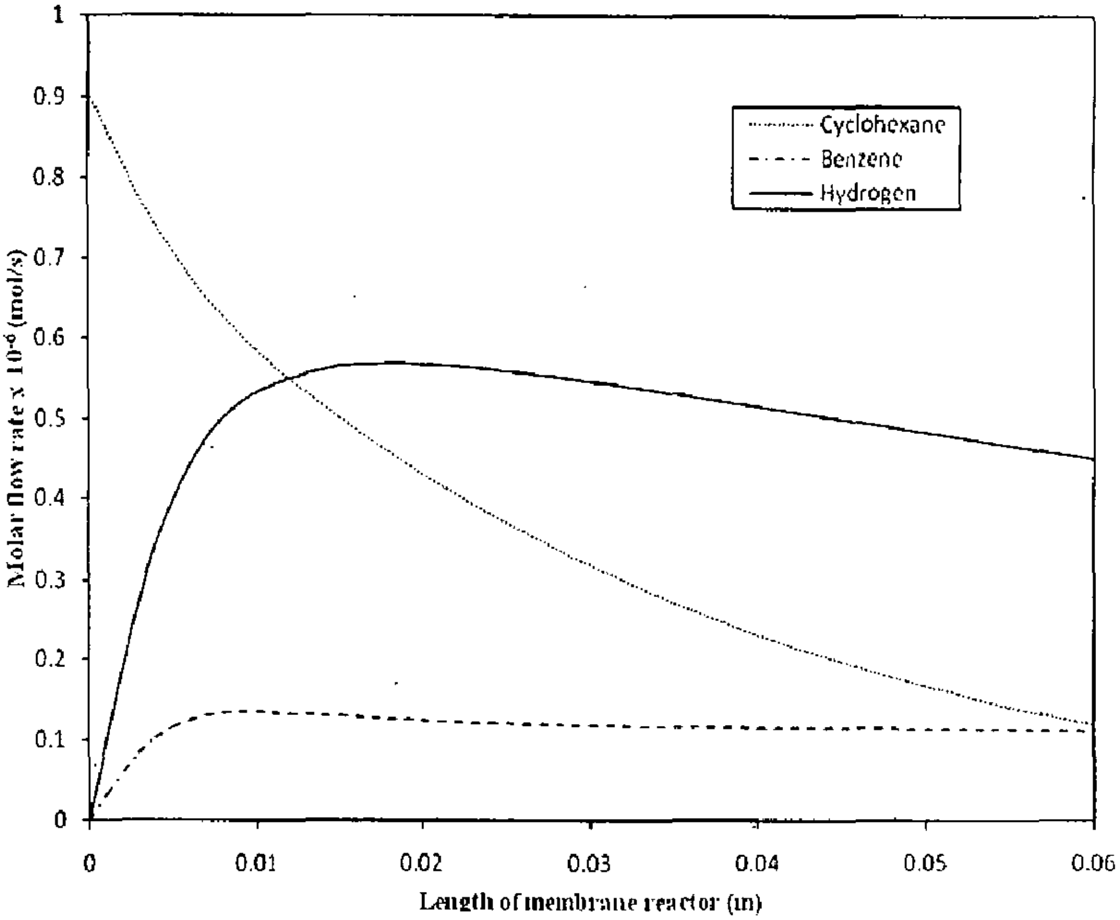

Fig.4.8: Variation in the molar flow rate along the length of the membrane reactor in the reaction side at 473 K with no H_2 in the feed.

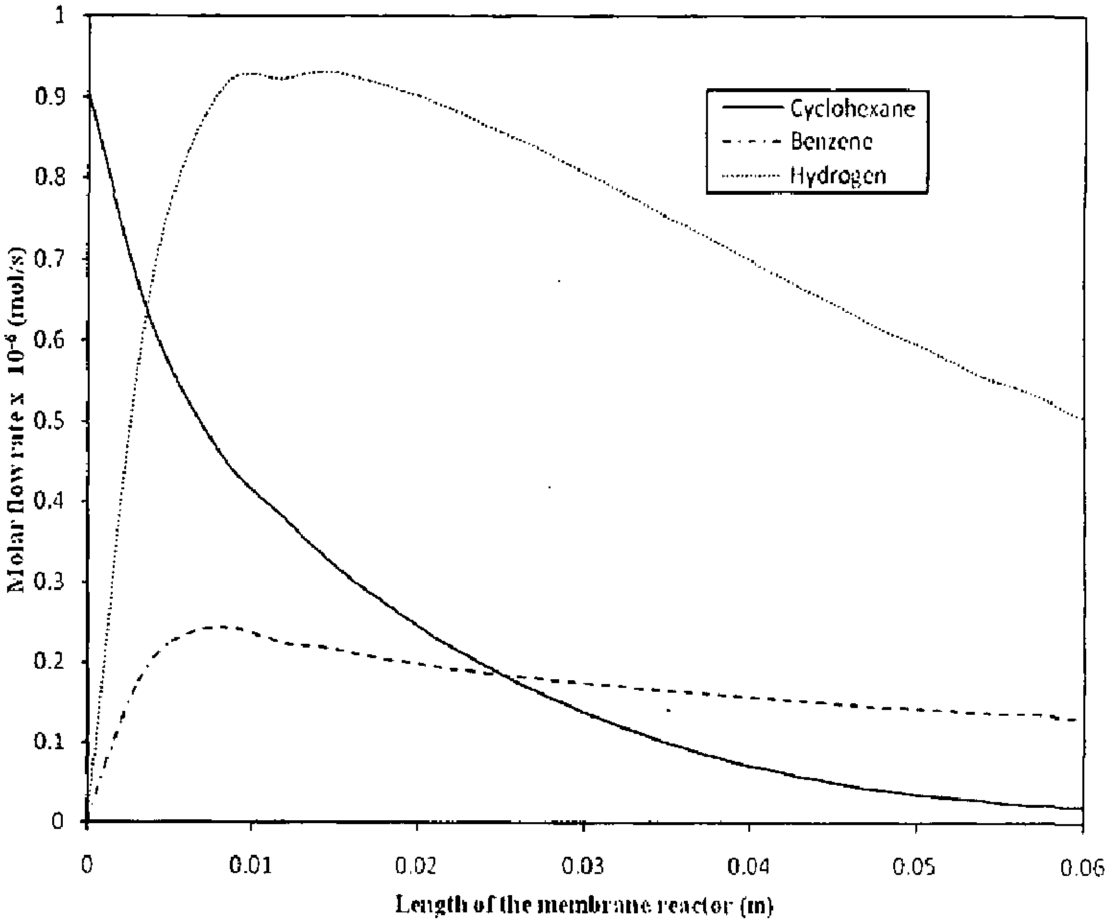

Fig.4.9: Variation in the molar flow rate along the length of the membrane reactor in the reaction side at 490 K with no H_2 in the feed.

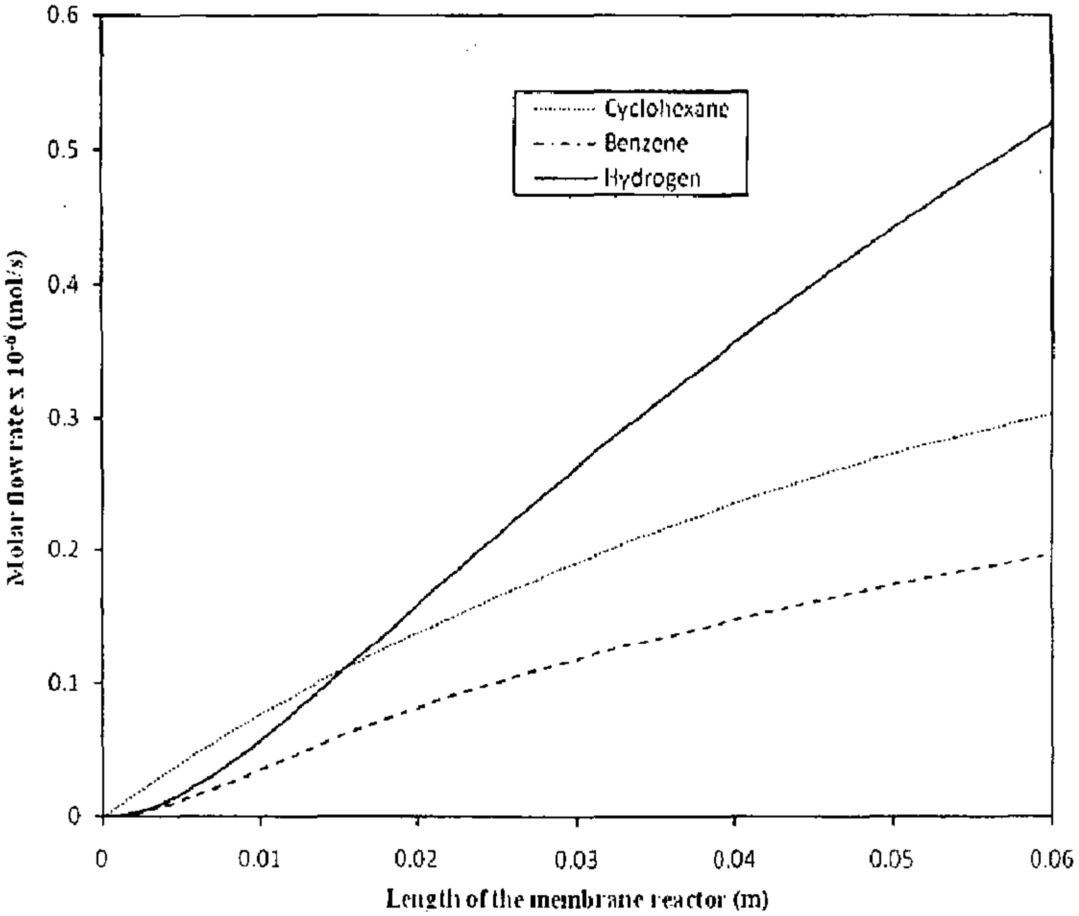

Fig.4.10: Variation in the molar flow rate along the length of the membrane reactor in the permeate side at 448 K with no H_2 in the feed.

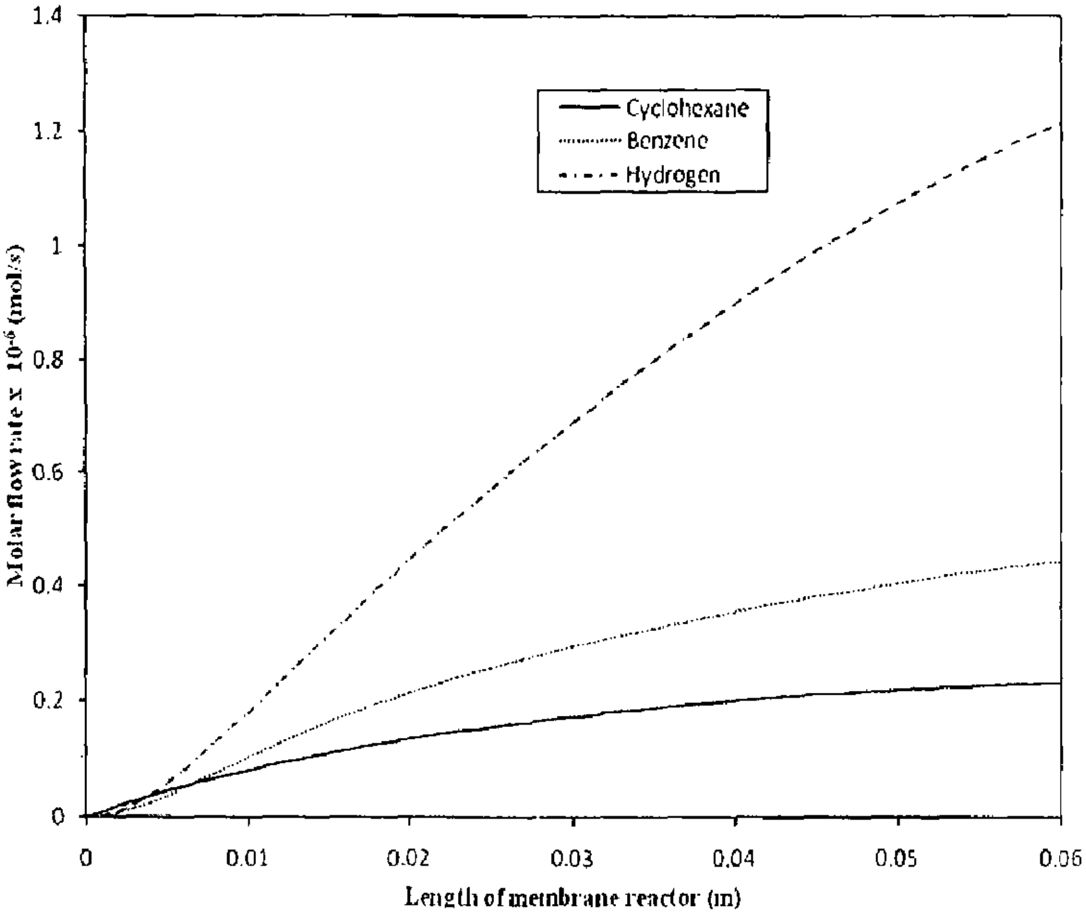

Fig.4.11: Variation in the molar flow rate along the length of the membrane reactor in the permeate side at 473 K with no H_2 in the feed.

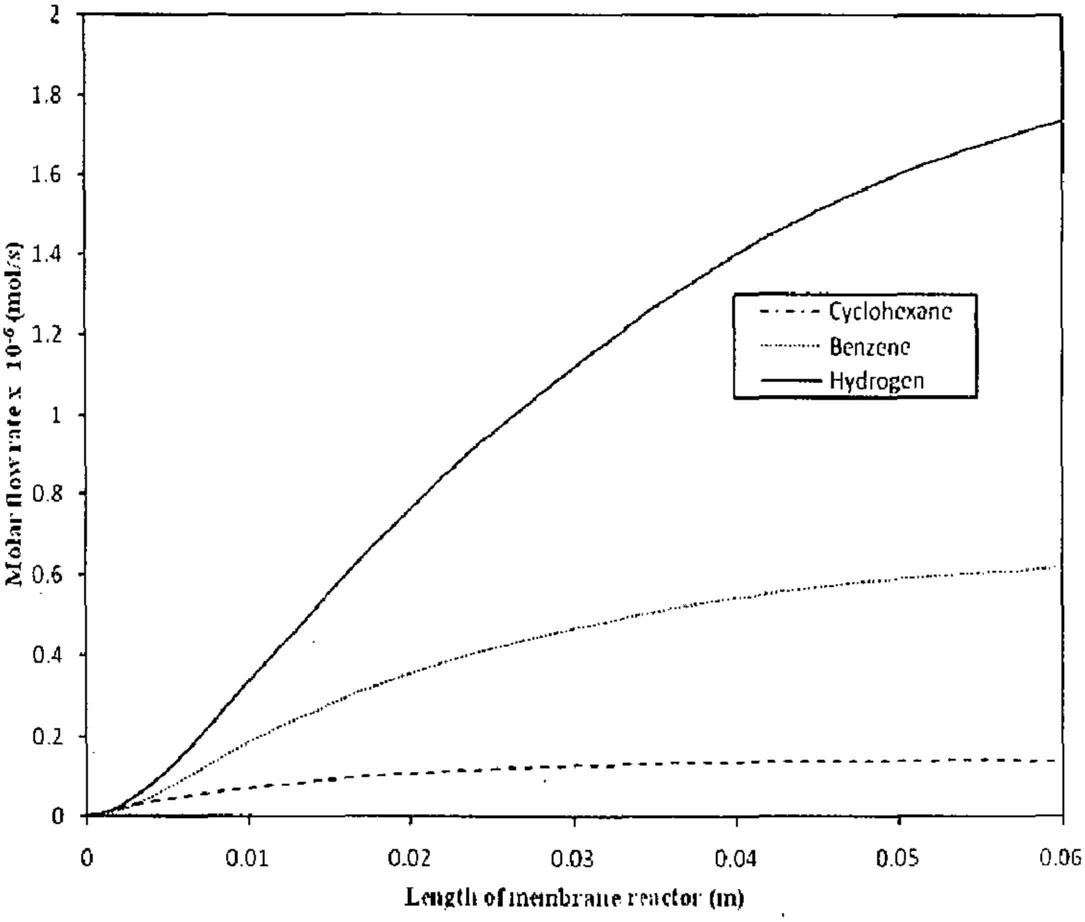

Fig.4.12: Variation in the molar flow rate along the length of the membrane reactor in the permeate side at 490 K with no H_2 in the feed.

benzene. As the temperature increases (Fig 4.11 and 4.12) the reaction rate of endothermic dehydrogenation reaction increases. Consequently, the conversion of cyclohexane increases and partial pressure of cyclohexane in the reaction side decreases. At the same time the flow rate of benzene and hydrogen increases. This results in higher permeation rate of benzene and hydrogen through membrane. In Fig 4.11 and 4.12, therefore, the flow rate of cyclohexane is lowest while that of hydrogen is highest in permeate side of the reactor at higher temperature.

4.3.1.2 Hybrid reactor

This is a fixed bed reactor in conjunction with a membrane reactor. In a full length membrane reactor the permeation rate of cyclohexane resulting from the high partial pressure of cyclohexane, is always high in the beginning of the reactor. This indicates the significant loss of cyclohexane which is undesirable. In order to maximize the removal of hydrogen and benzene and to minimize the cyclohexane loss, the combination of conventional fixed bed and a membrane reactor has been considered. The cyclohexane can be sufficiently converted to benzene and hydrogen in the first stage of hybrid reactor (i.e. fixed bed) and achieve equilibrium. Then the mixture of product and unreacted cyclohexane is passed through the membrane reactor. Since a maximum amount of cyclohexane has been converted in fixed bed, the loss of cyclohexane can be reduced in the membrane reactor. In the present study at given operating conditions, the equilibrium is achieved at fixed bed length of 0.04m. This length is extended to 0.06 with membrane.

Fig 4.13, 4.14 and 4.15 provide the profiles of molar flow rate in reaction side of hybrid reactor at temperature of 448, 473 and 490 K respectively. At 448 K (Fig 4.13), beyond the length of 0.04m, the flow rate of cyclohexane decreases due to equilibrium shift towards right resulting from the permeation of products through the membrane. The flow rate of benzene and hydrogen also increases but at the same time, their permeation rate also increases which results in reduction in flow rates of benzene and hydrogen in membrane section. At higher temperature of 473 and 490 K, since the yield of hydrogen is very high in fixed bed (Table 4.2), the flow rate of hydrogen increases to a maximum value and then decreases in the membrane section due to permeation through the membrane. In addition to this, the flow rate of cyclohexane decreases rapidly at higher temperature of 490 K as compared to 473K because of high rate of conversion of cyclohexane.

Fig 4.16, 4.17 and 4.18 gives the variation of molar flow rate in the permeate side of hybrid reactor at temperature of 448 K, 473 K and 490 K respectively. These figures clearly show that the loss of cyclohexane is very small as compared to loss in full length membrane reactor. Flow rate of cyclohexane in all three figures is minimum. At very high temperature of 490 K, loss of cyclohexane is very small whereas separation of hydrogen is very high which promotes the high conversion of cyclohexane in reaction side. Table 4.2 indicates that hydrogen generation continues to increase with increase in temperature. This increase is more in hybrid reactor as compared to fixed bed reactor. Although yield of hydrogen in hybrid reactor is less than yield in full length membrane reactor, yet the hybrid reactor performance can be considered better at the expense of loss of reactant in full length membrane reactor. The selectivity remains same as 75% for hydrogen and 25% for benzene.

4.2 Feed with Hydrogen

From aforementioned results it is clear that a membrane reactor can maintain a higher yield than a conventional fixed bed reactor. The researchers (Jeong et al. [15]) in the literature investigated membrane reactor performance in terms of stability of membrane and catalyst under reaction conditions. It was concluded that the improvements in membrane stability as well as catalyst stability are needed before membrane reactor can be considered as realistic alternative to existing conventional reactor technology for cyclohexane dehydrogenation.

In the experimental studies, it was observed that in the absence of hydrogen in the feed, and continuous extraction of produced hydrogen through membrane, there may exist stability problems in the catalyst and membrane. The use of hydrogen in the reaction side feed makes the catalyst and membrane stable. Taking this aspect into account industrial processes generally use hydrogen stream in feed [5]. Therefore in this section the performance of the reactor has been studied under feed with hydrogen. The feed conditions and operating conditions are mentioned in chapter 3.

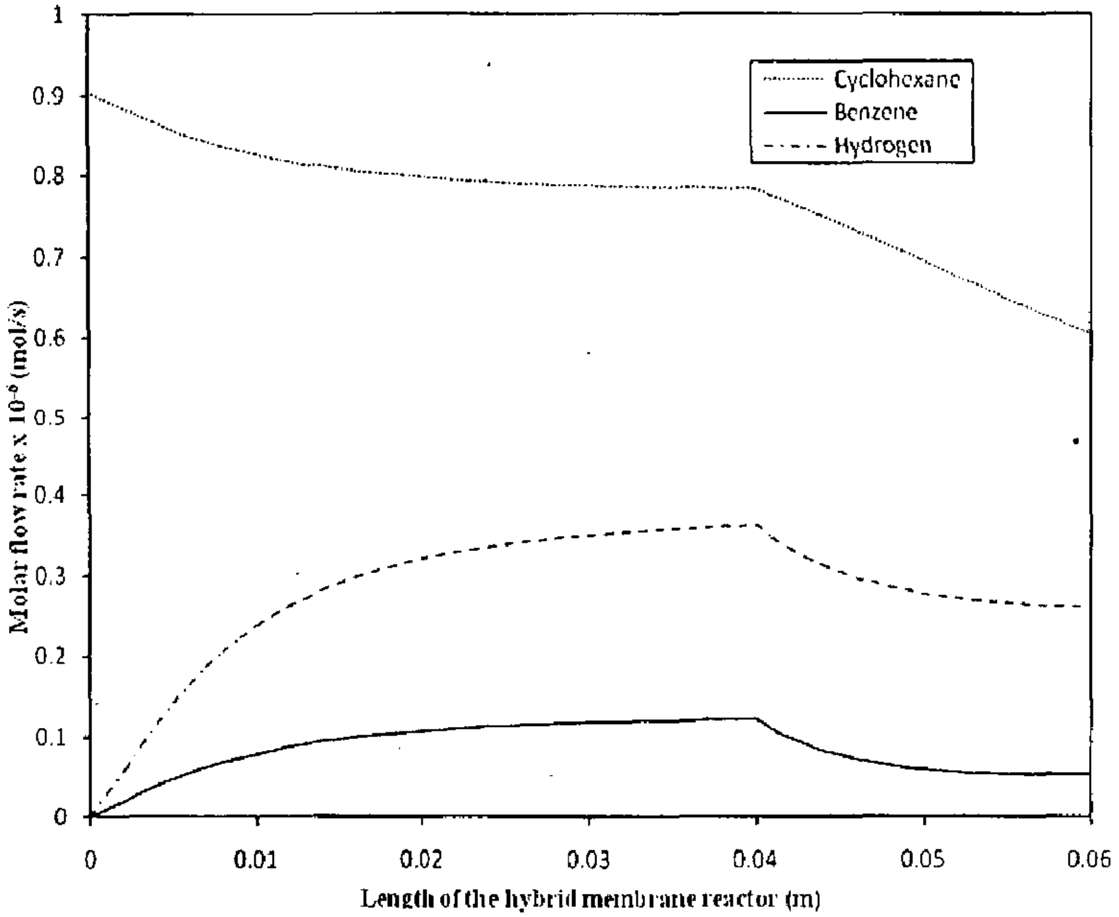

Fig.4.13: Variation in the molar flow rate along the length of the hybrid reactor in the reaction side at 448 K with no H_2 in the feed.

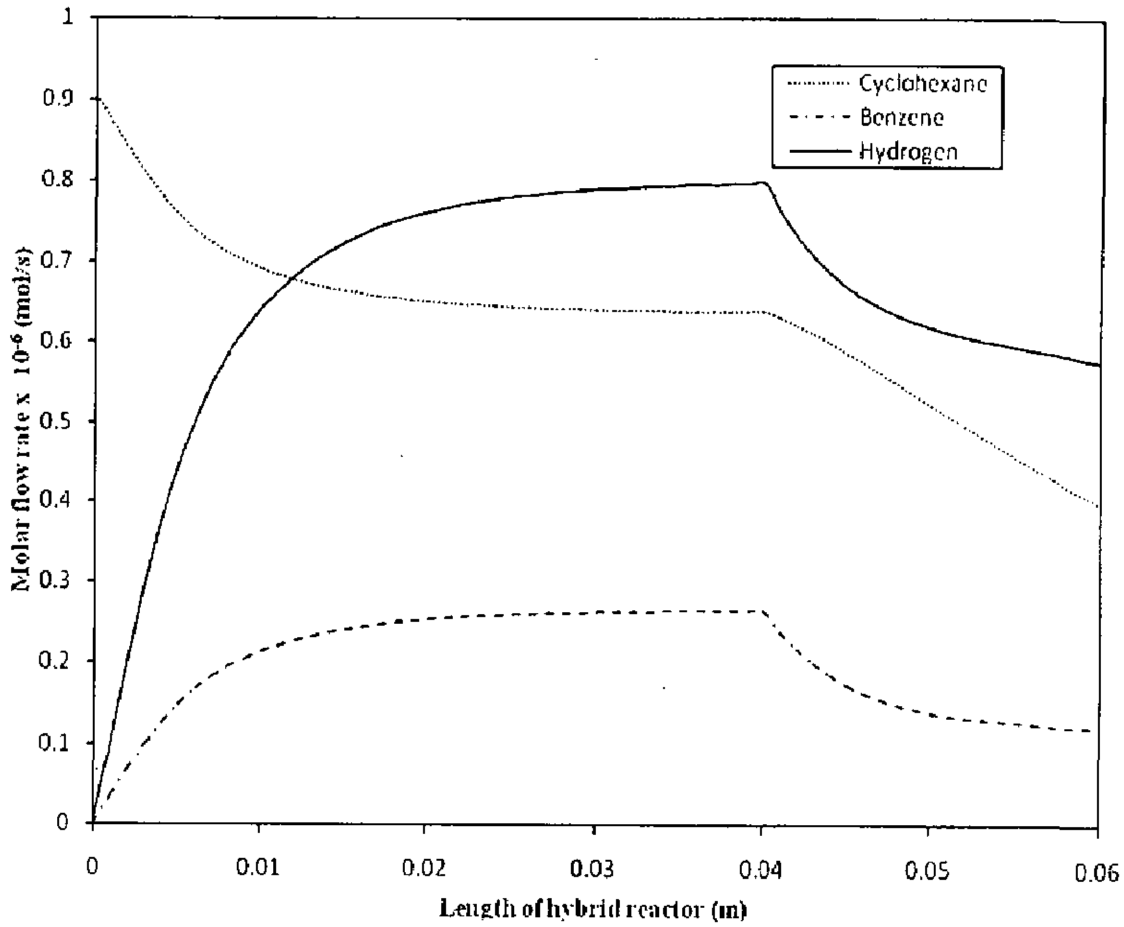

Fig.4.14: Variation in the molar flow rate along the length of the hybrid reactor in the reaction side at 473 K with no H_2 in the feed.

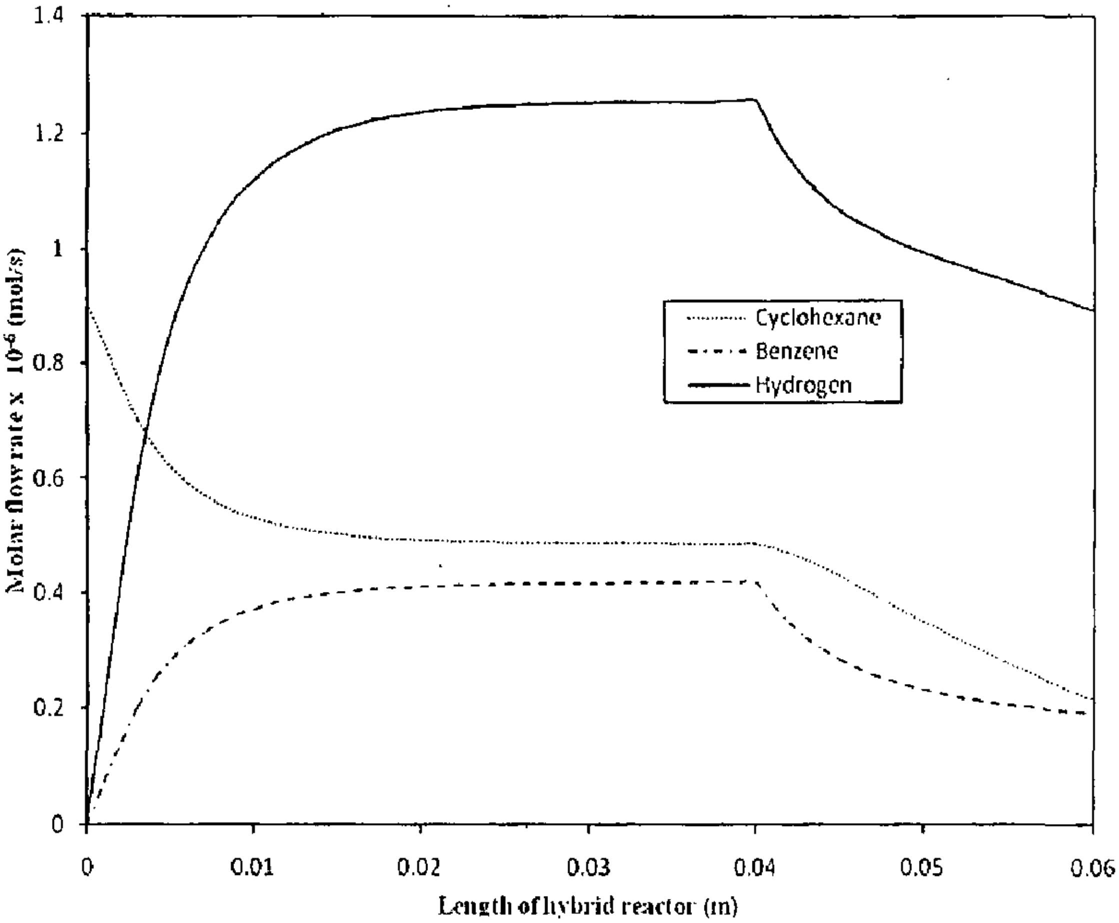

Fig.4.15: Variation in the molar flow rate along the length of the hybrid reactor in the reaction side at 490 K with no H_2 in the feed.

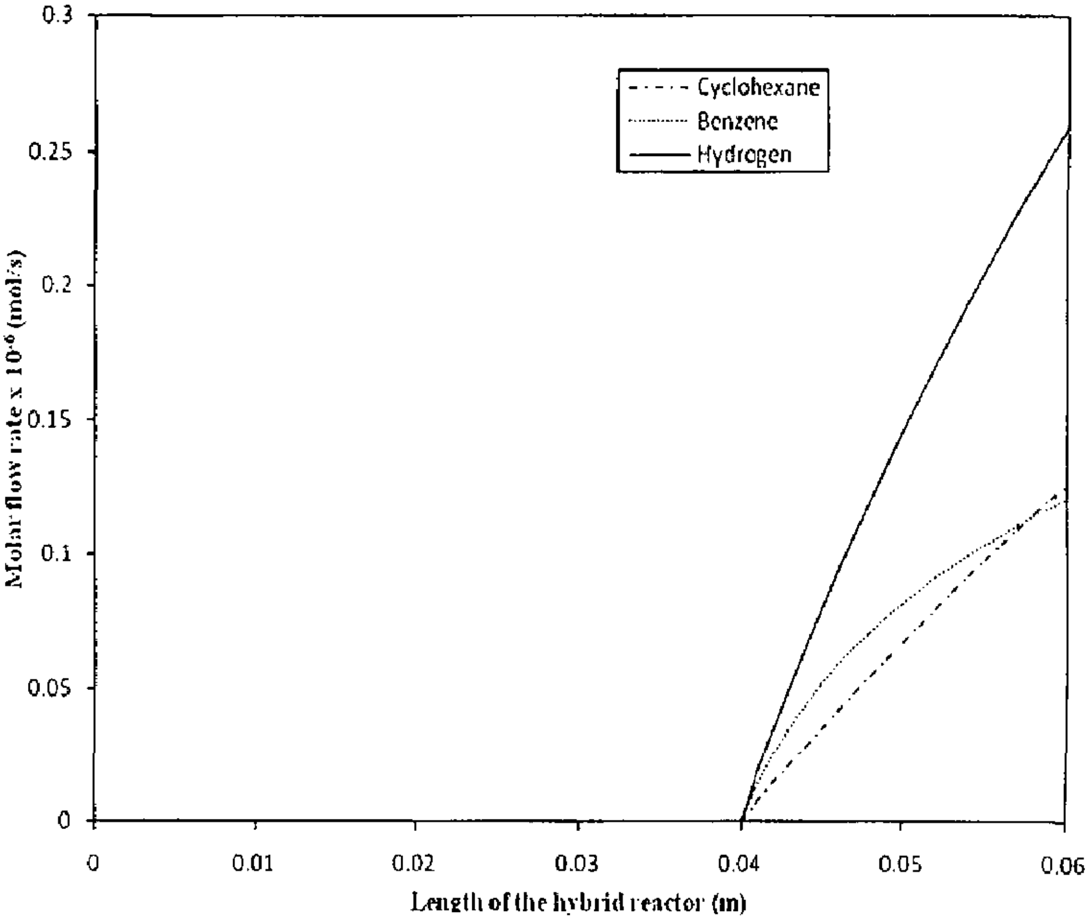

Fig.4.16: Variation in the molar flow rate along the length of the hybrid reactor in the permeate side at 448 K with no H_2 in the feed.

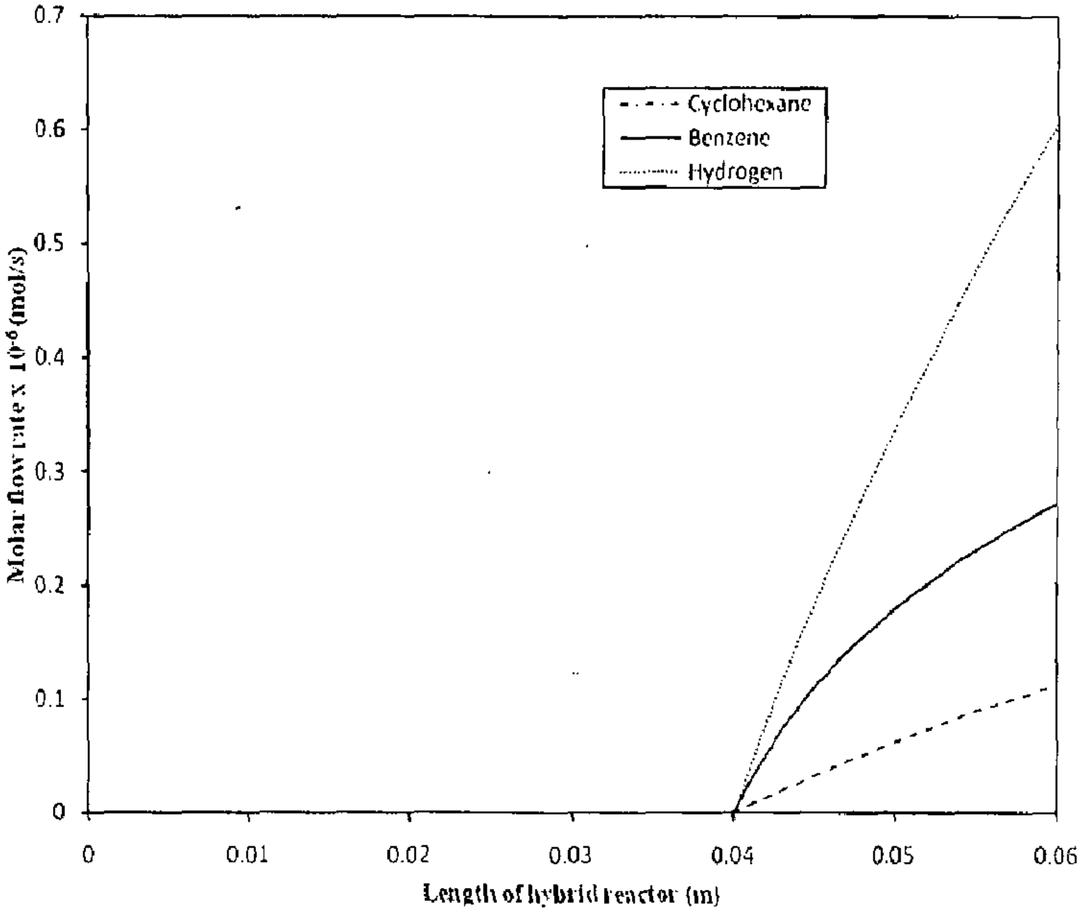

Fig.4.17: Variation in the molar flow rate along the length of the hybrid reactor in the permeate side at 473 K with no H_2 in the feed.

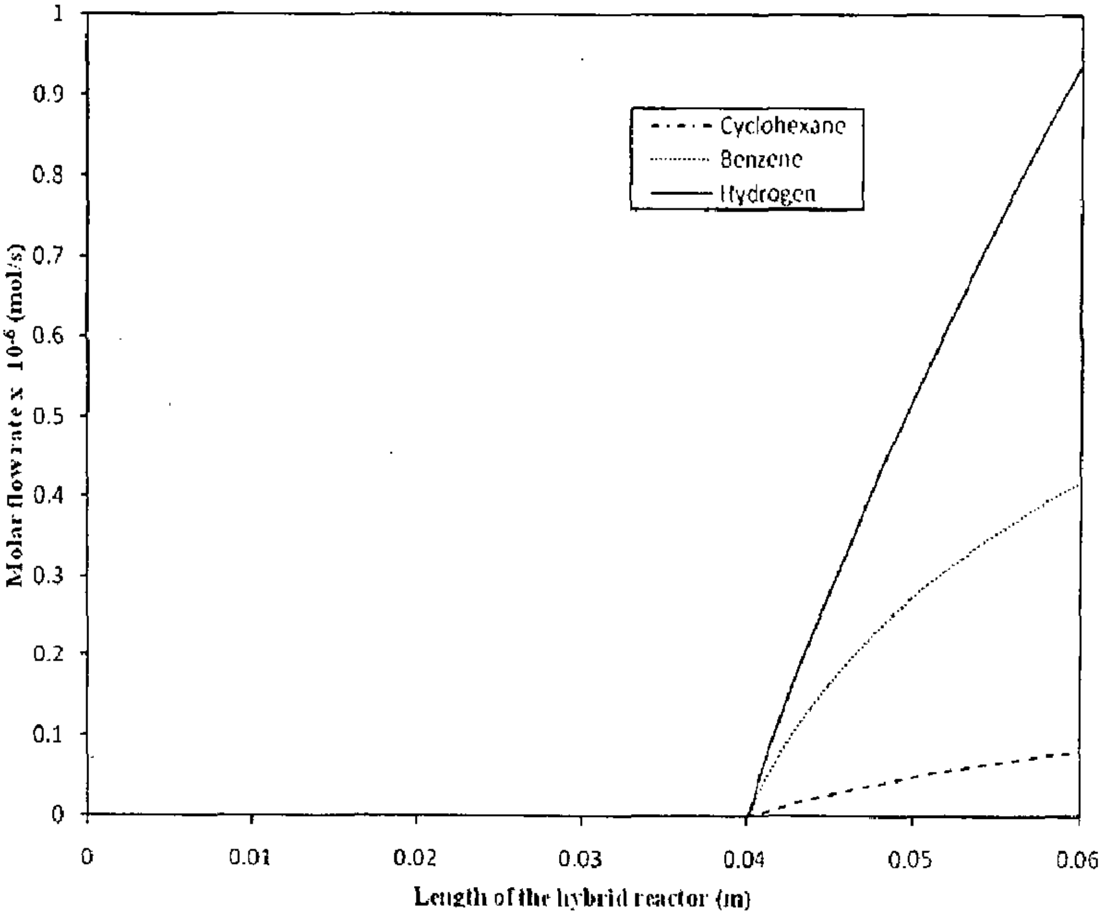

Fig.4.18: Variation in the molar flow rate along the length of the hybrid reactor in the permeate side at 490 K with no H_2 in the feed.

4.2.1 Effect of temperature on conversion of cyclohexane

Fig 4.19 shows percent conversion of cyclohexane at different temperatures in fixed bed hydrogen in the reactor. The conversion at various temperatures is less than the conversion estimated without hydrogen in the feed (Fig 4.2). The dehydrogenation reaction is reversible reaction and hydrogen is the product. On adding hydrogen in feed to the reactor promotes the reaction in the backward direction which results in the reduction in conversion of cyclohexane. For instance at 490 K the percent conversion is 46.29 with no hydrogen and conversion is 41.90 with hydrogen.

In full membrane reactor, the percent conversion is also lower than conversion with no hydrogen (Fig 4.20). At 490 K the conversion is 82.54% and with hydrogen it is 80.64%. For the hybrid type of reactor the variation in conversion of cyclohexane has been shown along the length of reactor in Fig 4.21, 4.22 and 4.23 at temperatures of 448 K, 473 K and 490 K respectively. The conversion increases along the length of the rector and also with temperature. The percent conversion at 473 is 43.65 with no hydrogen and it is 38.73 with hydrogen. From these illustrations it is observed that percent decrease in conversion of cyclohexane with hydrogen is maximum in fixed bed and minimum in case of full length membrane reactor. Hybrid reactor even on being between fixed bed and membrane reactor is considered better reactor configuration option at the expense of reactant loss.

4.2.2 Variation of molar flow rate along the length of reactor

4.2.2.1 Full length membrane reactor

The flow rates of cyclohexane, benzene and hydrogen in the reaction side of full length membrane reactor have been plotted in Fig 4.24, 4.25 and 4.26 at temperatures of 448 K, 473 K and 490 K respectively. The trends of all profiles are typical. The flow rate of hydrogen is higher than the flow rate flow rate of hydrogen in case of membrane reactor with no hydrogen as hydrogen is introduced with the feed. The flow rate of benzene is lowest. As temperature increases the flow rate of hydrogen increases rapidly (Fig 4.25 and 4.26) due to high conversion and then decreases due to high permeation through the membrane. At the same time the flow rate of benzene also increases while the flow rate of cyclohexane decreases along the length. The reduction in cyclohexane flow rate is sharp in the beginning due to high conversion rate at high temperature. These figures also reveal that as conversion increases the flow rate of benzene increases and reduction in flow rate of benzene due to permeation is low as compared to flow rate of hydrogen.

Variation in the molar flow rate of cyclohexane benzene and hydrogen in the permeate side of the membrane has been shown in Fig 4.27, 4.28 and 4.29 at temperatures of 448 K, 473 K and 490 K respectively. The flow rate of cyclohexane at low temperature of 448 K is higher than flow rate of benzene. This clearly shows the loss of reactant cyclohexane through membrane at low conversion. Although at high temperature the conversion of cyclohexane is high, the permeation of cyclohexane through membrane is in significant amount. The flow rate of hydrogen is higher than flow rate of hydrogen with no hydrogen as hydrogen is being added to the feed which makes the partial pressure of hydrogen higher at reaction side. Although conversion of cyclohexane is less, on adding hydrogen in the feed, the permeation rate of hydrogen becomes high due to additional amount of hydrogen in the feed.

4.2.2.2 Hybrid reactor

The major advantage of hybrid reactor is to reduce the reactant loss through a membrane. In the presence of hydrogen in the feed, conversion in the fixed bed decreases at given temperature and so correspondingly conversion in the hybrid reactor is also lower than the conversion with no hydrogen. Therefore the flow rate of cyclohexane in hybrid reactor with hydrogen is higher than in case of no hydrogen. On the other hand the flow rate of benzene is lower than that of with no hydrogen while the flow rate of hydrogen is higher at all temperatures (Fig 4.30 and 4.31). In Fig 4.32, at temperature 490 K, there is rapid increase in flow rate of hydrogen due to high production in fixed bed portion of hybrid reactor, and then it decreases. But at the exit of hybrid reactor its flow rate is still higher than the flow rate without hydrogen.

Fig 4.33, 4.34 and 4.35 indicates the flow rate variation in permeate side of hybrid reactor at temperature 448 K, 473 K and 490 K respectively. In all the figures the profile starts beyond the length of reactor as 0.04m. In membrane portion of reactor, the flow rate of hydrogen is very much higher than cyclohexane and benzene. It is also higher than the flow rate with no hydrogen.

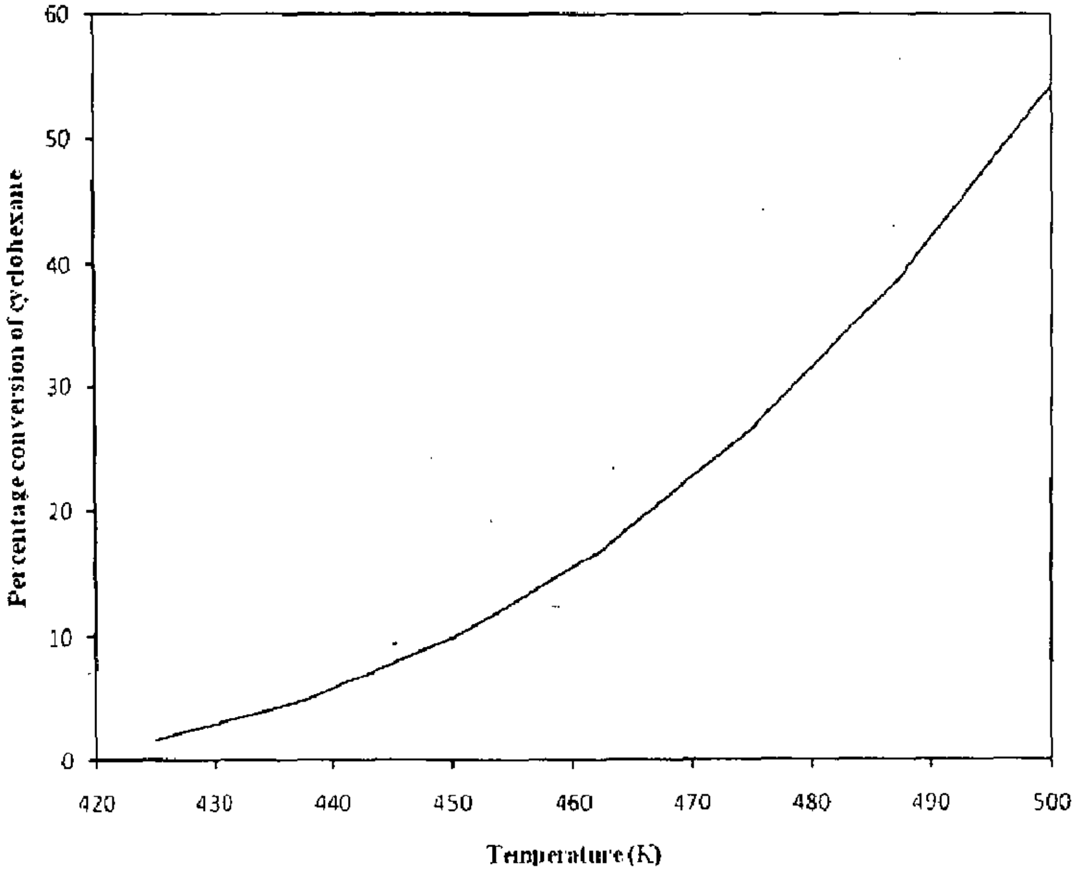

Fig.4.19: Variation of percent conversion of cyclohexane with temperature for fixed bed reactor with H_2 = 0.02 mol % in the feed side.

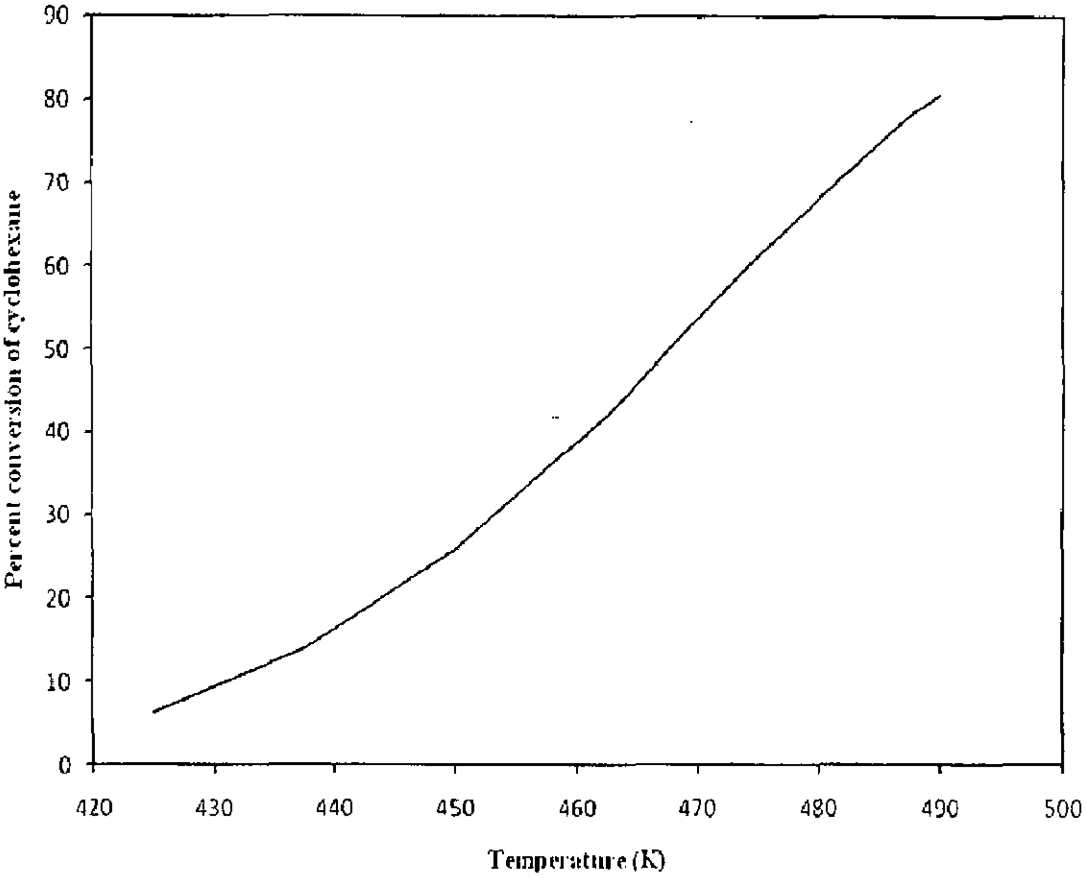

Fig.4.20: Variation of percent conversion of cyclohexane with temperature for membrane reactor with H_2=.02 mol % in the feed side.

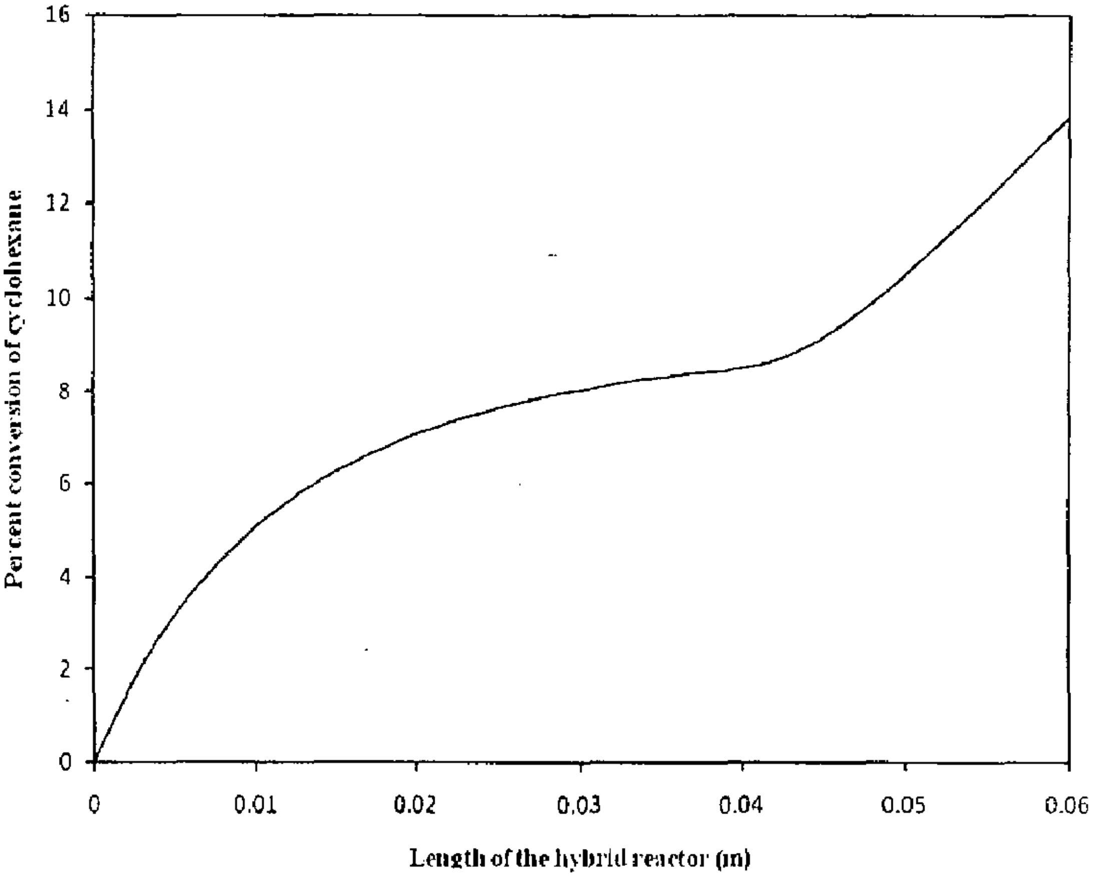

Fig.4.21: Variation of percent conversion of cyclohexane along the length of hybrid reactor at 448 K with H_2 = 0.02 mol % in the feed.

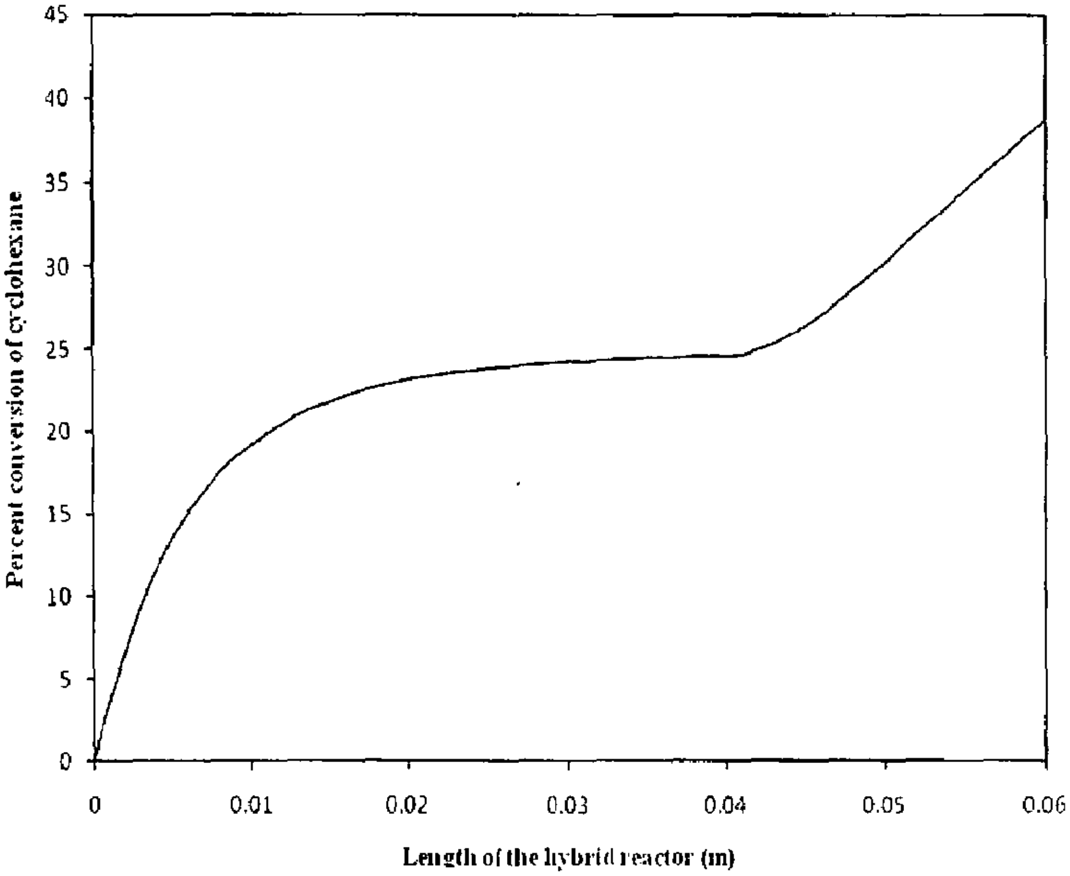

Fig.4.22: Variation of percent conversion of cyclohexane along the length of hybrid reactor at 473 K with H_2 = 0.02 mol % in the feed.

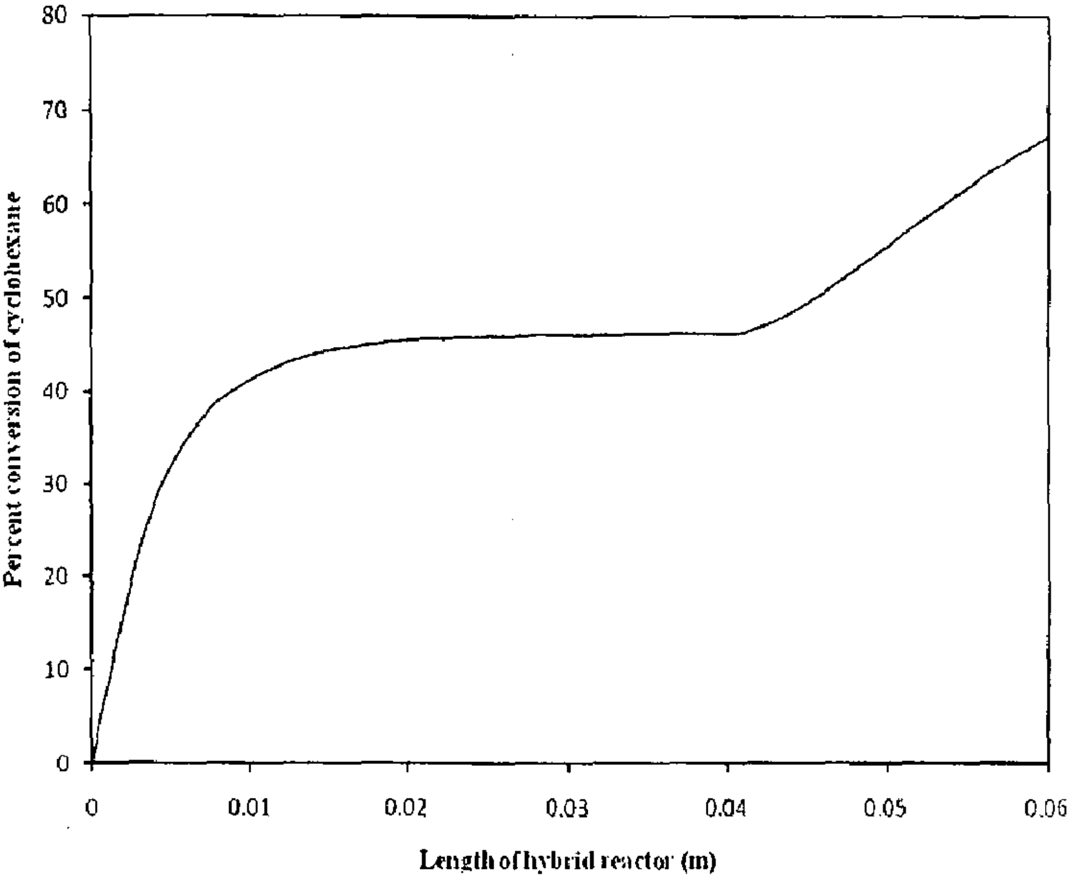

Fig.4.23: Variation of percent conversion of cyclohexane along the length of hybrid reactor at 490 K with H_2 = 0.02 mol % in the feed.

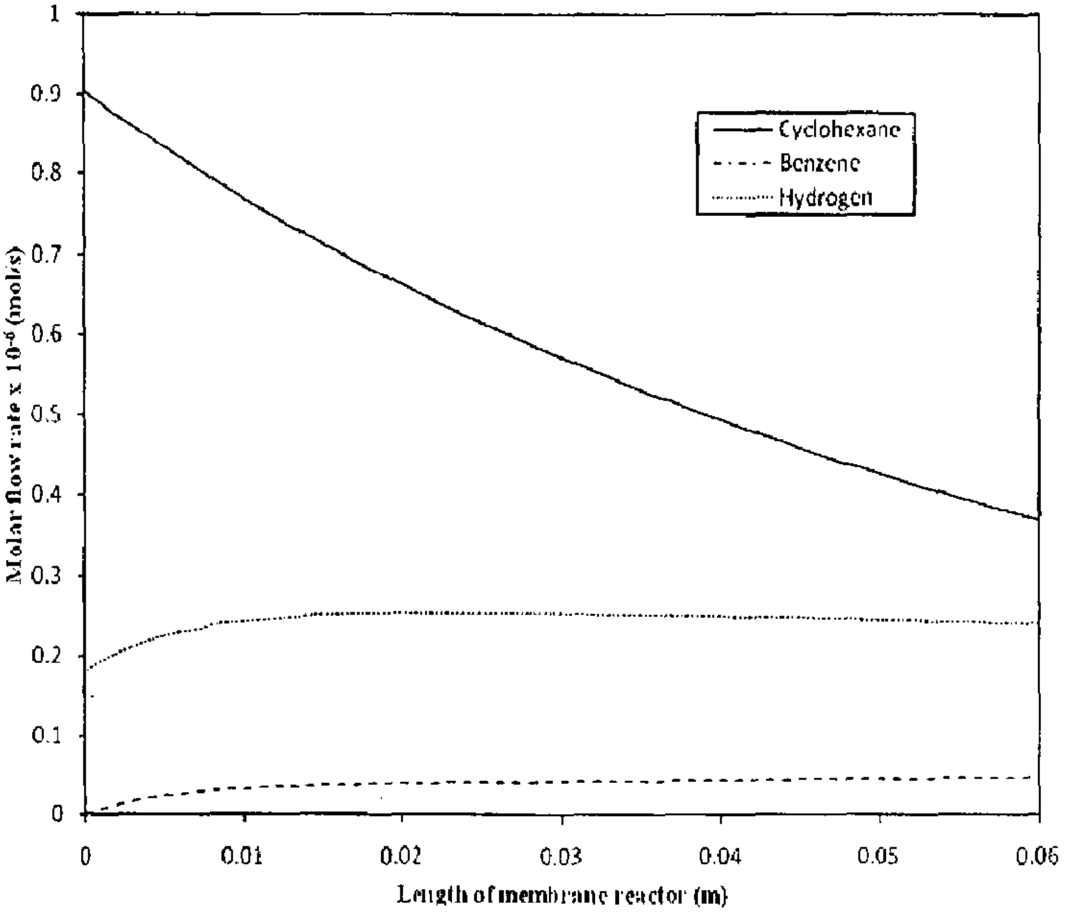

Fig.4.24: Variation in the molar flow rate along the length of the membrane reactor in the reaction side at 448 K with H_2 = 0.02 mol % in the feed.

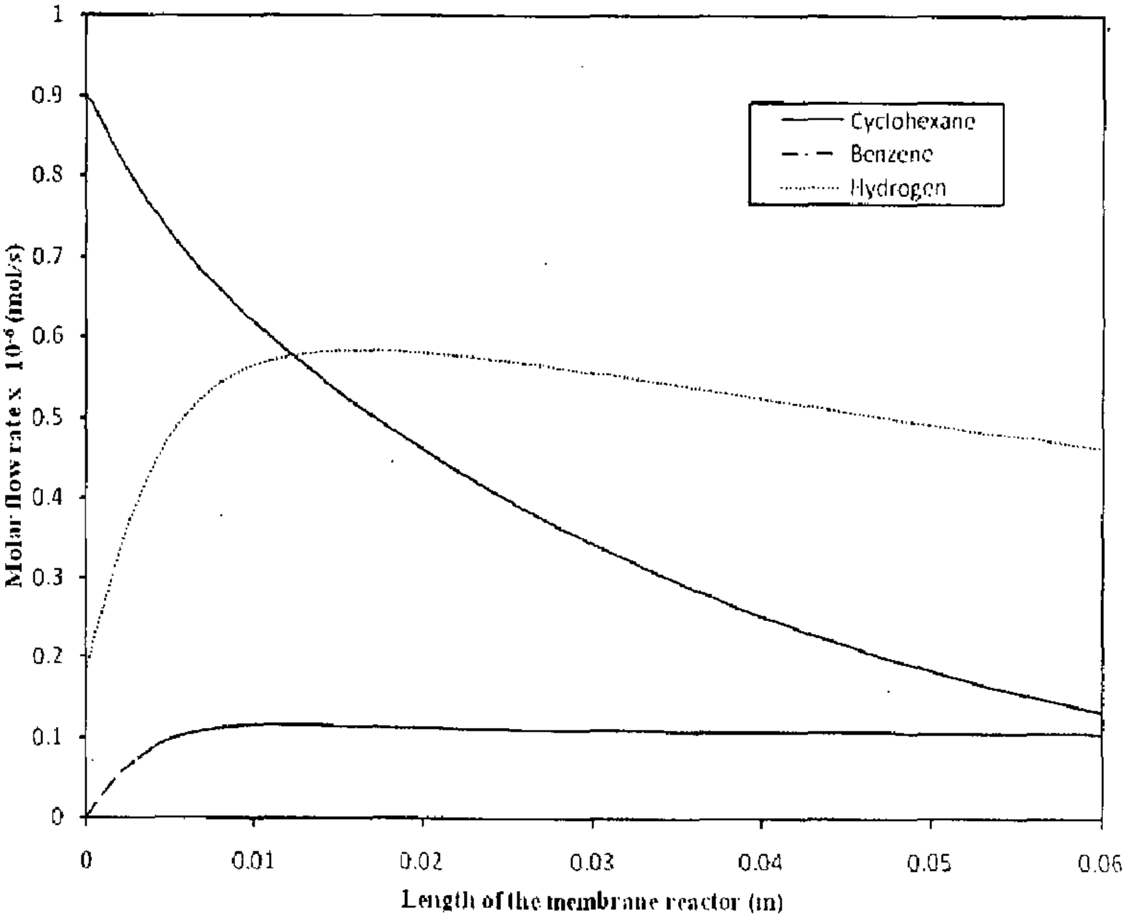

Fig.4.25: Variation in the molar flow rate along the length of the membrane reactor in the reaction side at 473 K with H_2 = 0.02 mol % in the feed.

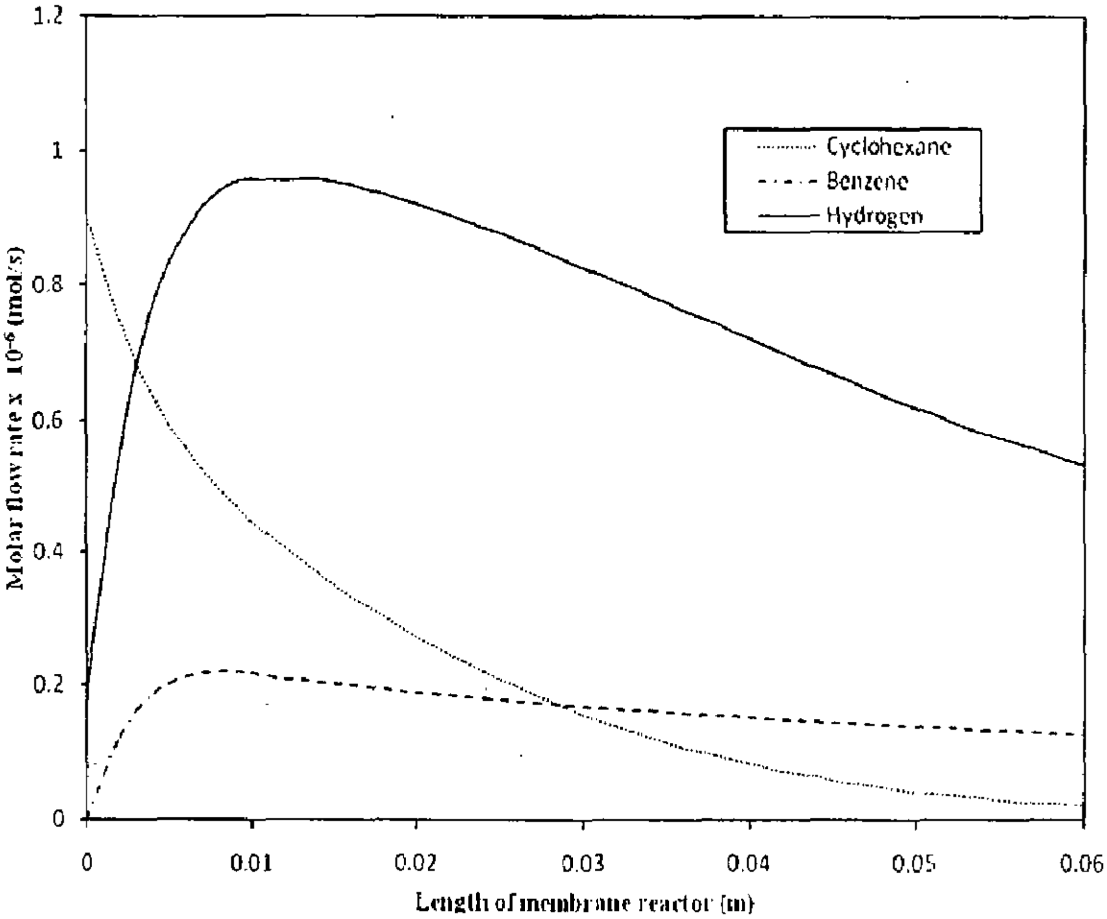

Fig.4.26: Variation in the molar flow rate along the length of the membrane reactor in the reaction side at 490 K with H_2 = 0.02 mol % in the feed.

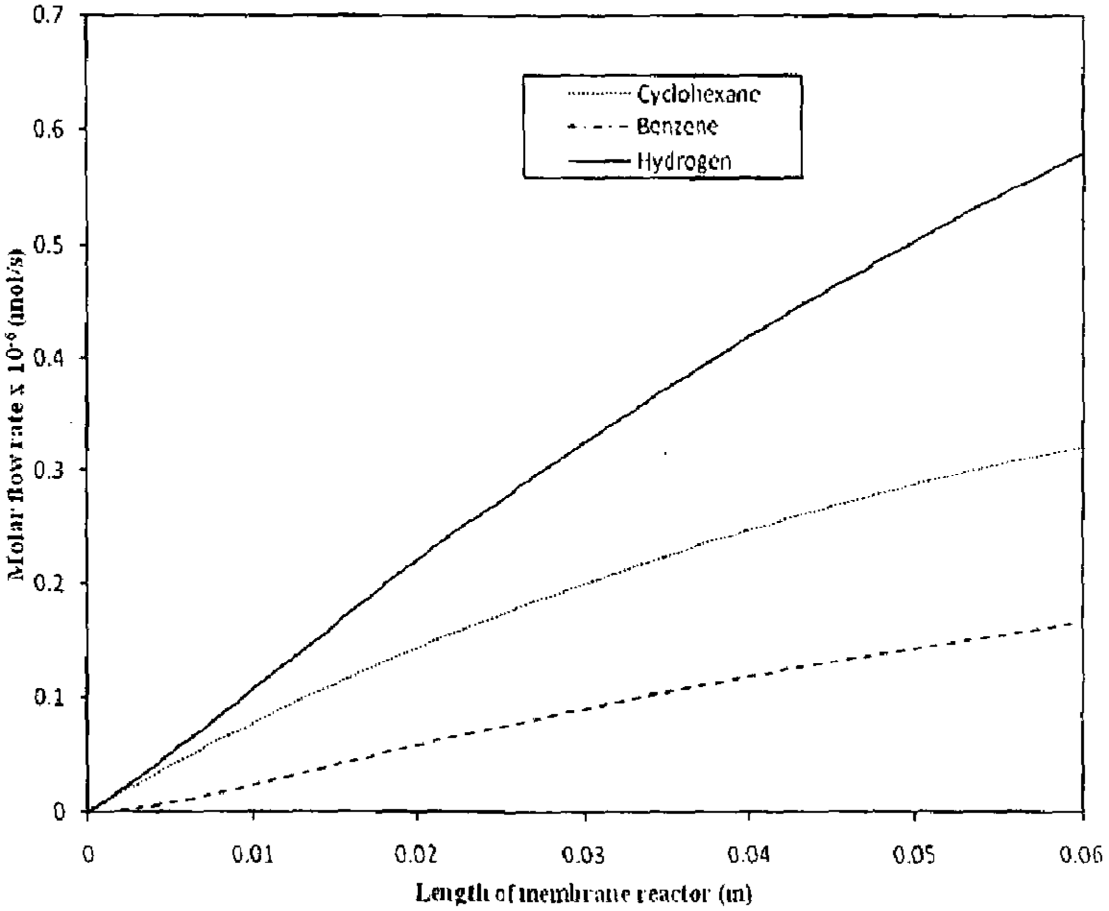

Fig.4.27: Variation in the molar flow rate along the length of the membrane reactor in the permeate side at 448 K with H_2 = 0.02 mol % in the feed.

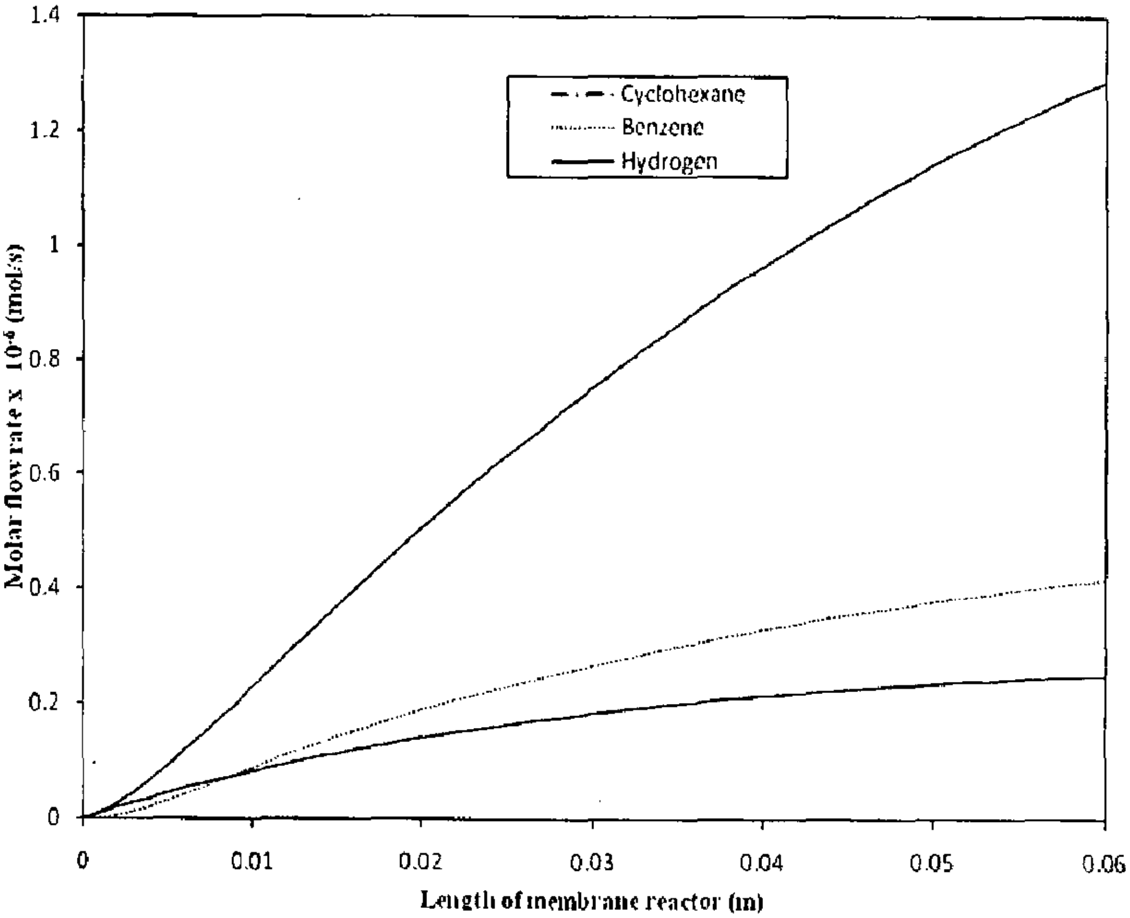

Fig.4.28: Variation in the molar flow rate along the length of the membrane reactor in the permeate side at 473 K with H_2 = 0.02 mol % in the feed.

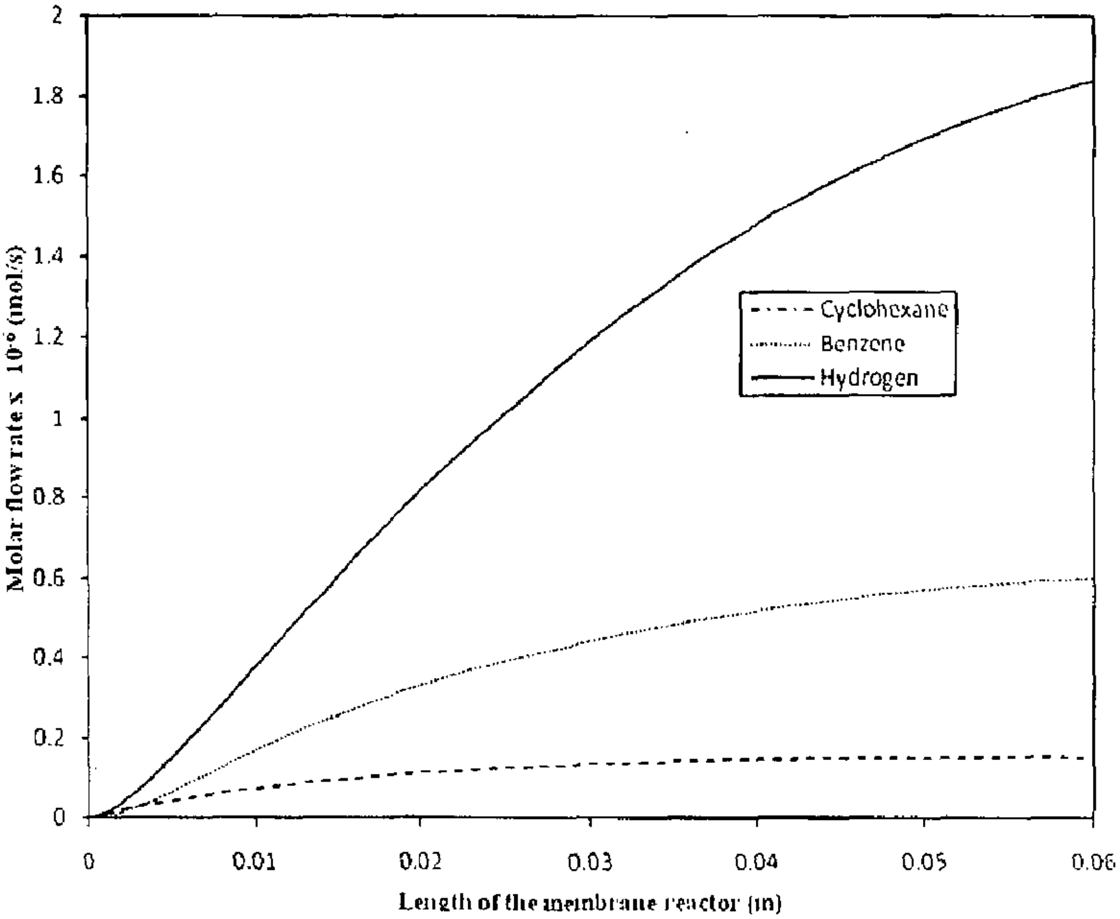

Fig.4.29: Variation in the molar flow rate along the length of the membrane reactor in the permeate side at 490 K with H_2 = 0.02 mol % in the feed.

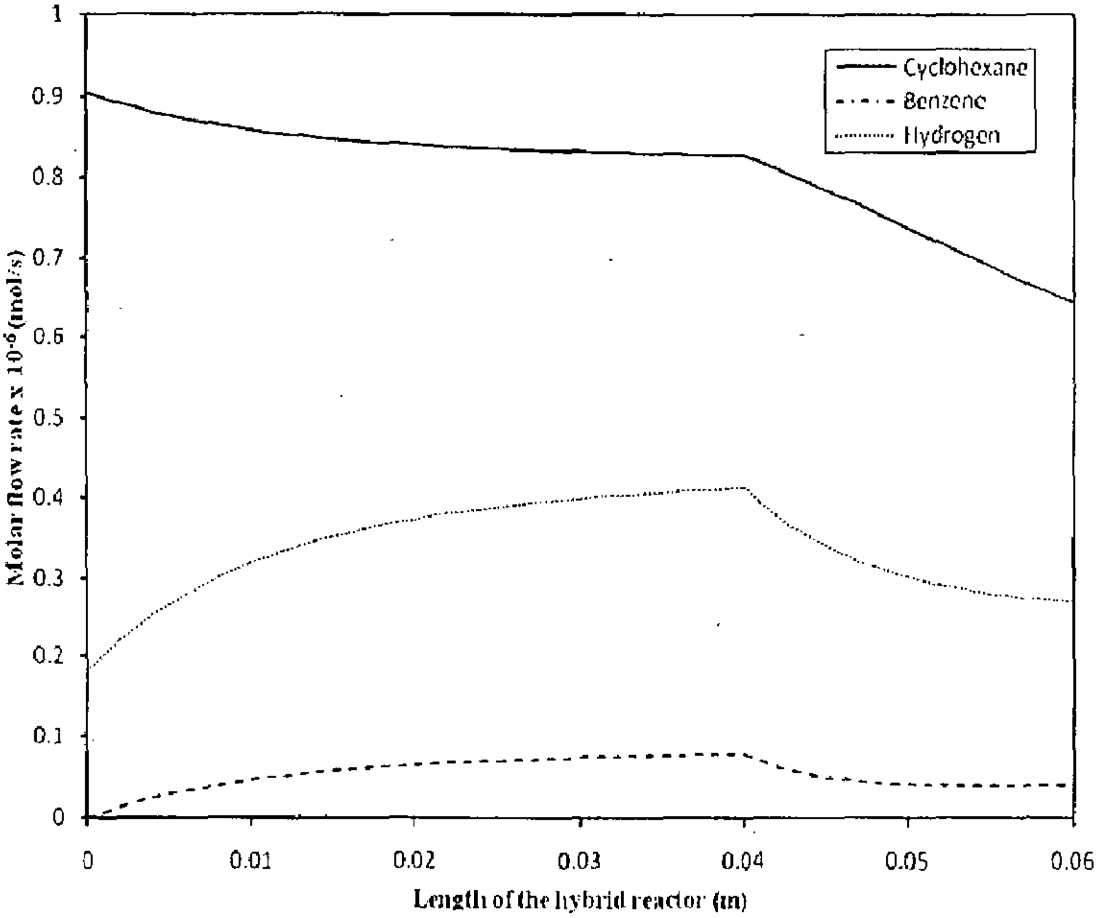

Fig.4.30: Variation in the molar flow rate along the length of the hybrid reactor in the reaction side at 448 K with H_2 = 0.02 mol % in the feed.

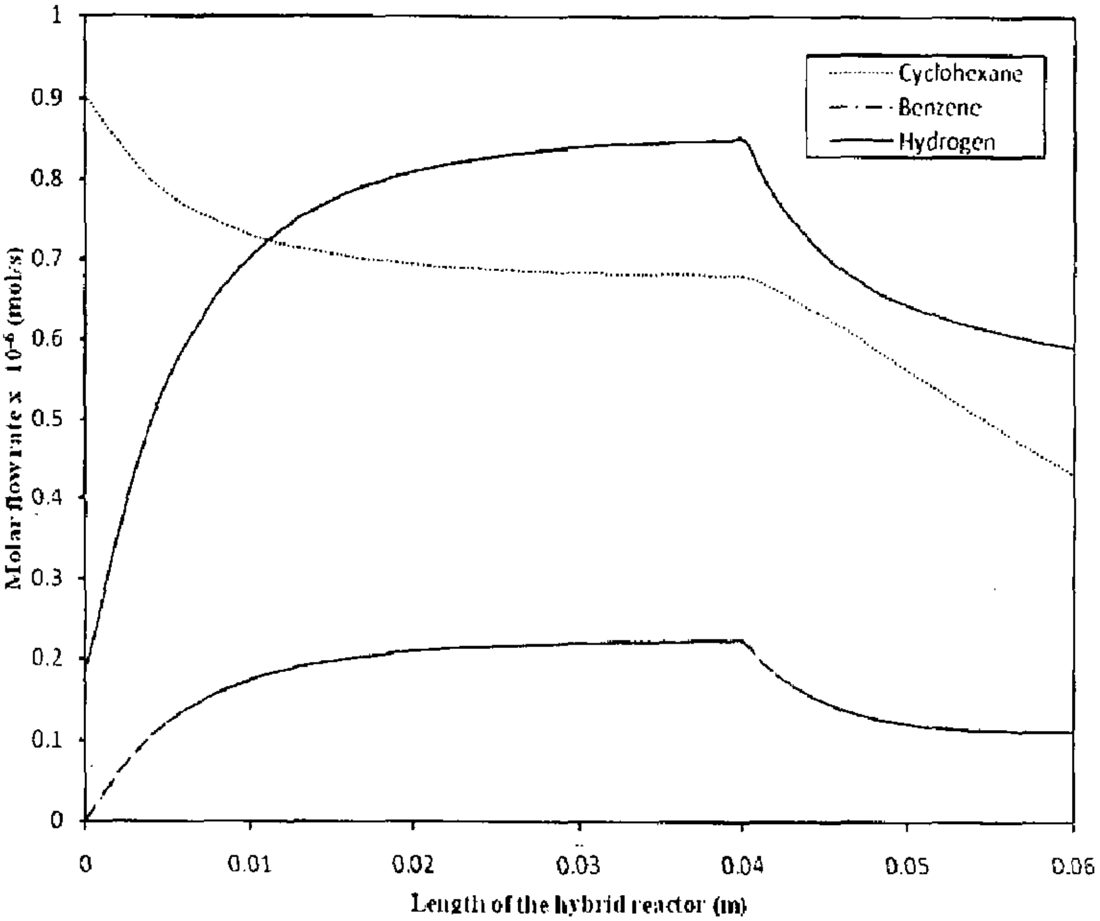

Fig.4.31: Variation in the molar flow rate along the length of the hybrid reactor in the reaction side at 473 K with H_2 = 0.02 mol % in the feed.

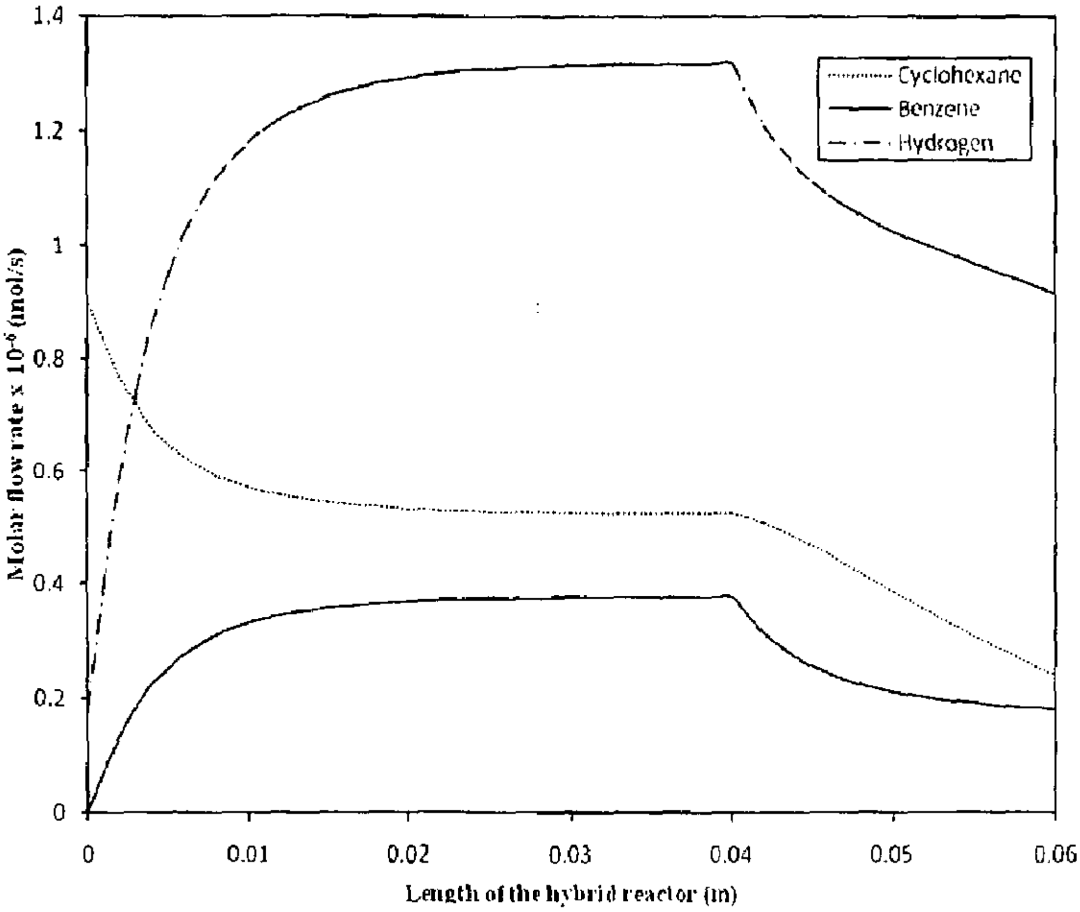

Fig.4.32: Variation in the molar flow rate along the length of the hybrid reactor in the reaction side at 490 K with H_2 = 0.02 mol % in the feed.

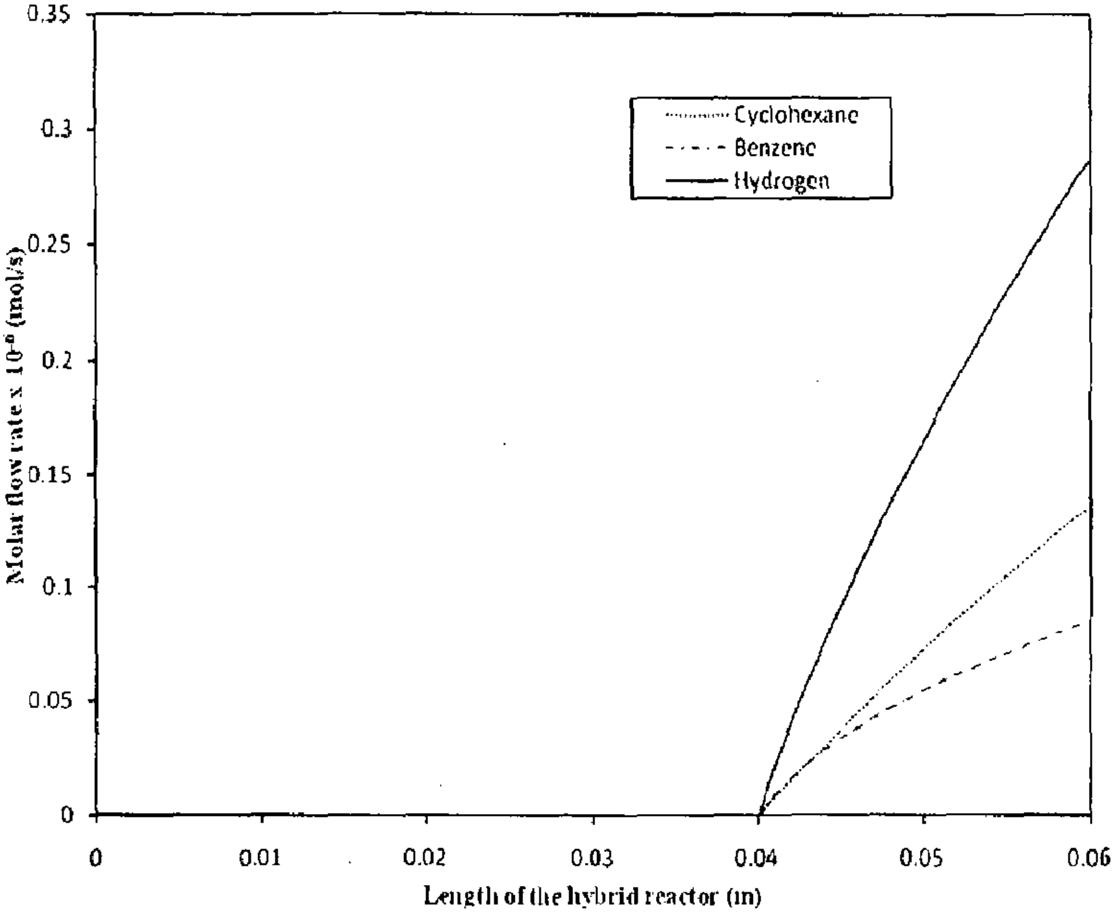

Fig.4.33: Variation in the molar flow rate along the length of the hybrid reactor in the permeate side at 448 K with H_2 = 0.02 mol % in the feed.

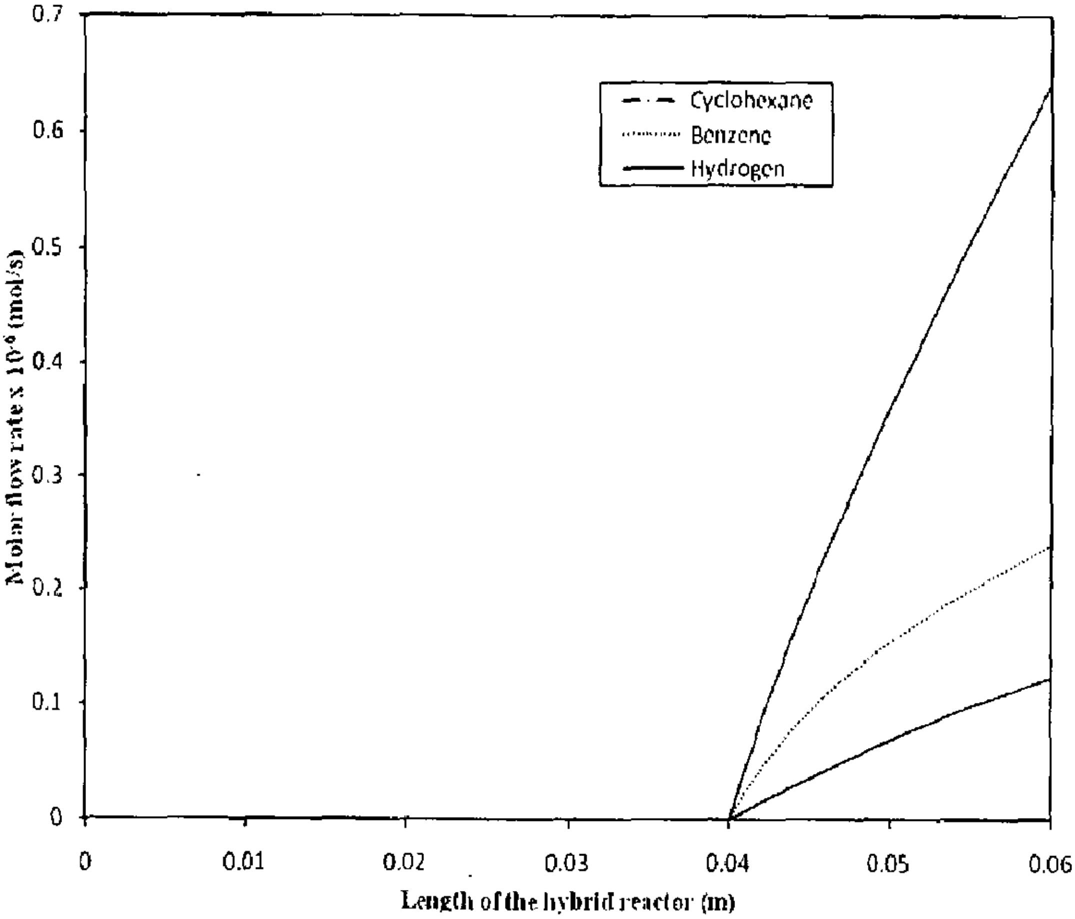

Fig.4.34: Variation in the molar flow rate along the length of the hybrid reactor in the permeate side at 473 K with $H_2 = 0.02$ mol % in the feed.

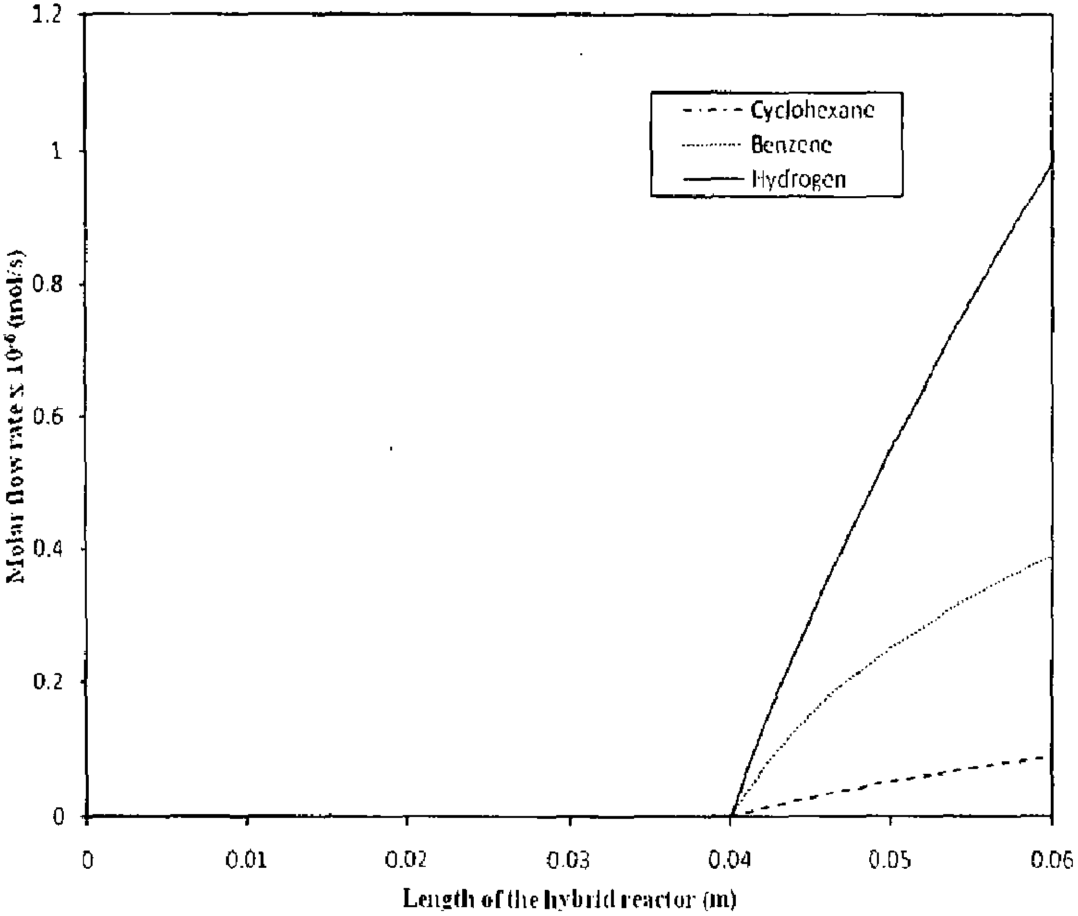

Fig.4.35: Variation in the molar flow rate along the length of the hybrid reactor in the permeate side at 490 K with H_2 = 0.02 mol % in the feed.

From the above results and their discussion, it can be concluded that hydrogen in feed provide practically the stability in the activity of membrane and catalyst as observed by many research workers. Although its presence in the feed reduces the conversion of cyclohexane, the hydrogen can be recovered from the outgoing stream and also selectivity of hydrogen becomes high in the product in comparison to the feed without hydrogen. Thus the addition of hydrogen in the feed is beneficial at the expense of deactivation of membrane and catalyst.

CHAPTER V

CONCLUSIONS AND RECOMMENDATIONS

5.1 Conclusions

The catalytic dehydrogenation of cyclohexane in a microporous membrane reactor was simulated by solving a one dimensional steady state isothermal mathematical model. A zeolite membrane (FAU type) was used in membrane reactor. Three reactor configurations namely conventional fixed bed, full length membrane reactor and hybrid reactor were studied with two feed conditions. In one feed condition argon and hydrogen were added to cyclohexane where as in second feed condition only argon was mixed with cyclohexane. The expressions which related permeance of components through FAU type membrane to temperature have been formulated on the basis of experimental data available in open literature. The model equations were solved by using "ode solver" of MATLAB at given operating and boundary conditions. The simulated results are as below:

- Conversion of cyclohexane increases with increase in temperature due to endothermicity of dehydrogenation reaction.
- The conversion is maximum upto a length of 0.04m in fixed bed reactor.
- In case of full length membrane reactor the conversion is higher than the conversion in fixed bed due to separation of the products from the reaction side by membrane.
- The conversion in hybrid reactor lies in between fixed bed reactor and full length membrane reactor. Although the conversion is lower in hybrid reactor than full length membrane reactor the performance of hybrid reactor may be considered superior at the expense of high cost and high reactant loss in full length membrane reactor.
- The yield of hydrogen increases with increase in temperature whereas the selectivity remains same at all temperatures since no side reaction has been considered in the present study.

- Cofeed of hydrogen with cyclohexane restrains the coke formation on the catalyst and membrane thus maintaining the stability of both catalyst and membrane.
- The conversion with hydrogen in feed is lower than the feed without hydrogen. The valid reason for this reduction is the high concentration of hydrogen in reactor which is the product.
- The yield of hydrogen is higher in case of feed with hydrogen because hydrogen is fed with cyclohexane. This indicates that supplied hydrogen can be recovered from the exit of the reactor.

From these studies it can be concluded that the reduction in conversion can be accepted on commercial level in order to maintain the stability of catalyst and membrane.

5.2 Recommendations

- In modeling studies constitutive properties play an important role. Therefore various constitutive properties which include kinetic, physical and transport properties must be evaluated very carefully to get better simulated results.
- Experiment results collected from the literature are sometimes not in accordance with the given system therefore, it is recommended that experiment data must be evaluated in the laboratory by carrying out an experiment.
- Since lab data are quite different from those obtained from commercial scale therefore it is recommended that the model developed here must be tested with the data obtained from the industries. It will enhance the applicability of the model.

REFERENCES

[1] Abashar M.E.E., A. A. Al-Rabiah, Production of ethylene and cyclohexane in a catalytic membrane reactor, Chemical Engineering and Processing ,44 (2005) 1188–1196.

[2] Alia L.I., Abdel-Ghaffar A. Ali, S.M. Aboul-Fotouh, Ahmed K. Aboul-Gheit, Dehydrogenation of cyclohexane on catalysts containing noble metals and their combinations with platinum on alumina support, Applied Catalysis A: General 177 (1999) 99-110.

[3] Biniwale R.B., N. Kariya, H. Yamashiro, and Masaru Ichikawa, Heat Transfer and Thermographic Analysis of Catalyst Surface during Multiphase Phenomena under Spray-Pulsed Conditions for Dehydrogenation of Cyclohexane over Pt Catalysts, J. Phys. Chem. B 110 (2006) 3189-3196

[4] Caro J., M. Noack, P. Kolsch, R. Schafer, Zeolite membranes - state of their development and perspective, Microporous and Mesoporous Materials 38 (2000) 3-24.

[5] Ciavarella P., D. Casanave, H. Moueddeb, S.Miachon, K. Fiaty and J.-A. Dalmon, Isobutane dehydrogenation in a membrane reactor. Influence of operating conditions on the performance, Catalysis Today 67 (2001) 177-184.

[6] Coronas J., J. Santamaria, Catalytic reactor based upon porous ceramic membranes Catal., 51 (1999) 377.

[7] Dittmeyer R., Volker Höllein, Kristian Daubb, Membrane reactors for hydrogenation and dehydrogenation processes based on supported palladium, Journal of Molecular Catalysis A: Chemical 173 (2001) 135–184.

[8] Dixon A.G., Recent Research in Catalytic Inorganic Membrane Reactors, International journal of chemical reactor engineering, 1 (2003).

[9] Gokhale Y.V., Richard D. Noble, John L. Falconer, Effect of reactant loss and membrane selectivity on a dehydrogenation reaction in a membrane-enclosed catalytic reactor, Journal of Membrane Science 105 (1995) 63-70.

[10] Hassan M.H., J. Douglas Way, Paul M. Thoen, Anne C. Dillon, Single component and mixed gas transport in a silica hollow fiber membrane, Journal of Membrane Science 104 (1995) 27-42.

[11] Itoh N, Eisuke Tamura, Shigeki Hara, Tomohiro Takahashi, Atsushi Shono, Kazumi Satoh, Takemi Nambac, Hydrogen recovery from cyclohexane as a chemical hydrogen carrier using a palladium membrane reactor, Catalysis Today 82 (2003) 119–125.

[12] Itoh N., A membrane reactor using palladium, AIChE Journal, 33 (September 1987) 1576-1578.

[13] Itoh N., Yuji Shindo, Kenji Haraya, and Toshikatsu Hakuta, A membrane reactor using microporous glass for shifting equilibrium of cyclohexane dehydrogenation, Journal of chemical Engineering of Japan 21 (1998) 399-404.

[14] Jeong B-H., Ken-Ichiro Sotowa, Katsuki Kusakabe, Catalytic dehydrogenation of cyclohexane in an FAU-type zeolite membrane reactor, Journal of Membrane Science 224 (2003) 151–158.

[15] Jeong B-H., Ken-Ichiro Sotowa, Katsuki Kusakabe, Modeling of an FAU-type zeolite membrane reactor for the catalytic dehydrogenation of cyclohexane, Chemical Engineering Journal 103 (2004) 69–75.

[16] Jeong B-H., Yasuhisa Hasegawa, Ken-Ichiro Sotowa, Katsuki Kusakabe, Shigeharu Morooka, Permeation of binary mixtures of benzene and saturated C4–C7 hydrocarbons through an FAU-type zeolite membrane. Journal of Membrane Science 213 (2003) 115–124.

[17] Jia W., S. Murad, Molecular dynamics simulations of gas separations using faujasite-type zeolite membranes, Journal of Chemical Physics, 120 (2004) 4877-4885.

[18] Kariya N., Atsushi Fukuoka, Masaru Ichikawa, Efficient evolution of hydrogen from liquid cycloalkanes over Pt-containing catalysts supported on active carbons under "wet–dry multiphase conditions", Applied Catalysis A: General 233 (2002) 91–102.

[19] Kusakabe K., T. Kuroda, K. Uchino, Y. Hasegawa, and S. Morooka, Gas Permeation Properties of Ion-Exchanged Faujasite-Type Zeolite Membranes, AIChE Journal, Vol. 45 (June 1999) 1220.

[20] Lechuga F.T., C.G. Hill Jr., M.A. Anderson, Effect of dilution in the experimental dehydrogenation of cyclohexane in hybrid membrane reactors, Journal of Membrane Science 118 (1996) 85-92.

[21] Mohan K., Rakesh Govind, Analysis of a cocurrent membrane reactor, AIChE Journal, 32 (1986) 2083.

[22] Shelekhin A.B., A.G. Dixon and Y.H. Ma, Adsorption, permeation, and diffusion of gases in microporous membranes. II. Permeation of gases in microporous glass membranes, Journal of Membrane Science, 75 (1992) 233-244.

[23] Sirkar K.K., Purushottam V. Shanbhag, and A. Sarma Kovvali, Membrane in a Reactor: A Functional Perspective, Ind. Eng. Chem. Res. 38 (1999) 3715-3737.

[24] Sun Y.M., Soon-Jai Khang, A Catalytic Membrane Reactor: Its Performance in Comparison with Other Types of Reactors, Ind. Eng. Chem. Res. Vol 29 (1990) 232-238.

[25] Tavolaro A., Enrico Drioli, Zeolite membranes, WILEY-VCH Verlag GmbH, D- 69469 Weinheim, 1999.

[26] Weyten H., Jan Luyten, Klaas Keizerb, Louis Willems, Roger Leysen , Membrane performance: the key issues for dehydrogenation reactions in a catalytic membrane reactor, Catalysis Today 56 (2000) 3-11.

[27] Zaman J., A. Chakma, Inorganic membrane reactors, Journal of.Membrane Science, 92 (1994) 1-28.

[28] Zhou L., Progress and problems in hydrogen storage methods, Renewable and Sustainable Energy Reviews , 9 (2005) 395–408.